PALYNOLOGY OF THE PERMIAN SANANGOÉ–MEFIDEZI COAL BASIN, TETE PROVINCE, MOZAMBIQUE AND CORRELATIONS WITH GONDWANAN MICROFLORAL ASSEMBLAGES

Kierra Caprice Mahabeer

A Dissertation submitted to the Faculty of Science, University of the Witwatersrand, in partial fulfilment of the requirements for the Degree of Master of Science

June, 2017

The financial assistance of the National Research Foundation (NRF) towards this research is hereby acknowledged. Opinions expressed and conclusions arrived at, are those of the author and are not necessarily to be attributed to the NRF.

Declaration

I hereby certify that this Dissertation is my own unaided work. It is being submitted for the degree of Master of Science at the University of the Witwatersrand, Johannesburg. It has not been submitted before for any degree or examination at any other University.

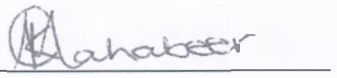

Kierra Caprice Mahabeer

June 2017

Acknowledgements

My deepest gratitude goes to my supervisors Prof. Marion Bamford and Dr. Natasha Barbolini. Without their help and guidance this dissertation would not be possible. Thank you for always pushing me further and making me a better researcher.

Thanks also goes to Dr. Jennifer Fitchett for the R script as well as for training in the statistical programs used in this study. Thank you to Eurasian Natural Resources Corporation (Mozambique Limitada) for access to core. Thank you to Dr. John Hancox for always being willing to assist with any questions and for facilitating access to core and for providing geological core logs. Thanks also goes to Prosper Bande for assistance with laboratory preparation.

I am grateful for the financial assistance from the National Research Foundation the Palaeontological Scientific Trust (PAST) and the University of the Witwatersrand.

Finally, I would like to thank and dedicate this dissertation to my mother. Thank you for making it possible for me to further my studies.

Abstract

This study investigated the palynology of three boreholes (boreholes 12 ESD 231, 871L_D012 and 12 ESD 218) from the Sanangoé-Mefidezi Basin in the Tete Province, Mozambique in order to correlate the coal seams in Mozambique with other Gondwanan palynofloral assemblages. A total of 56 samples were prepared and examined with 27 of them being palynologically productive. All samples were prepared using the standard palynological preparation methods of Phipps and Playford (1984) and were examined and photographed under light microscopy. Palynomorph grains were generally fragmented due to transportation in high energy depositional environments, but identification to genus or species level was possible in most cases. A total of 41 taxa were identified which represented lycopods, sphenophytes, ferns, peltasperms, conifers and glossopterids.

Statistical methods of clustering were applied as an unbiased method of subdividing palynomorph abundances through the three cores into zones and subzones. Four zones (the *Scheuringipollenites ovatus-Deltoidospora directa* Zone, the *Scheuringipollenites ovatus-Alisporites potoniei* Zone, the *Protohaploxypinus limpidus-Weylandites lucifer* Zone and the *Protohaploxypinus limpidus-Striatopodocarpites cancellatus* Zone) and two sub-zones (the *Punctatisporites gretensis* Subzone and the *Platysaccus papilionis* Subzone) were established for the Sanangoé-Mefidezi Basin.

Granulatasporites subreticulatus and *Plicatipollenites* sp. were found to be restricted to the "Platform Facies", whilst a number of taxa were present in two formations only. These restricted ranges can be utilised in future exploration work in the basin to determine which unit an unknown sample derives from.

Correlations between the palynozones of the Sanangoé-Mefidezi Basin and assemblages from southern Africa, Antarctica and Australia were possible, suggesting an age range of Artinskian–Capitanian for the Vúzi, Moatize and Matinde formations. The thermal maturity index determined from palynomorph colour yielded a range of 4 to 5 on the Thermal Alteration Index of Batten (1980),

indicating the potential for oil and wet gas production with transition into dry gas. This bodes well for future mining operations in the area.

Palynological sampling of new cores in the Sanangoé-Mefidezi Basin would permit a more detailed record of the species present in these rocks, and would also determine whether the palynological event marking the base of the Matinde Formation can be laterally traced across the basin. Although reliable radio-isotopic dates can be difficult to obtain, absolute ages for the Sanangoé-Mefidezi Basin rocks would be very useful in precisely calibrating the ages of the palynozones for future fossil fuel exploration as well as correlation with other Gondwanan palynoassemblages.

Keywords: Permian, Palynology, Mozambique, Gondwana, Sanangoé-Mefidezi Basin.

Contents

List of Figures

List of Tables

List of Plates

1. Introduction

1.1. Palaeopalynology

Palaeopalynology (hereafter referred to as palynology) is the study of fossilized palynomorphs, including those of mainly marine origin such as dinoflagellates, scolecodonts and chitinozoans, as well as terrestrial pollen and spores (Traverse, 2007). Palynomorphs contain sporopollenin and/or chitin which makes the cell walls of the palynomorphs very resistant to degradation (Traverse, 2007). This is an important factor in the success of palynological research as sporopollenin allows the outer wall of palynomorphs to be preserved for millions of years. In terrestrial deposits, pollen and spores are microscopic representatives of their parent plant taxa which allows for comparisons to other floras (palaeoecology) as well as tracing changes in palaeoclimate (Moore *et al.*, 1991). Palaeopalynology is a very useful tool as it can allow for reconstruction of palaeoenvironments, biostratigraphic correlation as well as providing relative ages for strata using vegetation history (Moore *et al.*, 1991).

1.2. Limitations of palynology

While palynomorphs are generally very resistant, some limitations do exist. For example, palynomorphs subjected to high pH and temperatures, and high-energy and oxidizing environments, are vulnerable to destruction, therefore volcanic and metamorphic rocks, very weathered rocks, coarse-grained sandstones and "red beds" are some of the environments that often do not preserve fossil palynomorphs (Traverse, 2007).

1.3. Application of palynology in coal mining

Palynology plays an important economic role as it can be used to correlate coal seams in different sedimentary basins, and aid in fossil fuel exploration. Since most of southern Africa's energy currently comes from fossil fuels, it is essential that new resources be efficiently exploited, and palynology can assist in this (Falcon, 1989). Although coal swamps can be mainly localized

environments (Traverse, 2007), they are not necessarily completely autochthonous deposits. Falcon (1975) showed that the physical components of coals indicate the dominant parent floras of a region, meaning that deposits in southern Africa can be partially allochthonous in terms of palynofloras. Palynology can also be used to describe why coal has different physical and chemical properties. Due to the different environments in which floras grow, the chemical composition of coals can differ, causing a variation in coal quality influencing the flammability of the coals (Falcon, 1975). Falcon (1975) noted that production of higher volatility coal can be associated with an increase in the number of spores, pollen, cuticles, waxes, resins as well as the amount of sporopollenin present. However, certain palynomorphs, waxes and resins can affect the coking ability of some coals adversely (Falcon, 1975). Barbolini (2010) also noted the importance of post-depositional thermal influence on fossil fuel deposits, as this can affect the hydrocarbon potential of coal.

1.4. Pollen

Pollen is produced by flowering land plants in large quantities, however not all of this pollen is used in the reproductive cycle of plants (Moore & Webb, 1978). This in turn means that the excess pollen that is not appropriated by the plant falls to the ground and accumulates on the soil or water surfaces (Moore & Webb, 1978). Due to natural weathering cycles this pollen becomes buried and due to the resistant nature of the pollen, is preserved for millions of years under the right conditions. Pollen and spores can be an important environmental proxy, as they represent both the environment and nature of the plants they originate from. Chemical preparation enables the pollen to be separated from the rock matrix in which it was deposited and studied under microscopy. Species identifications and counting facilitate comparisons of palynological assemblages from different areas, allowing for biostratigraphic correlation of units.

In this study, the palynology of the Sanangoé-Mefidezi Basin will be researched and used to correlate the Tete Province, Mozambique strata with other coal bearing deposits in Gondwana. A relative age will be given to the coals of the Sanangoé-Mefidezi Basin based on the vegetation and correlations

established. The palynology will help determine the local and regional environments of Mozambique in Permian times as well as determine if the same or similar climate and vegetation existed in other parts of Gondwana.

1.5. Objectives

The main objectives of this study are to:

1. Identify all productive samples for palynomorphs (both pollen and spores);

2. Correlate with other coal seams and palynofloral assemblages in Gondwana and correlate with other Mozambican coal basins;

3. Assign a relative age to the Sanangoé-Mefidezi coals based on correlation;

4. Reconstruct the palaeoenvironment in which the coals were deposited;

5. Determine the thermal maturity of the coals.

1.6. Hypothesis

The palynofloras of the Sanangoé-Mefidezi Basin will correlate with other Permian coal sequences in Gondwana, particularly the Tete Province coals in Mozambique, and through these palynological correlations, allow a more precise age assignment for the Sanangoé-Mefidezi coal strata.

2. Geological Background and Literature Review

2.1.1. Geological Background

The Karoo Basins in south central Africa reflects a time when Pangaea rifted to form Laurasia and Gondwana during the late Palaeozoic–early Mesozoic (Catuneanu *et al.*, 2005). The areal extent of the basin is approximately 550,000 square kilometres and is a foreland basin forming an asymmetrical cross section (Cadle *et al.,* 1993). All of the economically important coal bearing strata in the main Karoo Basin of South Africa are Permian in age (Cairncross, 2004). Changes in tectonic and climatic conditions are the main factors in variations in coal horizons of Karoo Basin sediments (Catuneanu *et al.*, 2005). The Karoo Supergroup was deposited from the Carboniferous to Jurassic and comprises four groups, namely the Dwyka, Ecca, Beaufort and Stormberg groups (Smith, 1990). The upper Stormberg Group is capped with volcanic eruptions which formed the Drakensberg and Lebombo groups (Johnson, 1996) and terminated Karoo sedimentation.

The Ecca Group is of the most importance economically as it comprises the main coal bearing strata of the Karoo Supergroup and was deposited in marine and fluviodeltaic environments (Johnson, 1996). There are three formations, namely the Pietermaritzburg Formation (oldest), the Vryheid Formation (most important for coal) and the Volksrust Formation (youngest). The Vryheid Formation hosts most of South Africa's mined coal strata (Cairncross, 2001). Coal seams were formed by dense plant matter (dominated by *Glossopteris*) accumulating in swamps and forming layers of peat, which were subjected to increased pressure and temperature from overlying sediments during phases of subsidence (Falcon, 1989).

2.1.2. Mozambique basins

The Mozambique sedimentary basins were formed by two continental break-up phases (passive continental margins), the first of which was from the late Palaeozoic to the early-mid Jurassic, and related to the break-up of early

Gondwana (Cilek, 1989). The second break-up was associated with the separation of Madagascar and took place from the early-mid Jurassic to the mid-Cretaceous (Cilek, 1989). The extensional stresses applied to the continental masses caused the basins to sag at continental margins while the interior of the continents formed fracture basins (Cilek, 1989).

2.1.3. Background

The history of mining in Mozambique began in the early 1900's on a small scale commercial level but in 2004 the right to develop was won by an international company (Vale) which allowed for investments into the Tete Province coalfields (Hancox, 2016). This lead to the expansion of exploration and growth of mining in the coalfields (Hancox, 2016). As of 2015, three collieries are operating namely Moatize, Benga Mine (both are in the Moatize-Benga coalfield) and Chirodzi Mine (in the Sanangoé-Mefidezi coalfield) (Hancox, 2016).

2.1.4. Geology

The Tete Province of western Mozambique forms part of the mid-Zambezi Valley coal deposits, and the main coal bearing formations were deposited in an east-west trending tectonically controlled basin (Hancox, 2016). This basin extends from the west Lake Cahora Bassa to the Malawi border in the east (Hancox, 2016). The geology is controlled by the Zambezi rift which follows the underlying Sanangoe Shear Zone in the Precambrian basement (Lachelt, 2004).

The Karoo aged basin in Mozambique is situated in a number of graben to half graben-type basins (Catuneanu *et al.,* 2005). These basins were thought to have been once connected, but due to the Jurassic and Cretaceous extensional tectonics (rifts created from vertical crustal movements due to the break-up of Gondwana) and associated erosion, are now separate basins (Hancox, 2016; Catuneanu *et al.,* 2005). Five sub-basins currently exist namely the Chicoa-Mecucoe, Sanangoe-Mefidezi, Moatize, Muarazi and Minjova sub-basins (Vasconcelos, 2013; Hancox, 2016). The coal seams in Mozambique are mostly

inclined due to the former extensional and structural processes (Hancox, 2016). The rifting that occurred during the Jurassic allowed for a number of dolerite dykes to intrude the surrounding rock (Hancox, 2016). These dykes have therefore altered some of the coal grades (low volatile lean bituminous or semi-anthracitic coal) due to the excess heat (Hancox, 2016).

The Mozambique basins have a similar generalised stratigraphy to the main Karoo Basin of South Africa, with the Tete Province containing glacial origin deposits at the base (Vasconcelos, 2009). This is followed by fluvio-lacustrine clastic sediment formations (Vasconcelos, 2009), similar to the Dwyka and Ecca groups in South Africa. These groups are named both formally and informally (by mining companies) and are (in ascending stratigraphic order) the Vúzi Formation (comprising the "Tillite Series and "Platform Facies"), the Moatize Formation ("Productive Series"), the Matinde Formation and the Cadzi Formation (Hancox, 2016). These sedimentary sequences overlie the Precambrian rocks of mainly the Tete Suite (predominantly gabbro and associate anorthosites of Mesoproterozoic age) unconformably (Hancox, 2016; Meyer, 2009).

2.1.5. Vúzi Formation

The Vúzi Formation is the lowermost unit of the Karoo Supergroup in Mozambique and indicates the start of Karoo sedimentation (Vasconcelos, 2009). The rocks are mostly glacial tillites, interbedded sandstones (occasionally conglomeratic), thin siltstones and mudstone beds with smaller thin coal seams (GTK Consortium, 2006). This group is considered to be the equivalent of the Dwyka Group in the Karoo Supergroup, South Africa and therefore dated as late Carboniferous to early Permian (GTK Consortium, 2006). The deposition of these glacial and periglacial sediments varies in thickness across the basin due to the constrained palaeovalleys and associated weathering (Hancox, 2014). Above the Vúzi Formation is a thin 100m thick succession informally termed the "Platform Facies" (Hancox, 2014). These facies comprise diamictites with angular basement clasts, coarse grained sandstone, conglomerates and thin coal seams (Hancox, 2014). This sedimentary succession is an upward fining sequence reflecting the

gradual change from glacial deposition to swamp environments (Lakshminarayana, 2015). The Vúzi Formation coals are intermittent and of low quality (Hancox, 2016).

2.1.6. Moatize Formation

The Moatize Formation unconformably overlies the Proterozic basement rocks or the Vúzi Formation and is of the most importance economically as it contains six coal seams (Hancox, 2016). The main coal seams in the Moatize Formation are named from oldest to youngest as follows: the Souza Pinto, Chipanga, Bananeiras, Intermèdia, Grande Falèsia and Andre seams (Meyer, 2009). This formation is Cisuralian to Guadalupian in age and is equivalent to the Ecca Group of the main Karoo Basin (Vasconcelos, 2009). This sequence was deposited in a lacustrine, marginal swamp environment and comprises mostly mudstone, carbonaceous mudstone, sandstones, carbonaceous sandstones and coal (Meyer, 2009). The coal seams are classified into two types namely those which are hosted in thick carbonaceous mudstones and siltstones (Souza Pinto, Chipanga seams) and those bounded both above and below by sandstones (Intermèdia, Grande Falèsia and Andre seams) (Hancox, 2016). The seams vary in thickness and comprise mainly interbedded coal and carbonaceous mudstones with portions of thicker siltstone (Hancox, 2016). The coal found in the Moatize Formation is bright in apperence with duller bands due to the high quantity of vitrinite (Hancox, 2016).

2.1.7. Matinde Formation

The Matinde Formation disconformably overlies the Moatize Formation and is considered to be Guadalupian to Lopingian (Vasconcelos *et al.,* 2014). This is the uppermost unit of the Karoo Supergroup within the Moatize sub-basin and comprises coarse cross-stratified sandstone, siltstone and mudstone as well as a number of coal seams (Hancox, 2016). This formation was deposited in a fluvial environment with a wet temperate to hot arid climate (Vasconcelos *et al.,* 2014; Hancox, 2016). The same occurs with the Matinde Formation as with the Moatize

Formation, in which the coal seams are divided in two groups, namely those which are hosted by thick carbonaceous mudstones and siltstones (upper portion of the formation) and those bounded by sandstones (lower portion of the formation) (Lloyd, 2015; Hancox, 2016).

2.1.8. Cadzi Formation

The Cadzi Formation overlies the Matinde Formation and is Lopingian to early Triassic (Fernandes *et al.,* 2015). This formation is considered to be the equivalent of the Beaufort Group in the main Karoo Basin and comprises mainly arkosic sandstone (Fernandes *et al.,* 2015). The Cadzi Formation was deposited in hot and dry phases of fluvial and lacustrine environments (GTK Consortium, 2006).

Borehole logs displaying the lithostratigraphy from the core used in this study can be found in Appendix A.

2.1.9. Study Area

The study area for this research is located within the Sanangoé-Mefidezi Basin in the Tete Province, Mozambique (Figure 2.1). The majority of Mozambique's coal bearing strata are found in the mid-Zambezi Valley and are of Permian age, like those of South Africa (Cairncross, 2001). A high concentration of coal bearing deposits is found in the Productive Series (Moatize Formation) containing six coal zones (Ecca Group equivalent) (Lächelt, 2004). The Sanangoé-Mefidezi Basin was formed from Permian–Jurassic volcano-sedimentary fills related to extensional tectonics from the break-up of Gondwana (Pereira *et al.*, 2016). The Sanangoé-Mefidezi Basin is currently being mined via the Chirodzi Mine (Hancox, 2016). The core samples used in this research comes from three boreholes drilled for exploration in relation to the mining operations in the Sanangoé-Mefidezi Basin.

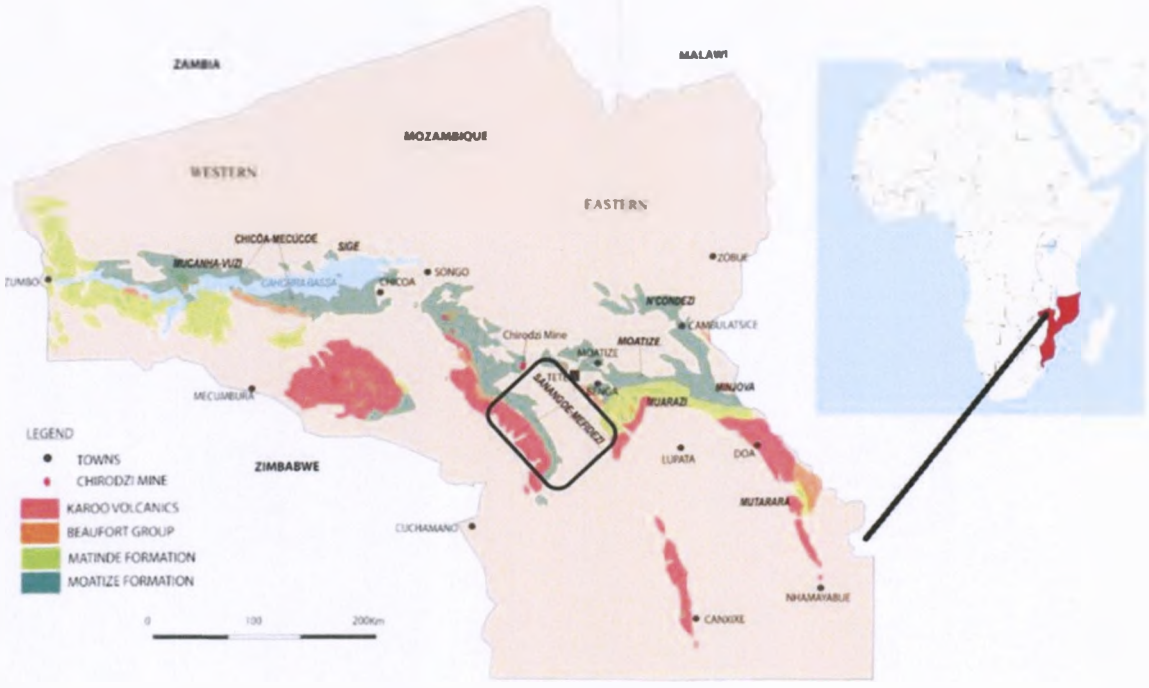

Figure 2.1: Map of Tete Province, Mozambique highlighting the basins and lithology including the study area (outlined in black box). A map showing location of the Tete Province in relation to Africa is highlighted in red. The lithological units displayed in the legend are in chronological order with the oldest unit at the bottom (adapted from Hancox *et al.*, 2016).

2.2. Literature Review

During Permian times glossopterids dominated the flora of almost all Gondwanan continents between 40° and 90° palaeoaltitude (McLoughlin, 2001), but a number of intra-Gondwanan floristic provinces are identifiable (Truswell, 1981).

Palynomorph assemblages show differences in regional composition from the same deposits, showing regional and provincial floral changes occurred (Barbolini *et al.*, 2016c).

For this study, only Gondwanan palynofloras between the palaeolatitudes 40° and 90° are reviewed as these localities form part of the Gondwanan floristic province and are most comparable for correlation with Permian coal seams of Karoo age (Figure 2.2). The Gondwanan palynofloras will be correlated to the palynoflora of the Sanangoé-Mefidezi Basin. The parts of Gondwana that will be examined are south-central Africa, Madagascar, India, Australia, Antarctica and South America.

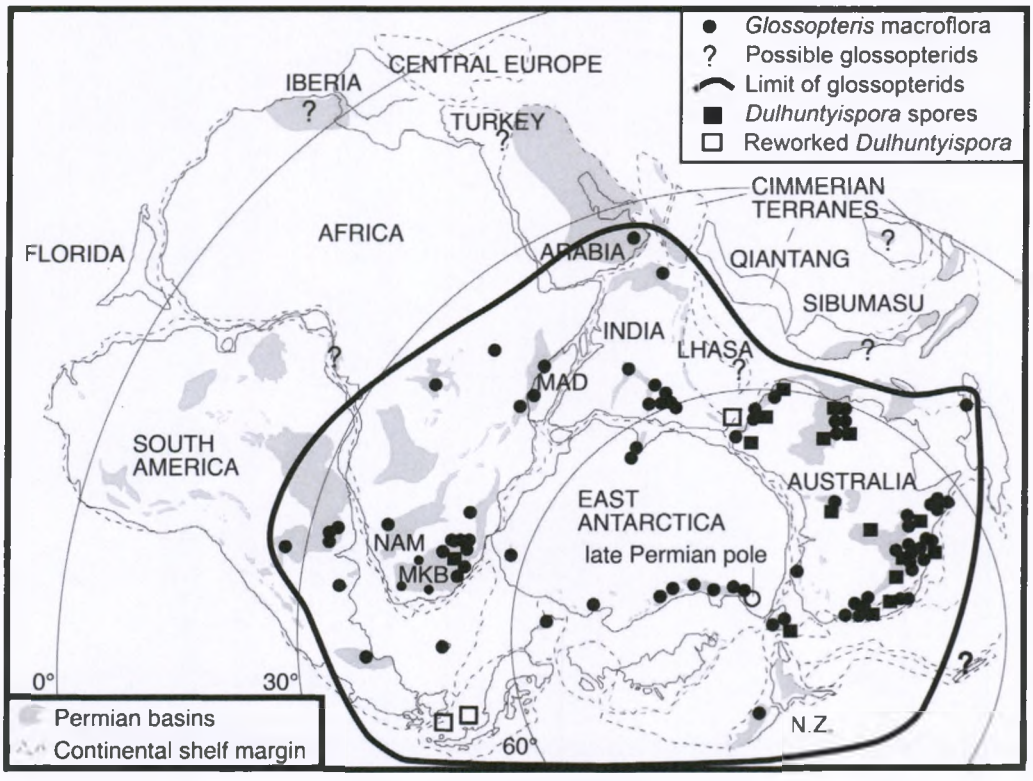

Figure 2.2: Map of Gondwana during the Permian showing the Gondwanan Floristic Kingdom between 40° and 90° (from Barbolini *et al.*, 2016c, modified from McLoughlin (2001, 2011)).

2.2.1. Africa

2.2.1.1. South Africa

Anderson (1977) erected a palynozonation scheme for the Karoo Basin and divided the Dwyka, Ecca and Beaufort groups into seven biozones according to the palynomorphs present. Zone 1 which represents the Dwyka Group plus the

Pietermaritzburg Formation of the Ecca Group has a low abundance and diversity of palynomorphs (Anderson, 1977; Barbolini, 2014).

Zone 2 represents the Pietermaritzburg and Vryheid formations (lower Ecca Group) and can be subdivided into four palynofloral zones namely subzones a to d (Anderson, 1977; Barbolini, 2014). Each subzone is dominated by different species. Subzone 2a is dominated by *Gondisporites punctatus* and *Gondisporites parvus* (Anderson, 1977). Subzone 2b is dominated by *Cirrabaculisporites plumsteadiae* and subzone 2c by *Gondisporites braziliensis* and *G. raniganjensis* (Anderson, 1977). Subzone 2d is dominated by *Pityosporites* (Anderson, 1977).

Zone 3 encompasses the Vryheid Formation (middle Ecca Group) is more abundant in palynomorphs when compared to zones 1 and 2. Spores are almost completely absent (Anderson, 1977). Zone 3 is divided into four palynofloral zones. Subzone 3a and b are dominated by *Granulatisporites austroamericanus*. Subzone 3b is distinguished by the appearance of *Gnetaceaepollenites*. Subzone 3c has a very diverse palynoflora and a number of species are present including the pollen genera *Vestigisporites, Vittatina, Pityosporites*, and *Lueckisporites* (Table 1.1). Subzone 3d includes the distinguishing species *Lueckisporites asulcus, Lueckisporites nyakapendensis* and *Protohaploxypinus goraiensis.*

Zone 4, spanning the Volksrust Formation (upper Ecca Group) shows a decrease in palynofloral diversity but five palynofloral subzones can be described. Subzone 4a is dominated by abundant *Gondisporites punctatus.* Subzone 4b is defined by the presence of *Granulatisporites trisinus*, *G. micronodosus, Polypodiisporites detritus* and *Weylandites lucifer*. Subzone 4c is defined by the abundance of *Lueckisporites asulcus* and *L. nyakapendensis*. Subzone 4d shows a number of new species initiating such as five species of *Granulatisporites*. Subzone 4e is similar to Zone 4c being dominated by *Lueckisporites asulcus* and *L. nyakapendensis*.

Zones 5 shows a decrease in palynofloral diversity and represents the Normandien Formation (Beaufort Group). Five palynofloral subzones can be defined. Subzone 5a shows a dominance of *Pityosporites maximus, Lueckisporites asulcus* and *L. nyakapendensis*. Subzone 5b is dominated by the above-mentioned taxa as well as

Weylandites lucifer. Subzone 5c is dominated primarily by *Weylandites lucifer* and *Scheuringipollenites maximus*. Subzone d is defined by the dominance of *Weylandites lucifer* and Subzone 5e by *Weylandites magmus*.

Zones 6 and 7 shows a steady decrease in palynofloral diversity and have similar palynomorph content (Table 2.1). Zone 6 is dominated by *Protohaploxypinus limpidus* and *P. micros* and Zone 7 is dominated by *Protohaploxypinus amplus*.

Table 2.1: Characteristic palynomorphs from the northern Karoo Basin, adapted by Barbolini (2014) after Anderson (1977).

Current stratigraphy (SACS, 1980)	**Original stratigraphy by Anderson (1977)**	**Reference Area**	**Zones**	**Characteristic Species (More commonly used names)**
Upper Balfour / Normandien Fm	*Daptocephalus* Zone (Beaufort Group)	Tetrapod- and macroflora - bearing floodplain deposits near Bergville / Harrismith	7	*Inaperturosporites inapertus* *Apiculatisporis bulliensis (Brevitriletes bulliensis)* *Apiculatisporis cornutus* *Weylandites lucifer (Vittatina lucifera)* *Alisporites ovatus (Pityosporites ovatus)* *Protohaploxypinus goraiensis (Pityosporites goraiensis)* *Protohaploxypinus amplus (Pityosporites amplus)* *Protohaploxypinus limpidus / P. micros (Pityosporites micros)*
Middleton & Lower Balfour formations	*Cistecephalus* Zone (Beaufort Group)	Tetrapod-bearing floodplain deposits near Graaff-Reinet	6	
Normandien Fm	*Tapinocephalus* Zone equivalent (Beaufort Group)	Near shore fluvial and fluvio-deltaic deposits from Welkom / Virginia	5	*Cyclogranisporites bharadwaji* *Weylandites lucifer (Vittatina lucifera)* *Weylandites magmus (Vittatina magma)* *Vittatina africana (Vittatina densa)* *Alisporites potoniei / Scheuringipollenites maximus (Pityosporites maximus)* *Lueckisporites asulcus*

				Lueckisporites nyakapendensis *Lueckisporites neohannonicus*
Volksrust Fm	upper Ecca	Delta front and shelf deposits from Welkom / Virginia	4	*Gondisporites punctatus* *Gondisporites parvus* *Gondisporites braziliensis* *Gondisporites variabilis* *Gondisporites splendens (Indotriradites splendens)* *Microbaculispora labyrinthica* *Deltoidospora directa (Microbaculispora directa)* *Microbaculispora finegranulata* *Microbaculispora mediogranulata* *Granulatisporites micronodosus (Microbaculispora micronodosa)* *Granulatisporites trisinus (Microbaculispora trisina)* *Microbaculispora gondwanensis* *Microbaculispora villosa* *Didecitriletes ericianus (Microbaculispora ericiana)* ~~*Dulhuntyispora dulhuntyi*~~ - actually *Dulhuntyispora granulata* (Backhouse, 1991) *Polypodiisporites detritus* *Weylandites lucifer (Vittatina lucifera)* *Lueckisporites asulcus* *Lueckisporites nyakapendensis* *Guttulapollenites hannonicus (Lueckisporites hannonicus)* *Lueckisporites neohannonicus*
Vryheid Fm	middle Ecca	Coals from Greylingstad / Bethal / Hendrina	3	*Mehlisphaeridium parvum* *Mehlisphaeridium fibratum* *Granulatisporites austroamericanus (Microbaculispora tentula)* *Granulatisporites trisinus (Microbaculispora trisina)* *Microbaculispora gondwanensis* *Converrucosisporites irregularis (Microbaculispora irregularis)* *Microbaculispora capilliformis* *(?Diatomozonotriletes townrowii)* *Apiculatisporis diversiformis*

				Apiculatisporis levis *Apiculatisporis bulliensis (Brevitriletes bulliensis)* *Apiculatisporis cornutus* *Vestigisporites rudis* *Vittatina nonsaccata* *Vittatina simplex* *Pityosporites levis* *Pityosporites fusus* *Protohaploxypinus goraiensis (Pityosporites goraiensis)* *Lueckisporites asulcus* *Lueckisporites nyakapendensis* *Lueckisporites welkomensis* *Guttulapollenites hannonicus (Lueckisporites hannonicus)* *Gnetaceaepollenites sinuosus* *Gnetaceaepollenites ovatus* *Gnetaceaepollenites bulbiger*
Vryheid Fm, Pietermaritzburg Fm	lower Ecca	Ladybrand borehole, Welkom / Virginia, Sasolburg	2	*Mehlisphaeridium irregulare* *Maculatasporites indicus* *Pilasporites calculus* *Pilasporites scissus* *Zinjisporites spinosus* *Gondisporites punctatus* *Gondisporites parvus* *Gondisporites raniganjensis* *Gondisporites braziliensis* *Concavisporites mortonii* (*Acanthotriletes* - laevigate form) *Horriditriletes ramosus* (*Acanthotriletes* - baculate form) *Granulatisporites microgranifer* (*Acanthotriletes* - granulate form) *Acanthotriletes tereteangulatus* (*Acanthotriletes* - spinate form) *Didecitriletes horridus (Microbaculispora eoericiana)* *Cirrabaculisporites plumsteadiae (Microbaculispora plumsteadi)* *Cirrabaculisporites lageniformis / Eccaspora plumsteadi (Microbaculispora lageniformis)* *Microbaculispora paramicronodosa*

				Pachytriletes densus *Apiculatisporis diversiformis* *Divaricrassus minor (Apiculatisporis minor)* *Apiculatisporis major (Apiculatisporis parmatus)* *Apiculatisporis levis* *Apiculatisporis bulliensis (Brevitriletes bulliensis)* *Apiculatisporis cornutus* *Polypodiisporites detritus* *Striatoabieites multistriatus (Vittatina multistriata)* *Weylandites lucifer (Vittatina lucifera)* *Marsupipollenites triradiatus (Vittatina triradiata)* *Pityosporites triassicus* *Alisporites tenuicorpus (Pityosporites tenuicorpus)* *Alisporites ovatus (Pityosporites ovatus)* *Alisporites potoniei / Scheuringipollenites maximus (Pityosporites maximus)* *Striatopodocarpites fusus (Pityosporites cancellatus)* *Protohaploxypinus amplus (Pityosporites amplus)* *Protohaploxypinus limpidus / P. micros (Pityosporites micros)* *Cycadopites cymbatus*
Pietermaritzburg Fm, Dwyka Group	Upper Dwyka Shales Dwyka Tillite	Glacial sequence of Welkom / Virginia	1	*Zinjisporites spinosus* *Granulatisporites austroamericanus (Microbaculispora tentula)* *Pachytriletes densus* *Punctatisporites gretensis* *Vestigisporites balmei* *Plicatipollenites gondwanensis (Vestigisporites gondwanensis)* *Cycadopites cymbatus*

Aitken (1993, 1994, 1998) and Falcon (1988, 1989) all worked on the Ecca Group (Vryheid Formation) in the Witbank/Highveld coalfield region. Aitken (1994)

focused on the No. 5 seam. The No. 5 seam showed evidence of being formed in a peat swamp and is dominated by striate pollen (Aitken, 1994). Correlation with Biozone F of MacRae (1988) was possible and an age of Aktastinian to Baigendzinian was determined for the No. 5 seam (Aitken, 1994). Aitken (1998) proposed ten palynofloral biozones for the Karoo Supergroup integrating previous work by MacRae (1988). Falcon (1988, 1989) focused mainly on the No. 2 seam in the Witbank/Highveld coalfield and assigned it an early Permian age (Falcon, 1989).

Aitken (1998) defined concurrent range zones based on the overlapping of two palynomorph taxa however a number of these taxa are seen to extend further than these range zones and are therefore actually abundance zone (Murphy & Salvador, 1999; Barbolini, 2014). For example, the species *Protohaploxypinus limpidus* extends throughout Biozones III – IX (Table 2.2). Falcon (1988, 1999) examined the No. 2 seam from the Witbank coalfield, Vryheid Formation. This seam was assigned an early Permian age and taxa from the Dwyka and Ecca groups were described.

Table 2.2: Concurrent Range Zones defined by Aitken (1998) for the Ecca and Beaufort groups redrawn by Barbolini (2014). Underlined taxa are distinctive species.

Lithology		**Biozone**	**Concurrent Range Zone**	**Characteristic Species**
Beaufort Group	Estcourt Formation	**X**	*Aratrisporites -Calamospora plicata*	*Aratrisporites* sp. *Calamospora tener* *Falcisporites stabilis*
		IX	*Ephidripites -Cycadopites*	*Ephidripites* sp. *Cirratriradites* sp. *Cycadopites follicularis* *Cycadopites nevesi*
		VIII	*Osmundacidites senectus-Alisporites potoniei*	*Osmundacidites senectus* *Alisporites potoniei* *Vitreisporites pallidus*
Ecca Group	Volksrust Formation			*Falcisporites stabilis* *Osmundacidites wellmanii* *Calamospora tener*

				Thymospora pseudothiessenii
		VII	*Protohaploxypinus limpidus-Lunatisporites pellucidus*	*Protohaploxypinus limpidus* *Lunatisporites pellucidus* *Protohaploxypinus amplus* *Lunatisporites* sp. *Tetraporina tetragona* *Lueckisporites* sp. *Chordecystia sp.* *Peltacystia venosa*
		VI	*Guttulapollenites hannonicus-Protohaploxypinus rugatus*	*Guttulapollenites hannonicus* *Protohaploxypinus rugatus* *Kraeuselisporites enormis* *Haplocystia pellucida* *Sporocystia eraducia* *Weylandites magmus* *Chordasporites australiensis*
	Vryheid Formation	**V**	*Lueckisporites virkkiae-Corisaccites alutas*	*Lueckisporites virkkiae* *Corisaccites alutas* *Protohaploxypinus limpidus* *Protohaploxypinus amplus* *Alisporites potoniei* *Granulatisporites trisinus* *Lunatisporites* sp. *Bascanisporites undosus* *Protohaploxypinus rugatus* *Guttulapollenites hannonicus*
		IVB	*Striatopodocarpites fusus-Weylandites lucifer*	*Striatopodocarpites fusus* *Weylandites lucifer* *Gnetaceaepollenites sinuosus* *Striatopodocarpites cancellatus* *Striatopodocarpites fusus* *Striatopodocarpites gondwanensis* *Protohaploxypinus amplus* *Protohaploxypinus goraiensis* *Protohaploxypinus diagonalis* *Protohaploxypinus limpidus*
		IVA	*Granulatisporites trisinus* Interval Zone	No distinctive taxa *Granulatisporites trisinus*
		III	*Striatopodocarpites cancellatus -Marsupipollenites triradiatus*	*Striatopodocarpites cancellatus*

				Marsupipollenites triradiatus *Alisporites potoniei* *Kraeuselisporites enormis* *Gnetaceaepollenites sinuosus* *Concavisporites mortonii* *Interradispora versus*
		II	*Mehlisphaeridium colliensis-Alisporites splendens*	*Mehlisphaeridium colliensis* *Alisporites splendens* *Deltoidospora directa* *Laevigatosporites vulgaris* *Florinites eremus*
		I	*Potonieisporites novicus-Cannanoropollis densus*	*Potonieisporites novicus* *Cannanoropollis densus* *Limitisporites monstruosus* *Lophotriletes novicus* *Acanthotriletes tereteangulatus* *Cannanoropollis mehtae* *Cannanoropollis obscurus* *Deltoidospora directa* *Granulatisporites papillosus* *Punctatisporites gretensis*

MacRae (1988) studied the Waterberg and Soutpansberg-Pafuri coal bearing basins and the palynology of two fossil plant slabs from Hammanskraal in the Springbok Flats Basin. Six biozones were erected (Biozone A–F). Notable floral changes are seen between Biozone A and B and the Carboniferous–Permian boundary was placed between the two biozones (MacRae, 1988). The palynomorphs of Biozone A reflect a cold climate with an abundance of monosaccates and triletes. Biozone B still has monosaccates and triletes present but shows an increase in aletes attributable to *Botryococcus* which suggests an increase in the water table due to deglaciation. Biozone C contains monosacates as dominant with triletes still being abundant indicating that a cold climate remained. Biozone D shows a distinct shift as monosaccates and triletes start to decrease and an increase in non-striate and striate bisaccate pollen is observed. This indicates warming of the climate. Biozone E shows similar amounts of non-striate and striate bisaccate pollen with a concomitant

decrease in monosaccates and an increase in zonotriletes. This biozone reflects a wetter environmental incursion. Bizone F is very similar to Biozone E, only being distinguished by a few new species initiations (MacRae, 1988). The age of the Hammanskraal locality is suggested to be Ufimian to lower Kazanian in age (MacRae, 1988). Figure 2.3 shows each biozone and their distinguishing species.

Zone	Name	Key Palynomorphs	Ellisras Basin	Tshipise Basin
F	*Striatopodocarpites fusus* – *Weylandites lucifer*	*Weylandites lucifer* *Gnetaceaepollenites sinuosus* *Striatopodocarpites fusus*		Mikambeni Formation
E	*Kraeuselisporites enormis* - *Striatopodocarpites cancellatus*	*Cirratriradites africanensis* *Kraeuselisporites enormis* *Alisporites potonieï* *Protohaploxypinus limpidus* *Striatopodocarpites cancellatus*	Grootgeluk Formation	
D	*Laevigatosporites vulgaris* – *Alisporites* sp. 1	*Deltoidospora directa* *Laevigatosporites vulgaris* *Alisporites* sp. 1 *Platysaccus radialis*	Enkelbult Formation	Madzaringwe Formation
C	*Cyclogranisporites gondwanensis* Interval Zone	No indicator taxa as Biozone C is an informal zone		Basement
B	*Potonieisporites novicus* – *Cannanoropollis densus*	*Verrucosisporites* sp. *Limitisporites monstruosus* *Cannanoropollis densus* *Potonieisporites novicus* *Cahenisaccites ovatus*	Wellington Formation	
A	*Plicatipollenites gondwanensis* – *Granulatisporites papillosus*	*Granulatisporites papillosus* *Plicatipollenites goraiensis* *Pteruchipollenites gracilis* *Cannanoropollis mehtae* *Cannanoropollis janakii*	Duvka Formation Basement	

Figure 2.3: Biozones and lithostratigraphy of the Ellisras and Tshipise basins (after Barbolini, 2014 redrawn from MacRae, 1988).

Barbolini (2014) examined the palynology of the Carboniferous–Jurassic Karoo Supergroup and correlated the vertebrate biozones of the main Karoo Basin using palynology. An abundance of monosaccate and bisaccate pollen was observed in the Vryheid, Volksrust, Normandien and Clarens formations (Barbolini, 2014). The palynofloral assemblages from South Africa could be correlated with those from Australia, New Zealand, Antarctica, South America and other parts of Africa (Barbolini, 2014).

2.2.1.2. Mozambique

Falcon *et al.* (1984) looked at the petrology and palynology of the Mucanha-Vúzi Basin in Mozambique. Only the coal seams were looked at and demonstrated a woody water-logged environment at the base of the seam, changing to a mangrove environment within the seam and ending in a peat swamp at the top of the coal seam. Falcon *et al.* (1984) studied two boreholes from the western Tete Province and designated three sub-assemblages. These are named the *Sulcatisporites Protohaploxypinus* Sub-Assemblage, *Protohaploxypinus-Vittatina-Striatopodocarpites* Sub-Assemblage, and *Protohaploxypinus-Vittatina-Guttulapollenites-Lueckisporites* Sub-Assemblage, after the distinctive species in each zone (Falcon *et al.*, 1984). An age of Guadalupian–Lopingian was assigned for the assemblages from the western Tete Province (Falcon *et al.*, 1984).

Pereira *et al.* (2016) studied the Moatize-Minjova Basin in Mozambique and identified two palynoassemblages for the Matinde Formation, one of which was assigned a late Permian age, and the younger, an early Triassic age. A significant palynofloral turnover can be seen from the older to the younger assemblage, and the palynofloras can be correlated with assemblages in Madagascar (Pereira *et al.*, 2016). A dominance of glossopterid pollen is noted from this assemblage. The dominant species are *Kraeuselisporites* sp. and *Lueckisporites virkkiae, Guttulapollenites hannonicus* and *Weylandites lucifer* (associated with conifers and pteridosperms). These palynomorph assemblages are most closely correlated with those from Madagascar, India and Pakistan.

Götz *et al.* (2017) examined the Permian climate of the Moatize Basin in Mozambique using the palynomorph assemblages. These palynomorph assemblages are from the eastern Tete Province and are seen to be younger than the samples in the western Tete Province (Götz *et al.*, 2017). The lowermost seam is named subzone H and is correlated with the *Protohaploxypinus-Vittatina-Guttulapollenites-Lueckisporites* Sub-Assemblage of Falcon et al. (1984). The uppermost seam is named subzone H^1 which represents the *Protohaploxypinus* Sub-Assemblage. This sub-assemblage can be correlated with the *Lueckisporites virkkiae* Interval Zone of the Brazilian Paraná Basin. Therefore, an age of Guadalupian–Lopingian is assigned for the entire section. This study can also be correlated with the Moatize Basin palynomorph assemblages from Pereira *et al.* (2016) which were said to be Lopingian in age.

2.2.1.3. Botswana

MacRae (1978) examined samples from north-east Botswana and erected three concurrent range zones (Figure 2.4). Concurrent Range Zone I was dominated by monosaccate pollen, Concurrent Range Zone II is abundant in bisaccates and Concurrent Range Zone III is dominated by bisaccate striate palynomorphs. Key *et al.* (1998) studied samples from south-west Botswana and assigned the palynomorphs a Carboniferous–Permian in age. Interestingly no coal seams were found in this region of Botswana (Key *et al.*, 1998). This area can be correlated with the northern Karoo Basin zones 1 to 3 of Anderson (1977).

Concurrent Range Zone I	Concurrent Range Zone II	Concurrent Range Zone III
SPECIES RANGE INITIATION: Lower limit of species range not defined in core $N1/_3$.	*A. tereteangulatus* *P. rotundus* *Apiculatisporites sp.* *Punctatosporites sp.* *T. pseudothiessenii* *Lophotriletes sp. A* *G. parviverrucosus* *C. parvus* *S. cancellatus* *P. leschiki* *S. rarus* *P. limpidus* *S. fusus* *Fimbriaesporites sp.* *P. micros* *S. splendens* *F. fimbriatus* *A. plicatus* *S. communis*	No new species — Upper limit of concurrent range zone III not defined in core $N1/_3$.
SPECIES RANGE TERMINATION: *N. ramosus* *C. ornatus* *P. gretensis* *C. splendens* *Densosporites sp.* *Z. restricta* *Z. bullatus* *G. vrystaatensis* *P. indicus* *P. distinctus* *V. radiatus* *V. obscurus* *V. densus* *C. ovatus* *E. elilaensis* *V. mehtae* *C. flavatus* *V. minima*	*D. directa* *M. tentula* *Apiculatisporites sp.* *P. calculus* *C. plicata* *Lophotriletes sp. A* *N. congoensis* *Punctatisporites sp.* *S. cancellatus* *P. leschiki* *V. sp. cf. V. trisecatus* *Tetraporina sp.* *S. fusus* *Fimbriaesporites sp.* *Q. horridus* *Z. eccensis* *T. thiessenii* *S. communis*	*P. novicus* *P. micros*
RESTRICTED SPECIES: *N. ramosus* *C. ornatus* *P. gretensis* *C. splendens* *Densosporites sp.* *Z. restricta* *Z. bullatus* *G. vrystaatensis* *P. indicus* *P. distinctus* *V. radiatus* *V. obscurus* *V. densus* *C. ovatus* *E. elilaensis* *V. mehtae* *C. flavatus* *V. minima*	*Apiculatisporites sp.* *Lophotriletes sp. A* *S. cancellatus* *P. leschiki* *S. fusus* *Fimbriaesporites sp.* *S. communis*	No restricted species
QUANTITATIVE CONTENT: (Supra-generic) Aletes : 20–40% Triletes : 20–35% Monosaccates : 20–30% Disacciatrileti : 0–15% Striatiti : 0–10% Plicati : 0–10% Monoletes : 0– 5% Zonotriletes : 0– 5%	Triletes : 40–70% Aletes : 20–70% Monoletes : 5–30% Disacciatrileti : 5–35% Striatiti : 5–30% Monosaccates : 0–10% Plicati : 0– 5%	Triletes : 20–55% Striatiti : 20–50% Aletes : 20–30% Disacciatrileti : 15–20% Plicati : 0–20% Monoletes : 0– 5%

Figure 2.4: Concurrent Range Zones I, II and III of north-eastern Botswana (MacRae, 1978).

Stephenson and McLean (1999) studied an assemblage from Morupule in south-east Botswana in the Kalahari Basin. Pollen found in the carbonaceous mudstones of this area were dominated by gymnosperm bisaccates, while small triletes dominated the coals. Some of the defining taxa are *Verrucosisporites pseudoreticulatus, Procoronaspora spinosa, Laevigatosporites colliensis, Striatopodocarpites cancellatus*, and *Granulatisporites micronodosus*. The Morupule assemblages correlate with the northern Karoo assemblages as well as those from the mid-Zambezi Basin, and an Aktastinian age was assigned for these rocks based on correlation with the Australian assemblages (Stephenson and McLean, 1999).

Barbolini (2010) and Barbolini and Bamford (2014) studied the palynology of a coal seam in the Mmamantswe region of Botswana. The assemblage was dominated by trilete and alete spores reflecting a floral assemblage of lower order lycopods, sphenophytes and ferns (Barbolini and Bamford, 2014). Distinctive taxa recovered from this study are *Brevitriletes levis, Cannanoropollis densus, Gondisporites raniganjensis, Platysaccus radialis, Scheuringipollenites ovatus* and *Verrucosisporites naumovae*. The palynofloral assemblage was divided into two zones, namely the lower Assemblage Zone 1 which correlates with Assemblage Zone 1, and the upper Assemblage 2 which correlates with Assemblage Zone 2 of Anderson (1977), Biozone C of MacRae (1988) and the No. 2 coal seam of Falcon (1988, 1989). An Asselian to early Artinskian age for the coal seam was determined based on these correlations (Barbolini and Bamford, 2014).

Modie & Le Hérissé (2009) examined palynomorphs assemblage from the Kalahari Karoo Basin of Botswana which comprise spores, pollen, acritarchs and chlorophycean algae. There are three assemblage zones designated the *Hamiapollenites bullaeformis* Biozone, the *Cyclogranisporites gondwanensis* Biozone and the *Platysaccus papilionis-Striatopodocarpites fusus* Biozone. The Kalahari Karoo Basin shows a close correlation with the Paraná Basin of South America. The *Cyclogranisporites gondwanensis* and *Platysaccus papilionis-Striatopodocarpites fusus* biozones correlate with the *Lueckisporites virkkiae*

Interval Zone of Brazil. The ages given for these assemblages are late Carboniferous (Kasimovian–Gzhelian) to late Cisuralian–early Guadalupian.

2.2.1.4. Zambia

Utting (1976) looked at the Luwumbu Formation of the Luangwa Basin in Zambia and two assemblages were recognised. The older assemblage was dominated by monosaccates, and the younger assemblage was dominated by striate and non-striate bisaccates as well as trilete spores (Utting, 1976). Utting (1978) examined the Siankondobo and Gwembe formations in the mid-Zambezi Basin of Zambia, which could be correlated with the Luwumbu Formation of Zambia.

Nyambe and Utting (1997) studied the Madumabisa and Interbedded Sandstone and Mudstone formations in the mid-Zambezi Basin in Zambia. Based on the palynofloras present the Siankondobo Formation was assigned an age of late Carboniferous (Gzhelian) to early Permian (Asselian to early Sakmarian) and is divided into three facies assemblages (Nyambe and Utting, 1997). The palynomorph assemblage of this formation is dominated by monosaccate pollen distinctive of the *Plicatipollenites indicus-Cannanoropollis obscurus* Zone (Utting, 1978; Nyambe and Utting, 1997). The Gwembe Formation overlies the Siankondobo Formation and was assigned an age of early Permian (Artinskian to Kungurian) (Nyambe and Utting, 1997).

The Maamba Sandstone member is at the base and is overlain by the Main Seam, which in turn is overlain by carbonaceous mudstones, silty mudstones, coaly mudstones, coal and siltstones or sandstone units (Nyambe and Utting, 1997). This basal member contains a palynomorph assemblage dominated by trilete spores with smaller amounts of bisaccate pollen (Nyambe and Utting, 1997). The overlying beds of the formation are dominated by trilete spores and bisaccate pollen therefore both the palynomorph assemblages can be allocated to

the *Brevitriletes levis-Scheuringipollenites maximus* Zone of Nyambe and Utting (1997), formerly the *Apiculatisporis levis-Vesicaspora potoniei* (LP) Zone of Utting (1978). This member is dated at Artinskian to Kungurian in age (Nyambe and Utting, 1997).

The Madumabisa Formation comprises mainly non-carbonaceous mudstones said to have been deposited in a lacustrine environment (Nyambe and Utting, 1997). The palynomorph assemblages consist predominantly of taeniate and non-taeniate bisaccate, monosulcate and polyplicate pollen as well as some rare trilete spores and algae (Nyambe and Utting, 1997). The palynomorph assemblage of the Madumabisa Formation can be correlated with the *Cistecephalus* reptile zone of North Luangwa and is said to be Tatarian in age (Nyambe and Utting, 1997).

The Escarpment Grit Formation is the next unconformable overlying formation and comprises mainly coarse grained arenaceous rock types which are unsuitable for palynological analysis (Nyambe and Utting, 1997).

The Interbedded Sandstone and Mudstone unit comprises fining upwards sandstones and mudstones which were deposited by a braided stream transitioning to a meandering stream (Nyambe and Utting, 1997). The palynomorph assemblage is dominated by non-taeniate bisaccate pollen and trilete spores (Nyambe and Utting, 1997). The unit was proposed as early or middle Triassic (late Scythian or Anisian) age (Nyambe and Utting, 1997).

Nyambe and Utting (1997) explained the changes in palynological assemblages from the lower Karoo Siankondobo Formation to the Gwembe Formation as being related to climate, particularly the increased warming of the climate and changes in humidity that occurred subsequent to Dwyka glaciation. This warming continued and the climate became more arid during the deposition of the Madumabisa Formation (Nyambe and Utting, 1997). It is noted that the Escarpment Grit Formation ("Upper Karoo") was not productive for palynomorphs, but other proxies suggest an adequate amount of rainfall existed for large trees to grow (Nyambe and Utting, 1997; Barbolini et al., 2016a). The deposition of the Interbedded Sandstone and Mudstone Formation is said to have

had a varied vegetational environment suggesting a seasonal rainfall existed (Nyambe and Utting, 1997).

System		Stage	Lith. Unit	Palynomorph Zone	Characteristic Taxa	Rock Unit
Triassic	Mid	Anisian	Stormberg	?		
	Early	Scythian		Unnamed	*Blyxosporites* sp., *Falcisporites stabilis*, *Alisporites* sp., *Sulcatisporites* sp., *Platysaccus queenslandi*, *Rimaesporites aquilonis*, *Lunatisporites pellucidus*, *Apiculatisporis* sp., *Calamospora* sp., *Verrucosisporites* sp., *Uvaesporites* sp., *Aratrisporites fischeri*, *Playfordiaspora crenulata* (*Guthoerlisporites cancellosus*)	Interbedded Sandstone and Mudstone Fm
Permian	Late	Tatarian	Beaufort	Unnamed	*Guttulapollenites hannonicus*, *Corisaccites alutas*, *Protohaploxypinus limpidus*, *Protohaploxypinus goraiensis*, *Stratopodocarpites* sp., *Sulcatisporites prolatus*, *Vitrensporites pallidus*, *Reticuloidosporites wirchiatus*, *Polypodisporites mutabilis*, *Weylandites lucifer*, *Botryococcus* sp.	Madumabisa Mudstone Fm
		Kazanian				
		Ufimian				
	Early	Kungurian	Ecca	*Brevitriletes levis* - *Scheuringipollenites maximus*	*Punctatisporites gretensis*, *Deltoidospora directa*, *Cirratriradites africanensis*, *Brevitriletes levis*, *Horriditriletes tiliformis*, *Protohaploxypinus limpidus*, *Protohaploxypinus amplus*, *Striatopodocarpites cancellatus*, *Striatopodocarpites rarus*, *Plicatipollenites indicus*, *Scheuringipollenites maximus*, *S. ovatus*, *Vittatina saccata*, *Cycadopites cymbatus*, *Pilasporites plurigenus*, *Circulisporites* sp.	Gwembe Coal Fm
		Artinskian				
		Sakmarian	Dwyka	*Plicatipollenites indicus* - *Cannanoropollis obscurus*	*Plicatipollenites indicus*, *Cannanoropollis obscurus*, *Brevitriletes cornutus*, *Acanthotriletes tereteangulatus*, *Zinspsorites eccensis*, *Microbaculispora micromodosa*, *Converrucosporites pseudoreticulatus*, *Cycadopites cymbatus*	Siankondobo Sandstone Fm
		Asselian				
Carboniferous	Late	Gzhelian		?	?	?

Figure 2.5: Palynozones of the Dwyka, Ecca, Beaufort and Stormberg Groups of Zambia (Barbolini *et al.*, 2016a redrawn from Nyambe and Utting, 1997).

The thermal maturity of the Gwembe, Madumabisa and Interbedded Sandstone and Mudstone formations is placed at a Thermal Maturity Index of 2 suggesting it is very low and most likely to have oil potential but liquid hydrocarbon potential is low (Nyambe and Utting, 1997). However, the depth at which the Gwembe Formation occurs could have the possibility of gas generation (Nyambe and Utting, 1997).

Barbolini *et al.* (2016a) reviewed the palynology, fossil plants and wood from the Luangwa and mid-Zambezi valleys in Zambia. A standardized subdivision was proposed for the area. Barbolini *et al.* (2016b) examined new palynology samples from the Madumabisa and Gwembe formations in order to attempt to date the formations more accurately. The Gwembe palynoassemblages are dominated by non-striate bisaccate pollen with the overlying Madumabisa Formation being

dominated by striate bisaccate pollen. Common species found in the Gwembe Formation include *Alisporites potoniei, Chordasporites waterbergensis, Striatosporites heyleri, Guttulapollenites hannonicus, Striatopodocarpites cancellatus* and *Potonieisporites novicus* (Figure 2.5). The Madumabisa Formation palynoassemblage comprised mostly *Cycadopites cymbatus, C. follicularis*, *Marsupipollenites triradiatus, Platysaccus papilionis, Weylandites lucifer, Calamospora plicata, Pakhapites fusus* and *Vittatina scutata* (Figure 2.5). The palynoflora represents a floral community of mostly ferns, pteridosperms, lycopods, sphenophytes, glossopterids and conifers. The Gwembe Formation palynoflora was correlated to assemblages from Australia, South Africa, Zimbabwe and Botswana and assigned a Guadalupian age. The Madumabisa Formation palynoflora was correlated with assemblages from Australia, Mozambique, East Antarctica and South Africa with a Lopingian age being assigned.

2.2.1.5. Congo

Kar and Bose (1967) studied the palynoflora of the Permian coal seam in the Greinerville Region in the Congo Basin. The dominant palynomorphs were trilete spores with bisaccates, striate bisaccates and non-striate bisaccates also being abundant (Kar and Bose, 1967). The common trilete spores found were *Punctatisporites, Lutorimites, Neocalamospora, Leiotriletes, Apiculatisporis, Cyclogranisporites, Microbaculispora, Indotriradites* and *Enigmaspora* and are found in all the seams (Kar & Bose, 1967). The common striate bisaccates that are abundant are characterized by *Strotersporites, Striatopiceites* and *Lunatisporites*. The non-striate bisaccates are represented by *Cuneatisporites, Raniganjiasaccites, Monoletesaccites, Valiasaccites, Jugasporites, Høegiasaccites* and *Walikalesaccites* (Kar & Bose, 1967). Monoletes, aletes, monosaccates, polysaccates, polyplicates and monocolpates were present in lesser abundances.

2.2.1.6. Tanzania

Hankel (1987) examined the late Permian to early Jurassic rocks of the Selous Basin in southern Tanzania. The late Permian Sumbadzi Member in

the Hatambulo Formation can be correlated to the lower Sakamena Formation in Madagascar.

2.2.1.7. Kenya

Hankel (1992) studied palynofloras of the Maji Ya Chumvi Formation in the Mombasa (Duruma) Basin in Kenya. The lower part of the basin correlates closely with the late Permian of Australia based on the palynoflora of the *Protohaploxypinus microcorpus* Zone (Henkel, 1992). The upper part of the basin correlates with the early Triassic *Lunatisporites pellucidus* Zone of Australia (Foster, 1982).

2.2.1.8. Zimbabwe

Falcon (1975) examined the palynology of the mid-Zambezi and Save-Tuli (Sabi-Limpopo) Basins of Zimbabwe. Carboniferous and Permian rocks were sampled from the Dwyka, Ecca and lower Beaufort groups. Changes are observed from monosaccate and trilete dominance in the Carboniferous to striate bisaccate pollen dominating in the Permian. Four assemblage zones are named: Assemblage Zone 1 (Dwyka Group and Lower Wankie Sandstone): *Virkkipollenites-Plicatipollenites* assemblage, Assemblage Zone II (black shales and coals: Transition Zone), Assemblage Zone III (Upper Wankie Sandstone): *Densosporites-Gondispora* assemblage, and Assemblage Zone IV (Madumabisa Mudstone): *Vittatina-Lueckisporites* assemblage (Falcon, 1975) (Figure 2.5).

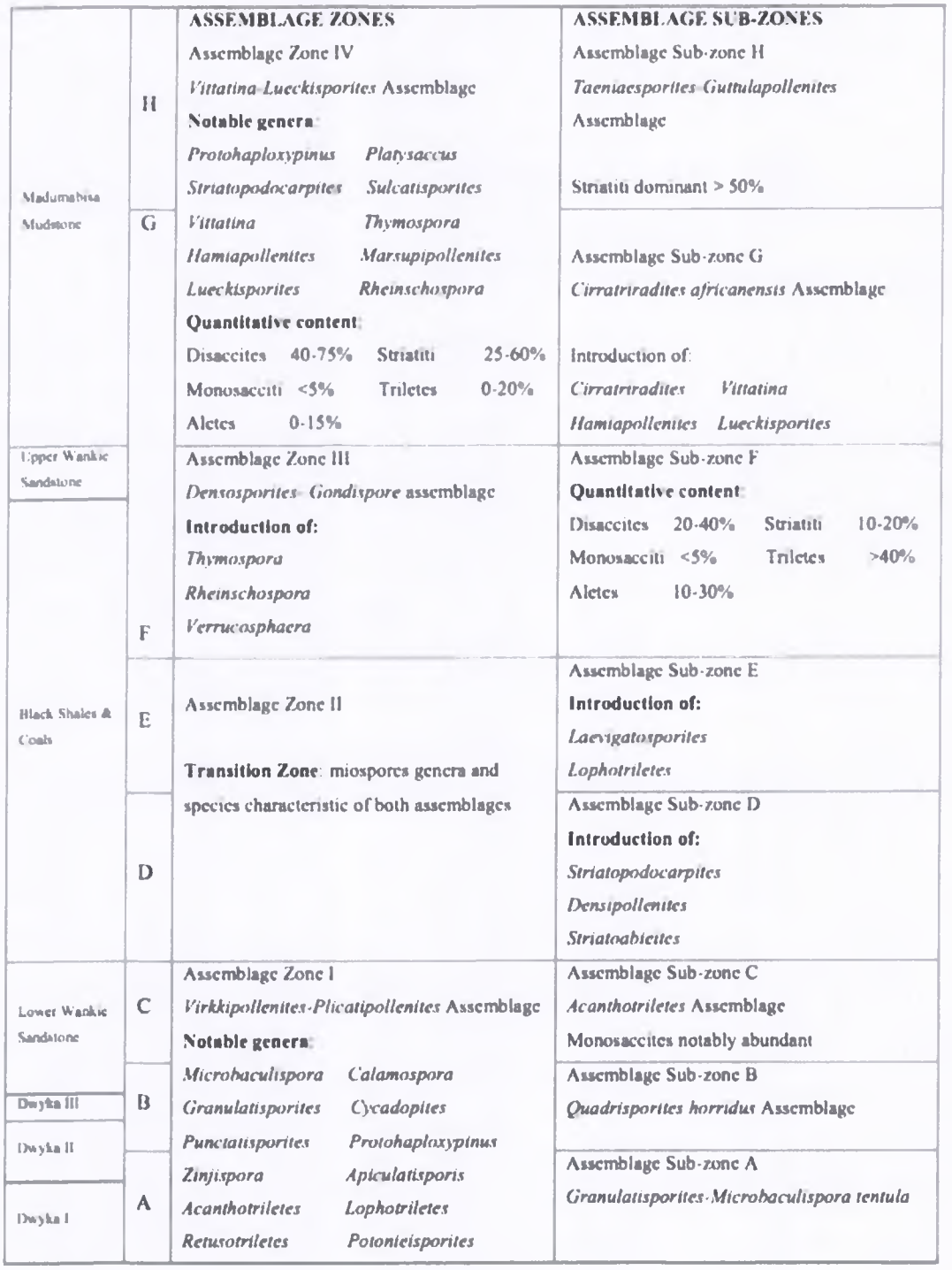

Figure 2.5: Diagram of four Assemblage Zones and eight Assemblage sub-zones of the Permian Matabola Flats borehole (after Barbolini, 2014 redrawn from Falcon, 1975).

2.2.2. Madagascar

De Jekhowsky & Goubin (1962) and Goubin (1965) studied the Morondava Basin (Sakamena Group) in Madagascar of late Permian to late Jurassic age, and drew up four major units and twelve pollen subzones. Wright & Askin (1987) then looked at the same basin and found a number of common palynomorphs for the late Permian. Based on correlations, the lower Sakamena assemblage was most closely correlated to the *Playfordiaspora crenulata* Zone in Australia (Foster, 1982). The middle Sakamena assemblage could be correlated to the *Protohaploxypinus microcorpus* and *Lunatisporites pellucidus* zones of Australia (Foster, 1982). The dominant species in the palynomorph assemblages from the Late Permian in Madagascar are *Guttulapollenites hannonicus, Weylandites* sp. and *Lueckisporites virkkiae* (Götz *et al.*, 2017). *Protohaploxypinus* sp. and *Striatopodocarpites* sp. are also commonly found in the assemblages from Madagascar (Götz *et al.*, 2017).

2.2.3. India

A large amount of palynological work has been carried out in India as the Gondwana basins of India range from Carboniferous to Cretaceous in age (Mukhopadhyay *et al.*, 2010). Vijaya *et al.* (2012) examined the Singrauli Gondwana Basin which spans the Permian and Triassic. Ten assemblage zones were described from this basin and could be correlated to other Indian and Australian zones (Vijaya *et al.*,2012).

Tripathi *et al.* (2012) looked at the Talchir, Barakar and Barren Measures formations in the Tatapani-Ramkola Coalfield, South Rewa Gondwana Basin. Five palynological assemblages were erected based on the palynoflora present namely the *Scheuringipollenites barakarensis, Faunipollenites varius, Gondisporites raniganjensis, Densipollenites magnicorpus* and *Krempipollenites indicus* zones (Tripathi *et al.*, 2012). Based on correlation the Talchir Formation can be dated as late early Permian, the Barakar Formation as late Permian in age and the Barren Measures Formation as early Triassic (Tripathi *et al.*, 2012).

Protohaploxypinus sp., *Striatopodocarpites* sp. and *Faunipollenites* sp. are the dominant species in India with a common occurrence of *Alisporites* sp., *Densipollenites magnicorpus, Striatisulcites ovatus, Tiwarisporites* sp., *Osmundacidites* sp. and *Weylandites* sp. (Götz *et al.*, 2017). However, *Guttulapollenites* are not very common in the Indian palynomorph assemblages (Götz *et al.*, 2017).

2.2.4. Australia

Australia has been studied in great detail palynologically and therefore is used in correlations with many other Gondwana palynofloral assemblages (Lindström & McLoughlin, 2007). Backhouse (1991) studied the Collie Basin in Western Australia and established eight zones in the Collie Coal Measures based on the appearance of key taxa such as *Pseudoreticulatispora pseudoreticulata, Striatopodocarpites fusus, Microbaculispora trisina, Praecolpatites sinuosus, Microbaculispora villosa, Dulhuntyispora granulata, Didecitriletes ericianus* and *Protohaploxypinus rugatus* (Backhouse, 1991). The zones based on the first appearances of these palynoflora are used to correlate three Permian sub-basins of the Collie Basin. The palynostratigraphy of the Collie Basin and the Karoo Basin were found to be similar below the *P. sinuosus* zone (Backhouse, 1991). The age of the Collie Basin was determined to be late Carboniferous/Asselian to early late Permian (Backhouse, 1991).

Mory and Backhouse (1991) examined the marine sediments of the Carnarvon Basin of western Australia. This basin is a very useful palynological type section has it has a near complete record for the Permian. Stage 2 is the oldest palynological zone and of Permian age. The *Pseudoreticulatispora confluens* Zone is defined by the appearance of *P. confluens* at the base and the appearance of *Pseudoreticulatispora pseudoreticulata* marks the top of the zone. *Cycadopites cymbatus* and *Densosporites rotundidentatus* are abundant in this zone but is not seen in high abundances in the overlying zones. This zone appears in the Lyons Group in western Australia.

The next overlying zone is the *P. pseudoreticulata* Zone and defines the lowest occurrence of this species. The top of this zone is marked at the first appearance of *Striatopodocarpites fusus.* The species *Diatomozonotriletes townrowii* appears at the base of this zone and is distinctive as it corresponds to Stage a/b in the Collie Basin. In the Carnarvon Basin this zone is found in the Callytharra Formation.

The overlying zone is the *S. fusus* Zone and is defined at the base with the appearance of this species. The coal measures in the Collie Bain show the appearance of *S. fusus* and *Laevigatosporites colliensis*. In the Carnarvon Basin this species' appearance is not as well defined. Mory and Backhouse (1997) notes this may be due to the lack of good palynological data from this zone. The top of this zone is taken as the appearance of *Didecitriletes byroensis* or the appearance of *Microbaculispora trisina*. The *S. fusus* Zone occurs in the upper Callytharra Formation (Mory and Backhouse, 1997).

The *D. byroensis* Subzone occurs next and forms part of the upper part of the *Striatopodocarpites fusus* Zone. *D. byroensis* occurs within a very limited interval and is distinctive so serves as a good datum in distinguishing the *S. fusus* and *Microbaculispora trisina* zones.

The base of the *M. trisina* Zone is marked by the species *M. trisina,* however this is not a very useful zone in correlating due to this species not being very consistent in abundance. The *M. trisina* Zone is always found overlying the *Didecitriletes byroensis* Subzone. The top of this zone is designated by the presence of *Praecolpatites sinuosus.*

The zone overlying the *M. trisina* Zone is the *P. sinuosus* Zone. This zone is marked by the appearance of *P. sinuosus* at the base. This species however is not easily identified and therefore some uncertainty exists with the base of this zone. The top of the zone is marked by the appearance of *Microbaculispora villosa.* The *M. trisina* Zone is part of the Coyrie Formation close to the basse of the Byro Group. The upper part of the zone forms part of the Coolkilya Sandstone.

The *M. villosa* Zone is marked by the appearance of the species *M. villosa.* The top of the zone is marked by the first appearance of *Dulhuntyispora granulata.* This zone is present in the Coolkilya and Mungadan Sandstones.

The *D. granulata* Zone is marked by the appearance of *D. granulata* at the base. The top of the zone is defined by the first appearance of *Didecitriletes ericianus*. The true thickness of this zone is unknown but it said to cover the Mungadan Sandstone and Binthalya Formation (Mory and Backhouse, 1997).

The overlying zone is the *D. ericianus* Zone and is marked at the base by the appearance of *D. ericianus.* The top of the zone is marked by *Dulhuntyispora parvithola.* This species is seen in the Collie Basin and is noted as being a good biostratigraphic marker in the Carnarvon Basin (Mory and Backhouse, 1997). This zone can be found in the rocks of the Peedamullah Shelf.

The youngest zone is the *D. parvithola* Zone which is marked by the first appearance of *D. parvithola* and correlated to the Upper Stage 5 of Price (1983) (Mory and Backhouse, 1997). The *D. parvithola* Zone forms part of the Kennedy Group and Chinty Formation (on the Peedamullah Shelf).

Barbolini (2016c) looked at spore and pollen zones from South Africa and Australia and calibrated them by radiometric dates. The radio-isotopic ages for both countries showed that key marker taxa have diachronous ranges. Barbolini (2016c) found that ranges of Permian pollen species are linked with palaeolatitude as well as plant distributions being affected by temperature, precipitation and seasonality.

2.2.5 Antarctica

Farabee *et al.* (1990) correlated Permian and Triassic palynomorph assemblages from the central Transantarctic Mountains, Antarctica in order to investigate age, correlation and palaeoenvironments of the area. Palynomorphs were obtained from the Buckley Formation and overlying Fremouw and Falla

formations. The Buckley Formation was correlated with the upper part of Australian Stage 4 or Stage 5 based on the presence of *Praecolpatites sinuosus* and *Protohaploxypinus microcorpus*. *Dulhuntyispora*, a distinctive species in the Australian Stage 5 is not found in the Buckley Formation palynomorph assemblage although the Buckley Formation was found to correlate most closely to the late Permian Australian Stage 5 (Farabee *et al.*, 1990). The Fremouw Formation is said to have comprised transported sediment and therefore the palynology may correspond to other lithological units. An age of Anisian is given based on *Aratrisporites parvispinosus* being present. This species is known to range from lower Triassic to lower Cretaceous in Australia. The Falla Formation assemblage is correlated as being most similar to Tasmania, South Australia and Queensland palynofloras. A Norian age is assigned based on *Polycingulatisporites crenulatus* and *Craterisporites rotundus* occurring together. Farabee *et al.* (1990) found the palynofloras of Antarctica to be most similar to Australian palynofloras.

Lindström (1995) studied the early Permian palynofloras of the Heimefrontfjella mountain range in Dronning Maud Land, Antarctica. Identifiable palynomorphs were found in three localities. The first and second localities reflected a periglacial, cold-climate, freshwater environment which contained early Permian Gondwana taxa. The palynomorph assemblage correlated most closely with late Stage 2 and the *P. confluens* Zone of Australia suggesting an Asselian-Tastubian age (Lindström,1995). The third locality was poorly preserved and correlated with the *M. trisina* Zone or Stage 3b of Australia with a possible Artinskian age (Lindström, 1995).

Lindström and McLoughlin (2007) examined palynofloras of the Permo–Triassic transition in the Prince Charles Mountains in Antarctica. The disappearances of coal-bearing strata and *Glossopteris*-dominated flora concur with the loss of approximately 32% of Permian pollen and spores. In the lowermost Triassic 34% of the remaining Permian taxa disappear and new Triassic taxa start to appear for the first time (Lindström and McLoughlin, 2007). From examination of the palynomorphs and comparison with other Gondwanan palynological assemblages, it is evident that warming had already begun in the Permian and that higher

latitude areas such as the mountainous regions were only affected later. The findings of this study suggested that although various regions in Gondwana were affected in different ways, the overall climate was thought to be sub-humid to semi-arid with not much seasonality across southern Gondwana (Lindström and McLoughlin, 2007).

2.2.6. South America

2.2.6.1. Brazil

The Paraná Basin of Brazil was re-examined by Souza and Marques-Toigo (2003, 2005) and Souza (2006) who erected new palynozonation zones for the Itararé Subgroup incorporating the intervals proposed by Daemon and Quadros (1970). These zones are the *Ahrensisporites cristatus* Interval Zone (AcZ) which was interpreted as Pennsylvanian (late Bashkirian to Kasimovian); the *Crucisaccites monoletus* Interval Zone (CmZ) which was assigned a late Pennsylvanian (Kasimovian to Gzhelian) age and the *Vittatina costabilis* Interval Zone (VcZ) which was dated as early Permian (early Cisuralian) in age (Souza and Marques-Toigo, 2003; 2005; Souza, 2006).

The palynology of the Amazonas Basin of northern Brazil was studied by Playford and Dino (2000) who established seven assemblage zones namely the: *Spelaeotriletes triangulus* Zone (Westphalian A-B); the *Striomonosaccites incrassatus* Zone (Westphalian C); the *Illinites unicus* Zone (Westphalian C); the *Striatosporites heyleri* Zone (Westphalian C-D); the *Raistrickia cephalata* Zone (Westphalian D); the *Vittatina costabilis* Zone (early Permian) and the *Tornopollenites toreutos* Zone (late Permian).

2.2.6.2. Argentina

Césari and Gutiérrez (2000) and Césari *et al.* (2011) studied the Carboniferous and Permian palynozones of central-western Argentina. Césari *et al.* (2011) proposed a palynozonation scheme for Argentina and correlated it using

radiometric dates from Brazil and South Africa. The palynozones are based on distinctive palynomorphs and are named as follows; the late Visean *Reticulatisporites magnidictyus-Verrucosisporites quasigobbetti* (MQ) Biozone; the Namurian (Serpukhovian and Bashkirian) *Raistrickia densa-Convolutispora muriornata* (DM) Biozone which is divided into three subzones; the early Permian *Pakhapites fusus-Vittatina subsaccata* (FS) Biozone and the Artinskian *Lueckisporites-Weylandites* (LW) Biozone (Césari *et al.*, 2011).

2.2.6.3. Uruguay

Beri *et al.* (2011) looked at the Permian San Gregorio to Yaguari formations of Uruguay. Two assemblage zones were erected namely the *Cristatisporites inconstans-Vittatina saccate* Assemblage Zone, assigned a Cisuralian age and the *Striatoabieites anaverrucosus-Staurosaccites cordubensis* Assemblage Zone which was said to be late Cisuralian–Guadalupian in age (Beri *et al.*, 2011). The first assemblage zone (covering the San Gregorio, Tres Islas and lower Melo formations) is characterised by trilete spores and monosaccate pollen with a lesser amount of non-taeniate bisaccate, taeniate bisaccate and plicate pollen (Beri *et al.*, 2011). The second assemblage zone represents the Melo Formation (Mangrullo and Paso Aguiar members) and is characterized by the dominance of bisaccate (taeniate and non-taeniate) pollen with some plicate and monosaccate pollen, and trilete and monolete spores (Beri *et al.*, 2011).

2.2.7 Conclusion

A superficial study was performed in order to form a basic overview of previous studies examined. However, there is still missing data that needs further examination of which the present study will contribute. A number of studies have been reviewed from the above-mentioned countries, and they possess distinct assemblages of palynomorphs from the Carboniferous, Permian and Triassic with major focus on the Permian due to this being the major coal bearing period. These assemblages are valuable for biostratigraphic correlation and age assignment, and are compared to the palynoassemblages from the "Platform Facies", Moatize and Matinde formations of the Sanangoé-Mefidezi Basin, Mozambique in Chapter 5.

3. Materials and Methods

The methods carried out for this study included laboratory preparation of palynological samples followed by microscope analysis and statistical analyses through C2 (Juggins, 2007) pollen diagram creation. The main purpose of laboratory work was to rid the samples of as much inorganic and organic matter (besides pollen) as possible in order to obtain the most palynomorph-rich residues in good condition. Chemical preparation methods generally followed Phipps & Playford (1984), with minor modifications dependant on sample lithology.

3.1. Sampling

The samples used in this study were derived from existing boreholes in the Sanangoé-Mefidezi Basin in the Tete Province, Mozambique. The borehole cores come from three boreholes namely 12ESD231, 11ESD012 and 12ESD218 (Figure 3.1). Boreholes were selected to build up a composite stratigraphy succession over 600 meters in depth. Sampling was carried out by Dr. John Hancox with the permission of Eurasian Natural Resources Corporation (Mozambique Limitada).

Borehole 12ESD231 consisted of basement rock with a thin section (1 meter) of Vúzi Formation and 60 meters of Platform Facies above. Borehole 11ESD012 intersected through 120 meters of Platform Facies and coal seams 4U to 6U. The third borehole examined is 12ESD218 which comprises the 4L to 9U coal seams. All the seams comprise mainly carbonaceous mudstones with interbedded coal seams.

For this study 56 samples were taken from the three boreholes and chemically prepared. Upon examination under the microscope 32 were found to be found productive (containing 250 or more palynomorphs) and were examined further.

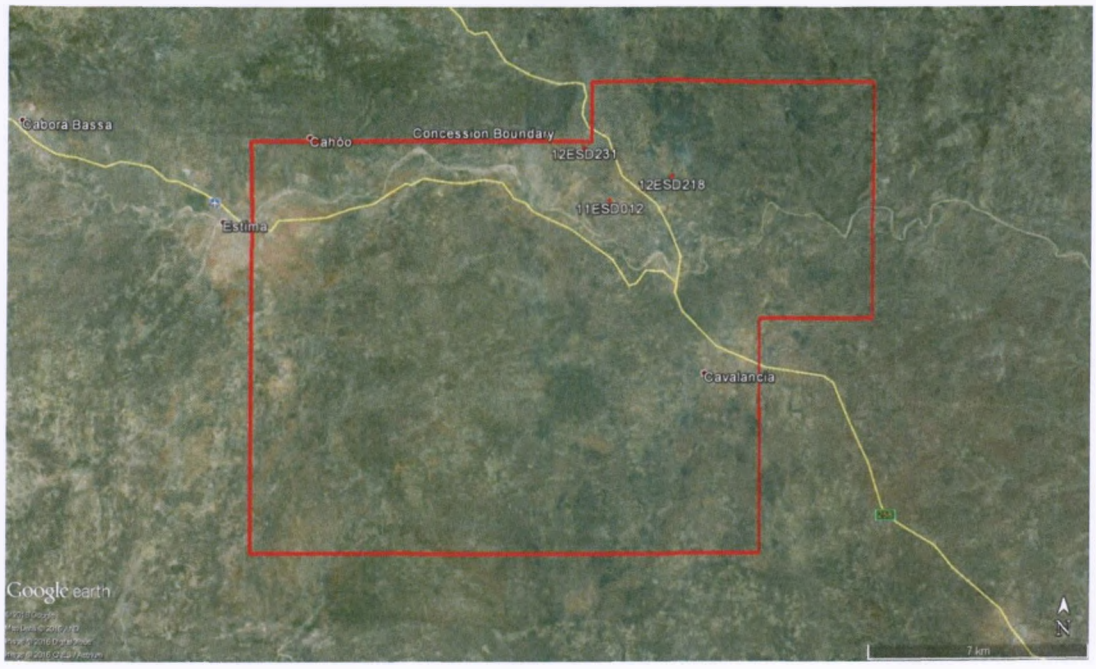

Figure 3.1: Google earth image showing borehole positions within the Tete province, Mozambique (outlined in red). Image courtesy of Dr. J. Hancox.

3.2. Maceration

A variety of acids were used in order to remove palynomorphs from the surrounding rock matrix, as palynomorphs are lithified together with inorganic minerals making up the rock matrix (Traverse, 2007). The standard methods of Phipps & Playford (1984) were used as these were previously found to be successful for Mozambique Permian samples (tested in Mahabeer, 2015). Figure 3.2 is a flowchart showing the simplified step by step process of maceration followed by a more detailed description of each chemical treatment.

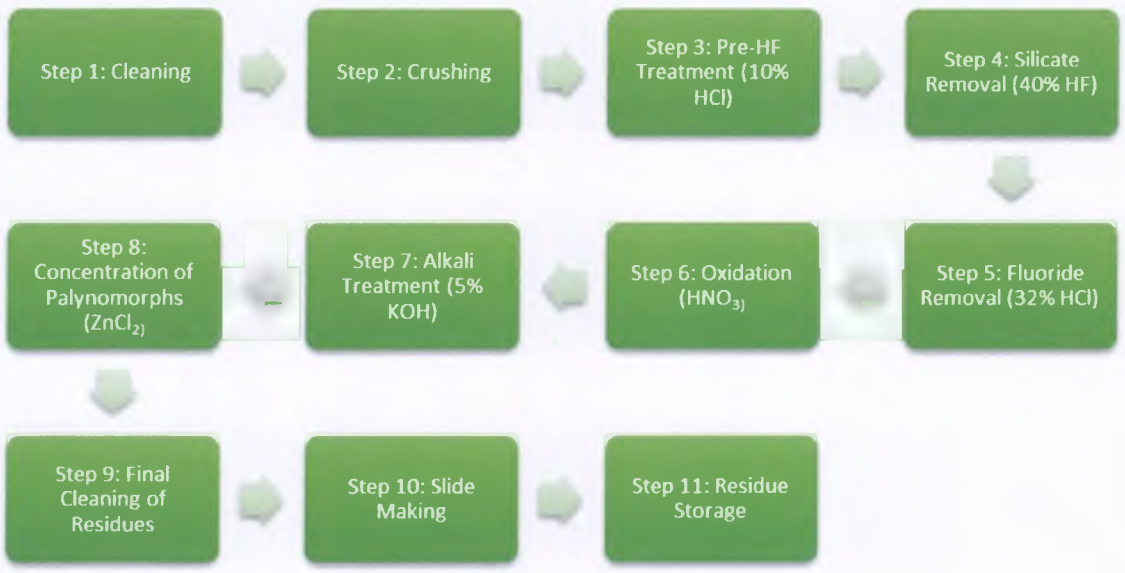

Figure 3.2: Flowchart demonstrating the step by step process of maceration and chemical preparation for Permian Mozambique palynomorphs.

Equipment

All equipment used during sample preparation was washed before and after use with boiling water and liquid soap (regular dishwashing liquid), with a final rinse in distilled water (Barbolini, 2010). When equipment was not in use it was stored in closed cupboards.

Step 1: Cleaning

The purpose of this first step is to remove all possible surface contamination on samples. The core is first broken into smaller pieces by knocking it on a hard surface with a hammer. The smaller pieces were weighed on a scale until they averaged between 15–18 grams. This size sample was sufficient to produce a productive sample abundant in palynomorphs. The core pieces were rinsed under tap water and scrubbed with regular dishwashing liquid and a clean tooth brush. The core was rinsed with tap water again unit it was clean of all soap, and then rinsed a final time with distilled water and left to dry on

clean tissue paper. This was repeated for all core pieces. A clean tissue paper was placed over all washed and sterilized core and left for approximately two hours to dry. The number of the core (assigned during sampling) was noted so samples could be kept in order.

Step 2: Crushing

Crushing was carried out in order to make the core in to a fine powder so that the acids could react adequately with the sediments. Washed pieces of core were crushed using a mortar and pestle (which had been washed with tap water, regular dishwashing liquid and a sponge; rinsed with distilled water and dried with a paper towel). After each sample was crushed into a fine powder it was transferred into a clean and sterilised (with distilled water), labelled beaker. The mortar and pestle were washed with tap water, regular dishwashing liquid and a sponge, rinsed with distilled water and dried with a paper towel. This process was repeated for each sample.

Step 3: Pre-HF Treatment

This step was carried out in order to remove all carbonates (both calcium and magnesium) from the sediments before the HF (hydrofluoric acid) treatment so that secondary fluoride precipitates would not form. Hydrochloric acid (HCl) was used to remove the carbonates. Approximately 10 ml of 10% HCl was added to each beaker containing the crushed core and stirred using Teflon stirring rods. The beakers were placed in a warm bath and heated to approximately 50°C and stirred occasionally. The reason for heating is to ensure the reaction goes to completion and the samples disaggregate effectively. The beakers were left for at least an hour in order for the samples to settle. If the supernatant was clear, the excess liquid was decanted and the remaining acid and sediment poured into clean, sterilised polypropylene centrifuge tubes and centrifuged three times with distilled water at 3000 revolutions per minute (r.p.m) for 5 minutes. Washing three times is necessary to ensure all soluble calcium and magnesium were washed out of the sample residues.

Step 4: Silicate Removal

40% HF was used to remove silica and silicates in order for disaggregation which results in the release of organic matter within the rock matrix. Approximately 30 ml of HF was added to each sample and stirred occasionally. A few drops of 32% HCl was added to each sample as it retards the formation of fluorosilicates. The beakers were placed in a hot bath for 30 minutes until the reaction was complete and samples were disaggregated. Samples were transferred into polypropylene centrifuge tubes and centrifuged three times with hot distilled water (more effective as fluorides and silicic acid are more soluble in hot distilled water) at 3000 r.p.m. for 5 minutes.

Step 5: Fluoride Removal

During silicate removal, any fluoride precipitates which might have formed need to be removed, as they obscure palynomorphs under the microscope. Therefore Step 5 is a preventative step in case this has occurred. Fluorides are more soluble in amplified temperatures and therefore warm to hot water needs to be used. The sample was agitated with small amounts of hot distilled water and mixed with stirring rods. The samples were transferred to beakers and filled with hot distilled water to the 125 ml mark. 125 ml of concentrated HCl was then added to each beaker, placed in a hot bath and stirred frequently. The samples needed to stay at boiling point in order for the reaction to reach completion. Thereafter the samples were removed from the heat, transferred to centrifuge tubes and centrifuged three times with hot distilled water at 3000 r.p.m. for 5 minutes. Each sample was mixed after each washing to ensure all acid was removed. An initial set of microscope slides was made in order to determine the thermal maturity and oxidation time needed for the samples. Due to the excess of organic matter seen, an oxidation time of 15–20 minutes was determined to be sufficient for the Permian Mozambique samples.

Step 6: Oxidation

Oxidation was carried out to remove most of the organic matter in order to concentrate the palynomorphs. This step needs to be performed with a great deal

of caution as palynomorphs can be oxidized and destroyed. Concentrated nitric acid (HNO_3) was used to oxidize the residues. Violent reactions are possible if pyrite is present in the samples and therefore needs to be carried out in beakers and in a fume hood. 20 ml of nitric acid was added to each residue and placed in a water bath for 15–20 minutes with constant stirring. The reaction is complete when the residues change colour from black to golden brown in colour. Once the reaction was observed to be complete the residues were removed from the heat, transferred from beakers into centrifuge tubes and centrifuged three times with distilled water at 3000 r.p.m. for 5 minutes.

Step 7: Alkali Treatment

An alkali treatment is performed to further concentrate the palynomorphs by removing any humic acids still present. 5% potassium hydroxide (KOH) is used with caution as it can corrode some parts of palynomorphs if left too long in the sample. Approximately 5 ml of KOH was added to each residue with a few drops of concentrated dishwashing liquid, which prevents clumping of particles. This step can be done directly in the centrifuge tubes, after which they were sealed and inverted several times to ensure mixing of the KOH and dishwashing liquid. The centrifuge tubes were filled with distilled water and centrifuged three times at 3000 r.p.m. for 5 minutes.

Step 8: Concentration of Palynomorphs using Zinc Chloride Solutions

In this step zinc chloride ($ZnCl_2$) at a specific gravity of 2.0 was used for a float-sink procedure in order to further concentrate the residues. The samples were acidified slightly by washing the residues with distilled water and adding a few drops of 10% HCl. The centrifuge tubes were half filled with $ZnCl_2$ and mixed well, then centrifuged once at 1000 r.p.m. for 2 minutes. After centrifugation the float fraction (supernatant) was poured into new labelled centrifuge tubes and the sink fractions were discarded. The tubes containing the supernatant were filled with distilled water and centrifuged three times at 3000 r.p.m. for 5 minutes.

Step 9: Final Cleaning of Residues

The final cleaning of the residues was carried out using a 20 µm sieve which was washed with dishwashing liquid, rinsed with tap water and then distilled water after each residue. The reason for sieving is to remove any extraneous particles smaller than 20 µm that obstruct palynomorphs in the final slides (Permian pollen is usually no smaller than 20 µm). Residues concentrated in Step 8 were mixed on the whirly mixer to make it easier to pour them onto the sieve using distilled water. Each residue was sieved with a few drops of dishwashing liquid to reduce clumping as much as possible (as soap has a mild deflocculating effect) and was sieved with distilled water until all the unwanted reside had passed through the sieve, and all dishwashing liquid was washed out. The residue on the sieve was washed into clean labelled beakers with as little distilled water as possible. The sieve was then cleaned and repeated for each residue.

Step 10: Slide Making

Permanent slides were made using glycerine jelly as the mounting solution. A hot plate was used at a low heat and clean, dust free microscope slides (75 x 25 mm and 1–1.2 mm thick) were labelled and placed on the hot plate. A test tube of prepared glycerine jelly was placed in a glass beaker with water on the hot plate in order to heat the jelly to melting point. A glass rod was used to place three drops of glycerine jelly on the microscope slide and spread it around. A plastic/glass pipette was used to place a few drops (no more than 3) of concentrated palynomorph residue onto the glycerine jelly and a clean glass rod was used to mix the residue and glycerine, distributing it evenly on the slide. Slides were left on the hot plate for a few minutes in order for the residue and glycerine jelly to melt and mix well. This was repeated for each residue using a clean pipette and glass rod for each slide. After the slides had been on the hot plate for a few minutes they were removed and glass coverslips (20 X 40 mm) were placed on each slide. Slides were then cleaned with tap water to remove excess residue and glycerine jelly and placed on the hot plate (inverted) for two minutes, then removed and left to cool in an inverted position for a day to bring

palynomorphs into one plane for easier microscope examination. The slides were then re-inverted and left to set for 2–3 days.

Step 11: Residue Storage

Remaining residues were transferred into new labelled storage tubes using a pipette and centrifuged once at 3000 r.p.m. for 5 minutes. The excess water was removed and tubes were kept in a cool dark place for storage.

3.3. Microscope Analysis

Microscope analysis was carried out using an Olympus BX51m light microscope for pollen analysis and counting. The slides were first counted to check if they were productive or non-productive depending on the number of palynomorphs present. The productive slides were determined by having 250 or more palynomorphs on them and if not were classified as non-productive. For particular samples slides had to be remade over in order to reach a count of 250 identifiable palynomorphs. Some slides were termed productive, but the majority of palynomorphs on the slide were fragmented and these were not included in the analysis.

The counting of palynomorphs was done under 400x magnification and high quality images were taken under 1000x magnification using a DIC prism (oil immersion) in order to capture the finer details on the grains. The ColourView Soft Imaging System, AxioCam ICc 1 camera and Analysis™ software were used for digital photography of the palynomorphs. Each taxon was identified to genus and species level where possible, based on shape, ornamentation, laesura type and colpi or sacci seen under the microscope (Figure 3.3), (this descriptive terminology used in palynomorph descriptions are taken from Traverse (2007)). The final step was to determine the thermal maturity of the palynomorphs based on colour and comparison with a thermal maturity scale. Thermal maturity w0061s determined from microscope slides that were prepared before the oxidation step in order to get the correct colour representation (as oxidation bleaches the palynomorphs).

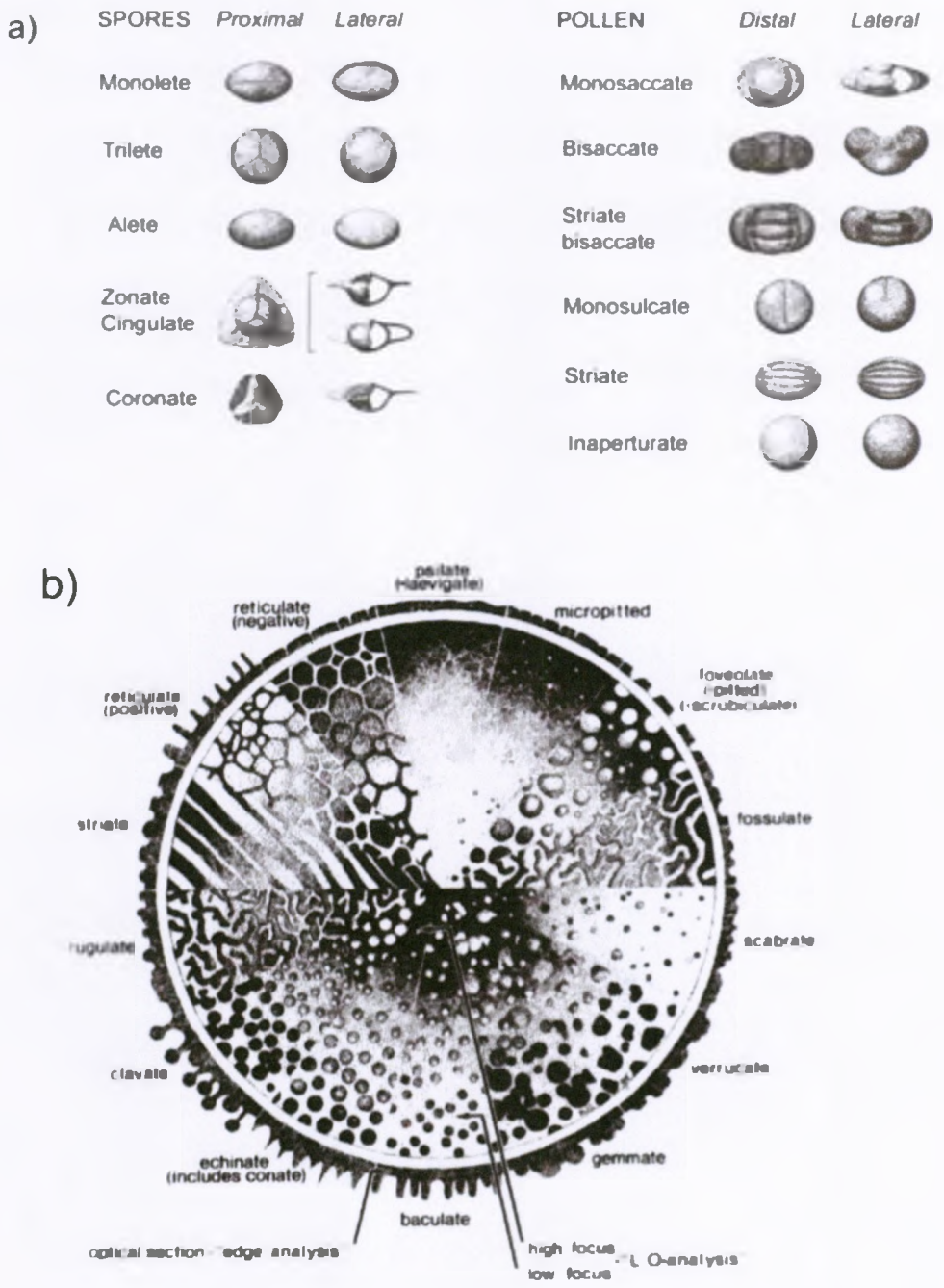

Figure 3.3: Distinctive morphological characters used to identify spores and pollen: (a) amb and (b) ornamentation and sculpture (modified from Traverse, 2007).

3.4. Statistical analysis

A statistical approach was used in order to determine the clustering of pollen into assemblage zones as well as any notable changes in environmental or climatic changes. The purpose of clustering of samples is to determine the samples with the greatest and least similarities within the pollen assemblages. This was attained by using CONISS (Constrained Incremental Sum of Squares) (Finkelstein *et al.,* 2005). This analysis allowed for comparison with already recorded regional and global changes.

All statistical analyses were carried out using the statistical coding interface R (Venables & Smith, 2015). The pollen plots were produced by using the program C2 (Juggins, 2007). The statistical analysis required that the raw data be split into three Excel spreadsheets (each representing a different borehole) reflecting the species' presence and abundances in percentages. All species that had an abundance of less than 2% were disregarded for statistical purposes only in order to prevent an uneven effect of rare species (Mackay *et al.,* 2012). The core logs were recorded in depth interval ranges and the mid-point depth for each range was calculated and recorded into the Excel spreadsheet. This mid-point depth then replaced the depth ranges. Adjustment needed to be performed on the dataset before clustering and PCA (Principal Component Analysis) could be performed. This required a square root transformation to be performed on the dataset. This transformation balances out the disproportions of high species counts to low species counts so that the environmental gradient is more proportionally distributed (Legendre & Birks, 2012).

3.4.1. Indirect Ordination/ Gradient Analyses

The ordination of vegetative samples is a special reflection of a two-dimensional system showing the species composition and the environmental conditions associated with it (Stevenson & Pan, 2004). This method allows for independent examination of the variation of samples from the environmental data and ordering

of the samples along a gradient (Stevenson & Pan, 2004). This is appropriate for the Sanangoe-Mefedezi Basin as the species composition changes over time, and this method allows for examination of possible environmental changes that could have led to changes in species composition (Stevenson & Pan, 2004). The method of ordination plots the sample data on a three-dimensional axis and therefore the type of analysis needs to be determined depending on the kind of data set used (Legendre & Birks, 2012). In order to determine which analysis should be used, the type of data needs to be determined i.e. whether it is unimodal or linear (Fitchett, 2015). Unimodal data are observed over long environmental gradients and show low diversity of each sample (more localized: alpha diversity) but a greater change in species over the environmental gradient (over time in all samples: beta-diversity) (Fitchett, 2015). Linear data differs in that it is the opposite of unimodal data. The data are more likely to have a higher species diversity in each sample but would have a shorter environmental gradient with less change between the samples (Fitchett, 2015). For the unimodal dataset Detrended Correspondence Analysis (DCA) would be used whereas for linear data Principal Component Analysis (PCA) would be used (Lepš & Šmilauer, 2003). For the Sanangoe-Mefedezi Basin the dataset was seen to be linear due to the high species variation within each sample but not much difference over the whole set of samples. This can also be tested statistically by running a DCA process to determine the number of species change over all the samples. The beta-diversity values are examined in standard deviation (SD) units (Mackay *et al.,* 2013). If the data has a SD value of four or more on the beta-diversity then the dataset is thought to be unimodal and therefore DCA is an appropriate method to be used (Mackay *et al.,* 2013). However, if a SD value of less than three for beta-diversity is observed then the dataset is said to be linear and PCA should be used (Mackay *et al.,* 2013).

Once PCA is complete bi-plots are produced with the data points plotted in a two dimensional space in relation to the first and second principal components (Lepš & Šmilauer, 2003). The species names are then inserted relative to the first and second principal components based on sample scores, allowing for visual examination of clusters as well as dominant species (Lepš & Šmilauer,

2003). The sample scores are then also used to plot pollen diagrams in order for pollen community changes over time to be examined (Legendre & Birks, 2012).

3.4.2. Clustering

The main purpose of clustering data is to divide the groups of samples according to their similarities. This allows for a clear identification of periods of environmental change and allows for examination of the relations that exist between the groups (Legendre & Birks, 2012). The method used in the study of the Sanangoé-Mefidezi Basin samples involved using a hierarchical agglomerative clustering. This means that the single samples were joined to form groups, and these smaller groups were then used to form bigger groups (i.e. locally similar) (Finkelstein *et al.*, 2005). The arrangement of these groups on a hierarchical system forms a dendrogram.

The current study used the CONISS method of clustering. This is most widely used in palaeoecological studies as it allows for the original sample order to be maintained which is essential when using borehole core data (in order for true depth to be maintained) (Legendre & Birks, 2012). The CONISS method uses Ward's minimum variance in order to cluster the data (Finkelstein *et al.*, 2005). Determination of the optimal number of groups is done by creating silhouette plots for all possible group numbers (Rosseeuw, 2009). These plots reflect the silhouette width which is a measure of each sample and all other samples in a cluster compared with the closest other cluster (Rosseeuw, 2009). The silhouette plots with the value closest to one is the optimal number of clusters, while the values closest to zero reflect the samples may lie between clusters (Rosseeuw, 2009). Negative values suggest that samples lie within the wrong cluster (Rosseeuw, 2009). The resultant dendrogram can then be colour coded and this colour coding can then also be used in the PCA diagrams allowing for adjacent comparisons (Finkelstein *et al.*, 2005).

3.4.3. Representation

The standard pollen diagrams are produced using the C2 program. This reflects the species counts against the depth from the core of each sample (Juggins, 2007). The sample score from the first and second principal components from PCA are also plotted on a diagram and indicate the change in species compositions (Legendre & Birks, 2012). These species are arranged according to their scores in order for the gradient of change of species to be clearly seen. From the CONISS method zones are demonstrated on a plot allowing for cluster analysis (Finkelstein *et al.*, 2005).

4. Results

4.1.1 Systematic Palynology

As no single classification system for palynology is under the protection of the International Code of Botanical Nomenclature, the system used for turmal classification of palynomorphs is determined at the discretion of the author based on the suitability of samples composition and time period being examined. For this study the most widely used system of Potonié (1956–1970) is used. This is a turmal system with the primary Anteturmas Sporites and Pollenites, which then contain further subdivisions. A total of 41 different taxa were identified in this study: 12 genus level identifications and 29 species level identifications. The overall preservation of palynomorphs was relatively degraded, so even though the Sanangoé-Mefidezi Basin samples are abundant in palynomorphs, identification of these grains is difficult. All descriptions are taken from the original description by the author (and subsequent amendments) as these are the defining features looked for when examining the palynomorphs under the microscope.

Micrographs of the different palynomorphs found are arranged in turmal group order. Due to degradation, fragmentation and orientation of certain palynomorphs, not all features may be seen in a single image, but all defining features were identified under the microscope in order to classify a grain. High resolution images of each species identified are included in the plates below (Plates 1-5). Scale bars represent 10μm on all images.

Note: For descriptions Borehole 12 ESD 231 is shortened to BH 231, Borehole 871L_D012 is shortened to BH 871 and Borehole 12 ESD 218 is shortened to BH 218.

Anteturma SPORITES

Turma TRILETES

Suprasubturma ACAVATRILETES

Subturma AZONOTRILETES

Infraturma LAEVIGATI

Genus PUNCTATISPORITES

Punctatisporites gretensis Balme & Hennelly 1956

Plate 1: (1).

DESCRIPTION: Spores radial, trilete. **Amb:** circular to sub-circular. Trilete mark slightly off-center. **Exine:** 1–2 µm thick; equator with sporadic gemmate to verrucate elements, about 2µm in height and base diameter. Plan view display isolated sub- circular to polygonal verrucae, 1–2µm across.

SIZE: 50 µm–60 µm.

STRATIGRAPHIC RANGE: "Platform Facies" and Moatize Formation.

TOTAL ABUNDANCE: BH 231: 58 specimens; BH 871: 84 specimens.

Genus DELTOIDOSPORA

Deltoidospora directa (Balme & Hennelly) Norris 1965

Plate 1: (2).

DESCRIPTION: Spores radial, trilete. **Amb:** triangular, interapices slightly convex, apices broad to slightly sharply rounded. **Laesurae:** distinct, straight to sinuous, extend to equator; occasionally develop Curvatura Imperfecta. **Exine**: 0.5–1µm thick, proximally laevigate; distal face commonly micro-granulate or scabrate, micropunctate to rarely foveolate.

SIZE: 45 µm–50 µm.

STRATIGRAPHIC RANGE: "Platform Facies", Moatize Formation and Matinde Formation.

TOTAL ABUNDANCE: BH 231: 77 specimens; BH 871: 95 specimens; BH 218: 130 specimens.

Infraturma APICULATI

Genus GRANULATISPORITES

Granulatisporites papillosus Hart 1965

Plate 1: (3).

DESCRIPTION: **Amb**: Triangular, apices rounded, interapices straight to slightly convex. **Aperture**: Trilete, laesurae straight to slightly sinuous, extending to the equator. Faint labra, generally narrow (less than 4 µm wide), present in some species. **Exine**: 1–2 µm thick, ornament of small grana spaced approximately 1–2 µm apart. Ornament appears reduced on the proximal surface of some specimens, although it is always obvious along the equator.

SIZE: 50 µm–55 µm.

STRATIGRAPHIC RANGE: "Platform Facies" and Moatize Formation.

TOTAL ABUNDANCE: BH 231: 50 specimens; BH 871: 97 specimens.

Genus HORRIDITRILETES

Horriditriletes ramosus (Balme & Hennelly) Bharadwaj & Salujha 1964

Plate 1: (4a, b).

DESCRIPTION: **Amb**: Triangular, apices rounded, interapices convex, straight to concave. **Aperture**: Trilete, laesurae extend ¾ to full radius of spores. Labra indistinct or absent, kyrtome not observed. **Exine**: 1–2 μm, ornament of bacula and spinae.

SIZE: 40 μm–45 μm.

STRATIGRAPHIC RANGE: "Platform Facies", Moatize Formation and Matinde Formation.

TOTAL ABUNDANCE: BH 871: 16 specimens; BH 218: 19 specimens.

Genus CONVERRUCOSISPORITES

Converrucosisporites naumoviae Backhouse 1991

Plate: 1 (5).

DESCRIPTION: Spores radial, trilete. **Amb:** sub-triangular, apices narrow to slightly broadly rounded, inter-apices convex. **Laesurae:** discernible to distinct, extend to equator; straight or sinuous with weakly developed labra. **Exine:** 0.5–1μm thick; sculptured with verrucae and subordinate grana to occasional gemmae-like sculpture at equator. Verrucae circular to sub-circular or polygonal

to elongate in form. Verrucae 1–2µm in diameter or up to 2 x 3µm in dimension. Sculpturing often reduced proximally.

SIZE: 40 µm–50 µm.

STRATIGRAPHIC RANGE: "Platform Facies", Moatize Formation and Matinde Formation.

TOTAL ABUNDANCE: BH 231: 53 specimens; BH 871: 38 specimens; BH 218: 127 specimens.

Genus VERRUCOSISPORITES

***Verrucosisporites* sp.**

Plate: 1 (6).

DESCRIPTION: Spores sub-circular with indistinct aperture. **Exine:** 1.5–2µm thick; equator bearing rounded verrucae, with subordinate low broad-based coni. Plan view with commonly flat verrucae, polygonal to elongate, defining a reticulate to near regulate pattern; brochi 1–3µm wide.

SIZE: 35 µm–40 µm.

STRATIGRAPHIC RANGE: "Platform Facies" and Moatize Formation.

TOTAL ABUNDANCE: BH 231: 10 specimens; BH 871: 10 specimens.

Subturma ZONOTRILETES

Infraturma ZONATI
Genus KRAEUSELISPORITES

Kraeuselisporites enormis Segroves 1970

Plate: 1 (7a, b, c).

DESCRIPTION: **Amb:** Roundly triangular to subcircular, outline irregular due to projecting spine. Aperture Trilete, laesurae extend to margin of central region and often traceable onto zona as folds extending in the direction of the laesure.

Laesurae: straight to slightly sinuous. **Exine:** exoexine 1–4 μm in central area, laevigate to finely granulate on the proximal surface. Zona continuous with the proximal exoexine, narrow, the margin defined by coni and spinae of variable size. Zone thin (less than 1 μm). Intexine thin, only observed when detached.

SIZE: 40 μm–45 μm.

STRATIGRAPHIC RANGE: Moatize Formation and Matinde Formation.

TOTAL ABUNDANCE: BH 871: 28 specimens; BH 218: 72 specimens.

Turma MONOLETES

Subturma AZONOMONOLETES

Infraturma LAEVIGATOMONOLETI

Genus LAEVIGATOSPORITES

Laevigatosporites vulgaris (Ibrahim in Potonié, Ibrahim & Loose) Ibrahim 1933

Plate 1: (8).

DESCRIPTION: **Amb**: Oval. **Aperture**: Monolete, laesura simple to weakly labrate, ¾ to almost entire longitudinal extent of spore, tapered at termini or curvaturate. **Exine**: Thin 0, 5 to 1 µm thick, laevigate to finely granulate or irregularly reticulate in appearance.

SIZE: 20 µm–30 µm.

STRATIGRAPHIC RANGE: "Platform Facies", Moatize Formation and Matinde Formation.

TOTAL ABUNDANCE: BH 231: 64 specimens; BH 871: 72 specimens; BH 218: 108 specimens.

Infraturma SCULPTATOMONOLETI

Genus THYMOSPORA

Thymospora pseudothiessenii (Kosanke) Wilson & Venkatachala 1963

Plate 1: (9).

DESCRIPTION: **Amb:** Subcircuar to weakly oval, outline irregular due to the large sculptural elements projecting from the equator. **Aperture:** Monolete, laesura extends over half the length of the spore, often obscured by ornament elements, but when evident the laesura is ill-defined. Some specimens show faint labra bordering the laesura. **Exine:** Variable in thickness due to ornamental elements, 0.5–3.5 µm thick. Ornament of verrucae on the entire surface which appear fused to form irregularly shaped rugulae.

SIZE: 30 µm–35 µm.

STRATIGRAPHIC RANGE: "Platform Facies", Moatize Formation and Matinde Formation.

TOTAL ABUNDANCE: BH 231: 9 specimens; BH 871: 88 specimens; BH 218: 139 specimens.

Turma ALETES

Subturma AZONALETES

Infraturma GRANULONAPTI

Genus GRANULATASPORITES

Granulatasporites subreticulatus (Samoilovich) Hart 1965

Plate 2: (1).

DESCRIPTION: **Amb**: Circular, subcircular or oval. **Aperture**: No aperture visible. **Exine**: 2–5 µm, ornament of fine grana closely spaced. This close spacing of the ornament may produce a faint reticulate optical effect.

SIZE: 30 µm–40 µm.

STRATIGRAPHIC RANGE: "Platform Facies".

TOTAL ABUNDANCE: BH 231: 48 specimens; BH 871: 76 specimens.

Anteturma POLLENITES

Turma PLICATES

Subturma MONOCOLPATES

Infraturma INTORTI

Genus CYCADOPITES

Cycadopites cymbatus (Balme & Hennelly) Hart 1965

Plate 2: (2).

DESCRIPTION: **Amb:** Elongately oval, length approximately twice the width.

Aperture: Sulcus or furrow extends full length of grain, open at ends and often narrow or closed in middle of the grain. **Exine:** 1μm or less, ornament of fine grana.

SIZE: 30 μm–40 μm.

STRATIGRAPHIC RANGE: "Platform Facies" and Moatize Formation.

TOTAL ABUNDANCE: BH 231: 71 specimens; BH 871: 129 specimens; BH 218: 27 specimens.

Genus MARSUPIPOLLENITES

Marsupipollenites striatus (Balme & Hennelly) Foster 1975

Plate 2: (3).

DESCRIPTION: **Amb**: Circular to subcircular with some grains oval. Outline irregular due to infrasculpture often visible along the equatorial plane. **Aperture**: Trilete, laesurae faintly labrate, generally small (3–14 μm length of single laesura) and sited proximally. Sulcus present distally, usually open and extending almost to the periphery of the grains. **Exine**: Less than 1 μm, infragranualte to slightly infrabaculate, elements arranged in rows which stimulates ribs or taeniae.

SIZE: 50 µm–60 µm.

STRATIGRAPHIC RANGE: "Platform Facies", Moatize Formation and Matinde Formation.

TOTAL ABUNDANCE: BH 871: 73 specimens; BH 218: 135 specimens.

Marsupipollenites triradiatus Balme & Hennelly 1956

Plate 2: (4).

DESCRIPTION: Pollen infrastriate, monosculcate, with small proximal trilete mark. **Amb:** circular to sub-circular or slightly longitudinally oval. **Laesurae:** poor to well distinct. Outline of sulcus weakly defined, extend full diameter but seem not to transcend outer margin or equatorial outline. **Exine:** about 1µm thick. Infrasculpture in taeniae-like rows, 1–2µm wide, separated by striations that converge at three points around grain, forming triangular shape; sets of striations appear confined to different faces.

SIZE: 20 µm–30 µm.

STRATIGRAPHIC RANGE: "Platform Facies", Moatize Formation and Matinde Formation.

TOTAL ABUNDANCE: BH 871: 16 specimens; BH 218: 82 specimens.

Turma SACCITES

Subturma DISACCITES

Infraturma DISACCITRILETI

Genus LIMITISPORITES

Limitisporites monstruosus (Luber in Luber and Waltz) Hart 1965

Plate 3: (5).

DESCRIPTION: Pollen bisaccate, monolete. **Amb**: slightly haploxylonoid to diploxylonoid. Laesura poorly distinct to discernible, straight to slight bending and widening in the centre. **Corpus**: distinct, darker, sub-circular to oval and occasionally slightly polygonal with near straight sides, transversely elongate, two or more transversely aligned to occasionally oblique and longitudinal intexinal folds; intexine 1µm thick. **Sacci:** crescentic to semi-circular in outline, joined by narrow lateral bladders 2–3µm wide, slightly inclined distally; infrapunctate and finely reticulate, brochi 1–2 µm wide.

SIZE: 50 µm–55 µm.

STRATIGRAPHIC RANGE: "Platform Facies", Moatize Formation and Matinde Formation.

TOTAL ABUNDANCE: BH 871: 27 specimens; BH 218: 69 specimens.

***Limitisporites* sp.**

Plate 2: (6).

DESCRIPTION: **Amb**: Weakly diploxylonoid. **Corpus**: Oval, elongated in the longitudinal direction. Intexine (less than 1 µm thick) laevigate to faintly granulate. Monolete aperture straight, of variable length and in some specimens bordered by narrow parallel darkened areas. **Saccus:** Bisaccate, sacci semicircular to more so, joining the corpus equatorially at a medium angle, lateral bladders (3– 10 µm wide) present. Distal saccus attachment subequatorial, overlap 6–12 µm, occasionally associated with circular folds. Proximally

exoexine covers the corpus, with granulate to fine irregular reticulation in this region. Sacci finely reticulate brochi 0.5–2 µm in diameter.

SIZE: 60 µm–65 µm.

STRATIGRAPHIC RANGE: "Platform Facies", Moatize Formation and Matinde Formation.

TOTAL ABUNDANCE: BH 871: 38 specimens; BH 218: 28 specimens.

Infraturma DISACCIATRILETI

Genus PTERUCHIPOLLENITES

Pteruchipollenites gracilis (Segroves) Foster 1979

Plate 2: (7).

DESCRIPTION: **Amb**: Haploxylonoid. **Corpus**: Indistinct, circular to slightly oval in the transverse direction. Exoexine on the proximal surface thin, laevigate with small irregular folds often observed. Distal saccus attachment indistinct, narrow overlap on the corpus and appears straight or slightly convex in polar view. **Saccus**: Bisaccate, sacci semicircular or slightly less than so in shape and may be connected by narrow (1–4 µm wide) lateral bladders.

SIZE: 80 µm–100 µm.

STRATIGRAPHIC RANGE: "Platform Facies", Moatize Formation and Matinde Formation.

TOTAL ABUNDANCE: BH 231: 56 specimens; BH 871: 101 specimens; BH 218: 94 specimens.

Pteruchipollenites landianus Balme 1970

Plate 2: (8).

DESCRIPTION: **Amb**: Diploxylonoid, not strongly so. **Corpus**: Distinct to indistinct, circular to subcircular. Exoexine on the proximal surface thin, granulate to finely reticulate. Distal saccus attachment subequatorial with a narrow saccus overlap onto the corpus (6–10μm wide). Cappula wide, oval to rectangular in shape. **Saccus**: Bisaccate, sacci larger than the corpus, semicircular to more than so in shape. Lateral bladders narrow to not developed. Sacci finely reticulate with the brochi less than 1 μm in diameter. Sacci show weak to fairly strongly developed radial folding near saccus bases.

SIZE: 60 μm–70 μm.

STRATIGRAPHIC RANGE: "Platform Facies" and Moatize Formation.

TOTAL ABUNDANCE: BH 871: 85 specimens; BH 218: 9 specimens.

Pteruchipollenites **sp.**

Plate 2: (9).

DESCRIPTION: **Amb**: Haploxylonoid. **Corpus**: Indistinct, oval in shape with elongation in the transverse direction, corpus larger than sacci along this axis. Exoexine of proximal surface thin, laevigate to finely granulate. Distal saccus attachment indistinct, straight to slightly convex, rarely associated with folding. Saccus overlap on corpus narrow. **Saccus**: Bisaccate, sacci semicircular to less than so in diameter and showing a slight radial elongation near the saccus attachment.

SIZE: 60 μm–70 μm.

STRATIGRAPHIC RANGE: "Platform Facies" and Moatize Formation.

TOTAL ABUNDANCE: BH 231: 14 specimens. BH 218: 21 specimens.

Genus ALISPORITES

Alisporites potoniei (Lakhanpal, Sah & Dube) Somers 1968

Plate 3: (1).

DESCRIPTION: **Amb:** Haploxylonoid, outline circular to oval, tending towards weakly diploxylonoid in some grains. **Corpus:** Indistinct to clearly defined, oval with elongation in the transverse direction. Distal saccus attachment lines parallel, forming narrow (1–8 µm wide) distal sulcus, rarely associated with folding.
Saccus: Bisaccate, sacci semicircular to greater than so, joined laterally by a narrow exoexinal connection. Sacci reticulate with brochi 2–4 µm in diameter with no obvious difference over the proximal side of grain.

SIZE: 70 µm–80 µm.

STRATIGRAPHIC RANGE: "Platform Facies" and Moatize Formation.

TOTAL ABUNDANCE: BH 231: 45 specimens; BH 871: 189 specimens.

***Alisporites* sp.**

Plate 3: (2a, b).

DESCRIPTION: **Amb:** Diploxylonoid. **Corpus:** Distinct, circular to sub-circular. Proximal surface intrareticulate. Distal saccus attachment subequatorial and associated with a narrow darkened band. Corpus distally sulcate, sulcus extending almost the full diameter in the transverse direction and narrow. **Saccus:** Bisaccate, sacci semicircular or more than so in shape, often overlapping

laterally. Sacci finely reticulate with a coarser reticulation superimposed on it and generally tending to be coarser away from the corpus.

SIZE: 60 µm–70 µm.

STRATIGRAPHIC RANGE: Moatize Formation.

TOTAL ABUNDANCE: BH 871: 11 specimens.

Genus SCHEURINGIPOLLENITES

Scheuringipollenites ovatus (Balme & Hennelly) Jansonius 1962

Plate 3: (3).

DESCRIPTION: Pollen bisaccate, distally sulcate. **Amb**: haploxylonoid, oval. Corpus elongate in transverse axis of grain, oval, outline poorly to rarely distinct. Sacci semi-elliptical, finely reticulate with brochi about 1µm wide. Distal sacci attachment sub-parallel, defining margin to a narrow sulcus that extend full length of corpus.

SIZE: 40 µm–60 µm.

STRATIGRAPHIC RANGE: "Platform Facies", Moatize Formation and Matinde Formation.

TOTAL ABUNDANCE: BH 231: 131 specimens; BH 871: 203 specimens; BH 218: 14 specimens.

Genus PLATYSACCUS

Platysaccus papilionis (Balme & Hennelly) Lele 1964

Plate 3: (4).

DESCRIPTION: **Amb:** Circular, subcircular, occasionally slightly oval. Margin smooth to slightly undulated. **Corpus:** Distinct, circular to subcircular, generally following the contour of the saccus margin. Proximal surface finely reticulate to coarsely granulate, exoexine thickens and may be detached.

SIZE: 40 µm–50 µm.

STRATIGRAPHIC RANGE: "Platform Facies", Moatize Formation and Matinde Formation.

TOTAL ABUNDANCE: BH 231: 64 specimens; BH 871: 123 specimens; BH 218: 102 specimens.

Infraturma STRIATITI

Genus HAMIAPOLLENITES

***Hamiapollenites* sp.**

Plate 3: (5).

DESCRIPTION: Pollen bisaccate, striate. **Amb**: diploxylonoid, with sacci and central body nearly identical in shape. **Corpus**: distinct, sub-circular to broadly oval elongate in transverse or longitudinal axis. Proximal cap with 7 taeniae oriented parallel to the long axis of the grain, approximately 5 taeniae in the distal area oriented transversely. Taeniae proximally infrapunctate and infrareticulate.

Sacci: nearly circular in shape, attached sub-equatorially.

SIZE: 40 µm–50 µm.

STRATIGRAPHIC RANGE: "Platform Facies", Moatize Formation and Matinde Formation.

TOTAL ABUNDANCE: BH 871: 57 specimens; BH 218: 161 specimens.

Genus LUECKISPORITES

***Lueckisporites* sp.**

Plate 3: (6).

DESCRIPTION: Pollen bisaccate, taeniate. **Amb**: diploxylonoid. **Corpus**: distinct, subcircular to broadly oval. Proximal cap divided into half by narrow cleft that generally tapers on either ends, and extends full diameter of corpus along grain longitudinal axis; a monolete mark may be visible at the center of the cleft. **Sacci:** semi-circular in shape, distal attachment parallel defining margins to sulcus about 6µm wide; infrastructure fine to micro-punctate or vermiculate.

SIZE: 50 µm–60 µm.

STRATIGRAPHIC RANGE: "Platform Facies", Moatize Formation and Matinde Formation.

TOTAL ABUNDANCE: BH 871: 34 specimens; BH 218: 115 specimens.

Genus LUNATISPORITES

***Lunatisporities* sp.**

Plate 3: (7).

DESCRIPTION: Pollen bisaccate, taeniate. **Amb:** moderate to slightly strongly diploxylonoid. **Corpus:** well defined, subcircular with slight elongation in longitudinal axis of grain; centre with discernible monolete mark occasionally enclosed within irregular cleft extending full diameter of corpus in longitudinal axis. Proximal cappa robust, divided into four longitudinal taeniae; microinfrastructure reticulate, punctate, vermiculate or granulate. **Sacci:** semi-circular to larger than semi-circle in shape, distal attachment straight, leaving gap about 8µm–12µm wide; infrastructure reticulate to vermiculate with punctae, occasionally radially arranged.

SIZE: 30 µm–40 µm.

STRATIGRAPHIC RANGE: "Platform Facies", Moatize Formation and Matinde Formation.

TOTAL ABUNDANCE: BH 871: 54 specimens; BH 218: 103 specimens.

Genus GUTTULAPOLLENITES

Guttulapollenites hannonicus Goubin 1965

Plate 3: (8).

DESCRIPTION: Pollen, asaccate, with generally circular outline. Constitutes a spherical central body with smooth exine about 2 µm thick, consisting of two individualized "balloons" at the distal pole. The proximal pole supports a large sub-equatorial dome as a sacciform bead. Exine of saccus, rnicroreticulate and outer fringe of the cappa, reticulate.

SIZE: 45 µm–50 µm.

STRATIGRAPHIC RANGE: "Platform Facies", Moatize Formation and Matinde Formation.

TOTAL ABUNDANCE: BH 871: 73 specimens; BH 218: 181 specimens.

Genus PROTOHAPLOXYPINUS

Protohaploxypinus limpidus (Balme & Hennelly) Balme & Playford 1967

Plate 3: (9a, b).

DESCRIPTION: **Amb**: Haploxylonoid, with an oval amb, often longitudinally elongated. **Corpus**: Discernible, indistinct in some specimens, subcircular to oval with elongation in the longitudinal direction. Proximal surface, fine to mediumly reticulate (brochi 0,4–5 µm in diameter) with 6–8 longitudinal taeniae separated by narrow clefts. Taeniae generally unbranched and of even width. Distal saccus attachment straight, two sides (roots) parallel and extend over the entire corpus in the transverse direction. **Exine**: Thin and showing little or no structure. **Saccus:** Bisaccate, sacci semicircular in shape, rarely joined by lateral bladders.

SIZE: 60 µm–70 µm.

STRATIGRAPHIC RANGE: "Platform Facies", Moatize Formation and Matinde Formation.

TOTAL ABUNDANCE: BH 871: 189 specimens; BH 218: 553 specimens.

Protohaploxypinus rugatus Segroves 1969

Plate 4: (1).

DESCRIPTION: Pollen bisaccate, taeniate. **Amb:** haploxylonoid to slightly diploxylonoid, slightly oval elongate in transverse axis of grain. **Corpus:** distinct,

broadly oval elongate in transverse axis of grain, short sides may be slightly flattened; infrastructure laevigate to rarely punctate. Proximal surface with approximately 10 longitudinal taeniae. **Sacci:** largely distally confined, only marginally exposed, less than semi-circular in outline; infrastructure finely reticulate or vermiculate to grana or just rarely punctate in some specimens. Cappula sub-rectangular, extend full length of corpus, sides well-defined by distinct transverse folds; slightly widens at lateral extremities.

SIZE: 40 µm–50 µm.

STRATIGRAPHIC RANGE: Moatize Formation and Matinde Formation.

TOTAL ABUNDANCE: BH 871: 44 specimens; BH 218: 162 specimens.

Protohaploxypinus goraiensis (Potonié and Lele) Hart 1964

Plate 4: (2).

DESCRIPTION: **Amb**: Haploxylonoid to weakly diploxylonoid. **Corpus**: Indistinct to discernible, circular to subcircular, if elongate then is usually slight and in the transverse direction. Proximal surface finely reticulate (brochi 1–2 µm in diameter) to coarsely granulate in appearance with 8–12 longitudinal taeniae separate by narrow clefts. Taeniae narrow, and may extend the full corpus length. Distal saccus attachment straight to sinuous with the two sides parallel, occasionally folding observed associated with this folding. Cappula 1/5 nor less than the corpus longitudinal dimension, exine thin and unstructured. **Saccus**: Bisaccate, sacci semicircular, occasionally greater than so, rarely joined by narrow lateral bladders. Sacci mediumly reticulate with brochi 2–4 µm in diameter.

SIZE: 60 µm–70 µm.

STRATIGRAPHIC RANGE: "Platform Facies", Moatize Formation and Matinde Formation.

TOTAL ABUNDANCE: BH 871: 60 specimens; BH 218: 177 specimens.

***Protohaploxypinus* sp.**

Plate 4: (3).

DESCRIPTION: Pollen bisaccate, taeniate. **Amb:** haploxylonoid, subcircular to broadly oval. **Corpus:** poorly distinct, outline broadly oval with elongation in transverse axis of the grain; some specimens bearing trilete marks. Proximal cap with about 6–9 relatively regular longitudinal taeniae separated by very fine striations; taeniae with well-defined curvi-linear terminations. **Sacci:** crescentic to almost semi-circular in shape; infrastructure reticulate, brochi fine to moderate 1–3. cappula sub-rectangular; narrow distal sulcus partially constricted at centre, fan-shaped at one or both ends.

SIZE: 50 μm–60 μm.

STRATIGRAPHIC RANGE: Moatize Formation.

TOTAL ABUNDANCE: BH 871: 18 specimens.

Genus STRIATOPODOCARPITES

Striatopodocarpites cancellatus (Balme & Hennelly) Hart 1963

Plate 4: (4).

DESCRIPTION: **Amb**: Moderately diploxylonoid. **Corpus**: Distinct, circular to semicircular. Proximal surface finely reticulate (brochi less than 0.5 μm in diameter) to granulate with 5–10 longitudinal taeniae separated by narrow clefts. Taeniae generally unbranched, of equal width and extend over the entire corpus.

Distal saccus attachment straight to slightly biconvex, folding occasionally associated with this attachment. Exine thin and showing little or no structure. **Saccus**: Bisaccate, sacci greater than semicircular in shape, radially folded near the saccus attachment, lateral bladders are seldom observed. Sacci fine to mediumly reticulate with brochi 1–4 µm in diameter often radially elongated near the saccus attachment.

SIZE: 30 µm–40 µm.

STRATIGRAPHIC RANGE: Moatize Formation and Matinde Formation.

TOTAL ABUNDANCE: BH 871: 113 specimens; BH 218: 540 specimens.

Striatopodocarpites fusus (Balme & Hennelly) Potonié 1958

Plate 4: (5).

DESCRIPTION: Pollen bisaccate, taeniate. **Amb:** strongly diploxylonoid.

Corpus: distinct, dark, circular to subcircular and oval elongate in transverse axis of grain; exoexine 1–2µm thick. Proximal cap with approximately 5–11 longitudinal taeniae, 2–3µm wide; finely infrapunctate or unstructured. **Sacci:** extremely large, greater than semi-circular in outline, distal attachment convex to straight and often touching at middle or leaving a narrow gap; finely reticulate with brochi 2µm wide, radially arranged near base. Cappula constricted or slit-like to very narrow, of the order of 1/10 of corpus.

SIZE: 30 µm–40 µm.

STRATIGRAPHIC RANGE: Moatize Formation and Matinde Formation.

TOTAL ABUNDANCE: BH 871: 71 specimens; BH 218: 296 specimens.

***Striatopodocarpites* sp.**

Plate 4: (6).

DESCRIPTION: **Amb:** diploxylonoid. **Corpus:** discernible to distinct, sub-circular to oval with elongation in the transverse axis. Proximal surface finely reticulate, multistriate. **Sacci**: crescentic to greater than semicircular in shape, mediumly reticulate.

SIZE: 30 µm–40 µm.

STRATIGRAPHIC RANGE: Moatize Formation and Matinde Formation.

TOTAL ABUNDANCE: BH 871: 12 specimens; BH 218: 3 specimens.

Genus STRIATOABIEITES

Striatoabieites multistriatus (Balme & Hennelly) Hart 1964

Plate 4: (7).

DESCRIPTION: **Amb**: Diploxylonoid. **Corpus**: Distinct, circular to oval with elongation in the longitudinal direction. Proximal surface laevigate to finely infrapunctuate with 12–20 longitudinal taeniae, separated by very narrow clefts. A narrow monolete aperture is frequently observed in the central part of the proximal surface between two taeniae. Distal saccus attachment straight, shorter than the corpus transverse dimension and usually associated with cresecentic folds. **Exine**: Appears structured. **Saccus**: Bisaccate, sacci greater than semicircular in shape. Sacci largest transverse dimension equal to or smaller than that of the corpus, finely to mediumly reticulate with brochi 1–4 µm in diameter.

SIZE: 45 µm–50 µm.

STRATIGRAPHIC RANGE: "Platform Facies" and Moatize Formation.

TOTAL ABUNDANCE: BH 871: 76 specimens.

***Striatoabieites* sp.**

Plate 4: (8).

DESCRIPTION: Amb haploxylonoid to weakly diploxylonoid. Corpus indistinct to discernible, oval in shape. Multistriate proximal surface, sacci crescentic in shape and finely reticulate, smaller than corpus in size.

SIZE: 40 µm–50 µm.

STRATIGRAPHIC RANGE: Moatize Formation.

TOTAL ABUNDANCE: BH 871: 3 specimens.

Genus WEYLANDITES

Weylandites lucifer (Bharadwaj & Salujha) Foster 1975

Plate 4: (9).

DESCRIPTION: **Amb**: Circular, subcircular to oval with elongation in the longitudinal direction. **Corpus**: Exine thin with laevigate taeniae separated by narrow clefts. Taeniae appear to form continuous loops which on crossing the equatorial margin turn approximately 90 degrees. Individual taeniae 1–4 µm wide. Distal surface appears to have an oval to circular area where taeniae are not present. **Sacci**: No sacci evident.

SIZE: 30 µm–40 µm.

STRATIGRAPHIC RANGE: "Platform Facies", Moatize Formation and Matinde Formation.

TOTAL ABUNDANCE: BH 871: 141 specimens; BH 218: 496 specimens.

Subturma STRIATICOLPATES

Genus PAKHAPITES

Pakhapites fusus (Bose and Kar) Menéndez 1971

Plate 4: (10).

DESCRIPTION: Pollen monocolpate, taeniate. **Amb:** longitudinally oval. **Exine:**

1–1.5 µm thick, infrapunctate or laevigate; divided into 10–14 transverse taeniae, 1–2µm wide. **Colpus:** extending full length of grain, centrally constricted, margins occasionally overlapping, fan-shaped at both extremities.

SIZE: 25 µm–45 µm.

STRATIGRAPHIC RANGE: "Platform Facies" and Moatize Formation.

TOTAL ABUNDANCE: BH 871: 67 specimens; BH 218: 4 specimens.

Subturma MONOSACCITES

Infraturma TRILETESACCITI

Genus PLICATIPOLLENITES

Plicatipollenites gondwanensis (Balme & Hennelly) Lele 1964

Plate 5: (1)

DESCRIPTION: **Amb:** Circular, subcircular, occasionally slightly oval. Margin smooth to slightly undulated. **Corpus:** Distinct, circular to subcircular, generally following the contour of the saccus margin. Proximal surface finely reticulate to coarsely granulate, exoexine thickens and may be detached.

SIZE: 65 µm–70 µm.

STRATIGRAPHIC RANGE: "Platform Facies", Moatize Formation and Matinde Formation.

TOTAL ABUNDANCE: BH 871: 99 specimens; BH 218: 20 specimens.

***Plicatipollenites* sp.**

Plate 5: (2)

DESCRIPTION: **Amb**: circular to slightly oval. **Corpus**: distinct. Exhibiting conspicuous intexinal fold system. **Saccus**: finely reticulate.

SIZE: 50 µm–60 µm.

STRATIGRAPHIC RANGE: "Platform Facies".

TOTAL ABUNDANCE: BH 871: 4 specimens.

Genus VITTATINA

Vittatina africana Hart 1966

Plate 5: (3)

DESCRIPTION: **Sacci:** The miospore is haploxylonoid in outline and does not show the development of sacci. The proximal cap is divided into from 9 to 22 longitudinal ribs. The longitudinal ribs meet in a regular fashion so that they form a concentric pattern. The more laterally situated proximal ribs curve round the terminal parts of the miospore and unite on the distal surface. Each terminal area is marked by from 2 to 7 transverse ribs. The inner rib of each terminal area is distinctly wider than the others. The central area is laevigate.

SIZE: 40 µm–50 µm

STRATIGRAPHIC RANGE: "Platform Facies", Moatize Formation and Matinde Formation.

TOTAL ABUNDANCE: BH 871: 126 specimens; BH 218: 162 specimens.

***Vittatina* sp.**

Plate 5: (4)

DESCRIPTION: Pollen striate. **Amb:** oval elongate to sub-circular or broadly oval. Proximal surface with about 11–19 taeniae perpendicular or oblique to long axis of grain, 1–3µm wide; infrastructure finely granulate and punctate. Distally with 3 narrow grooves or sulcus, sharply tapered at either ends, and parallel to long axis of grain.

SIZE: 50 µm–60 µm.

STRATIGRAPHIC RANGE: "Platform Facies" and Moatize Formation.

TOTAL ABUNDANCE: BH 871: 39 specimens; BH 218: 6 specimens.

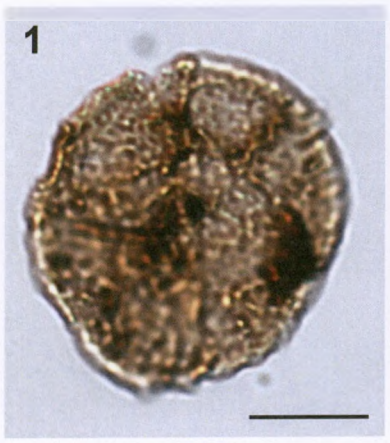

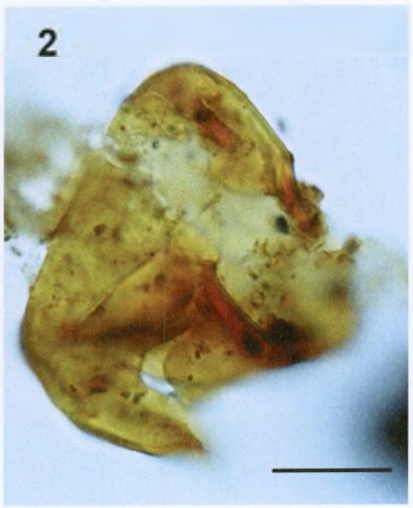

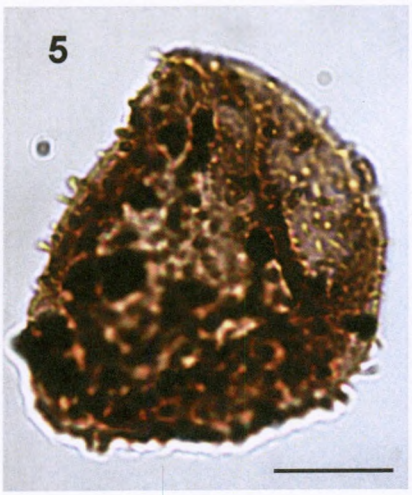

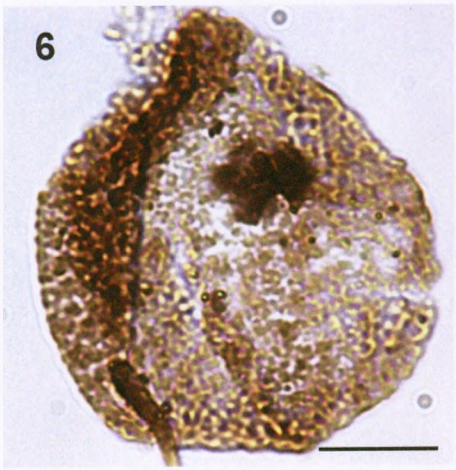

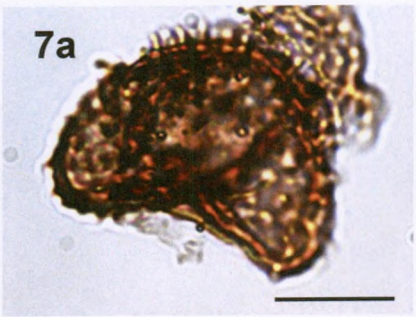

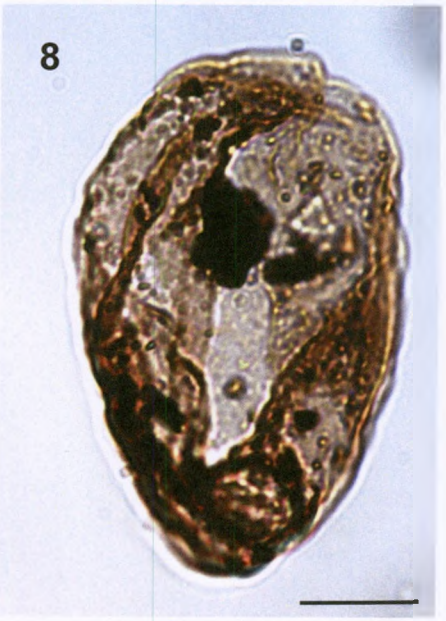

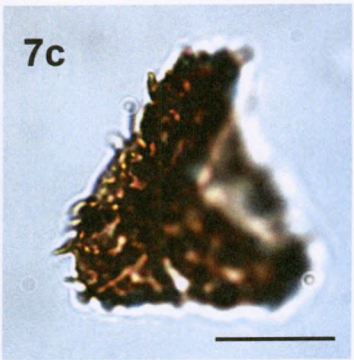

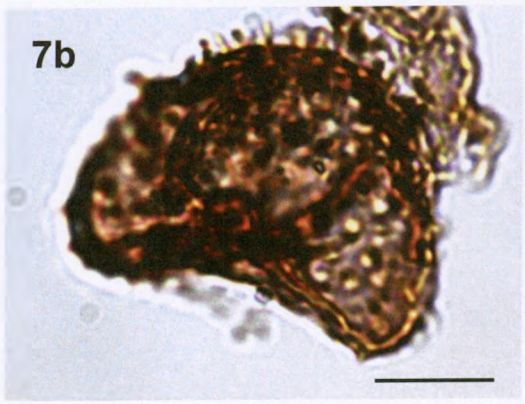

Plate 1

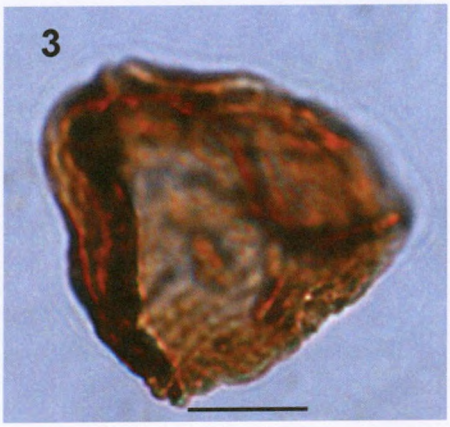

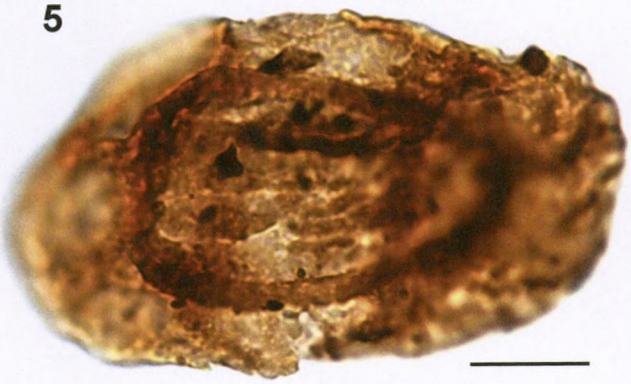

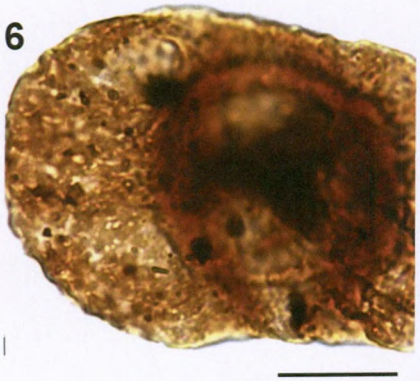

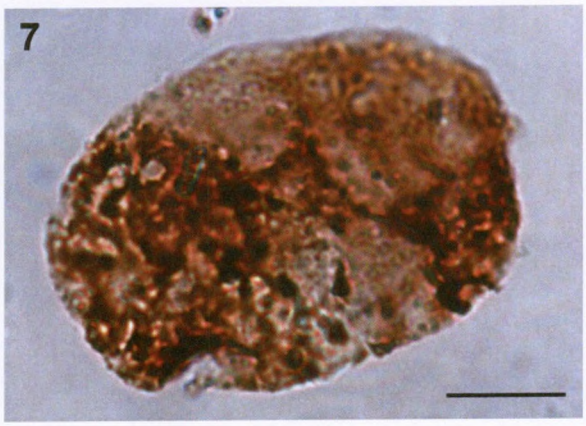

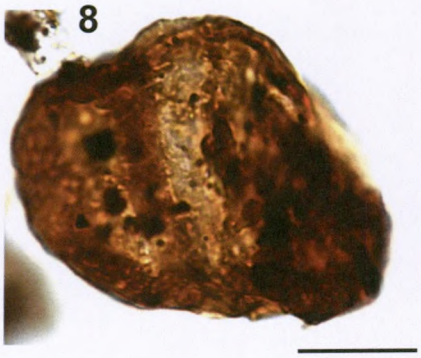

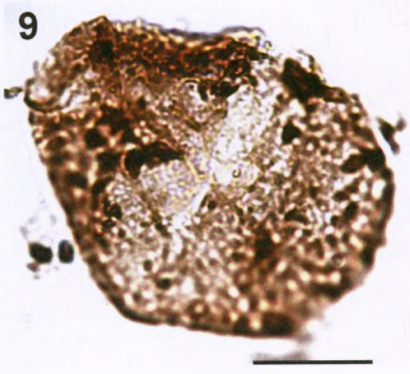

Plate 2

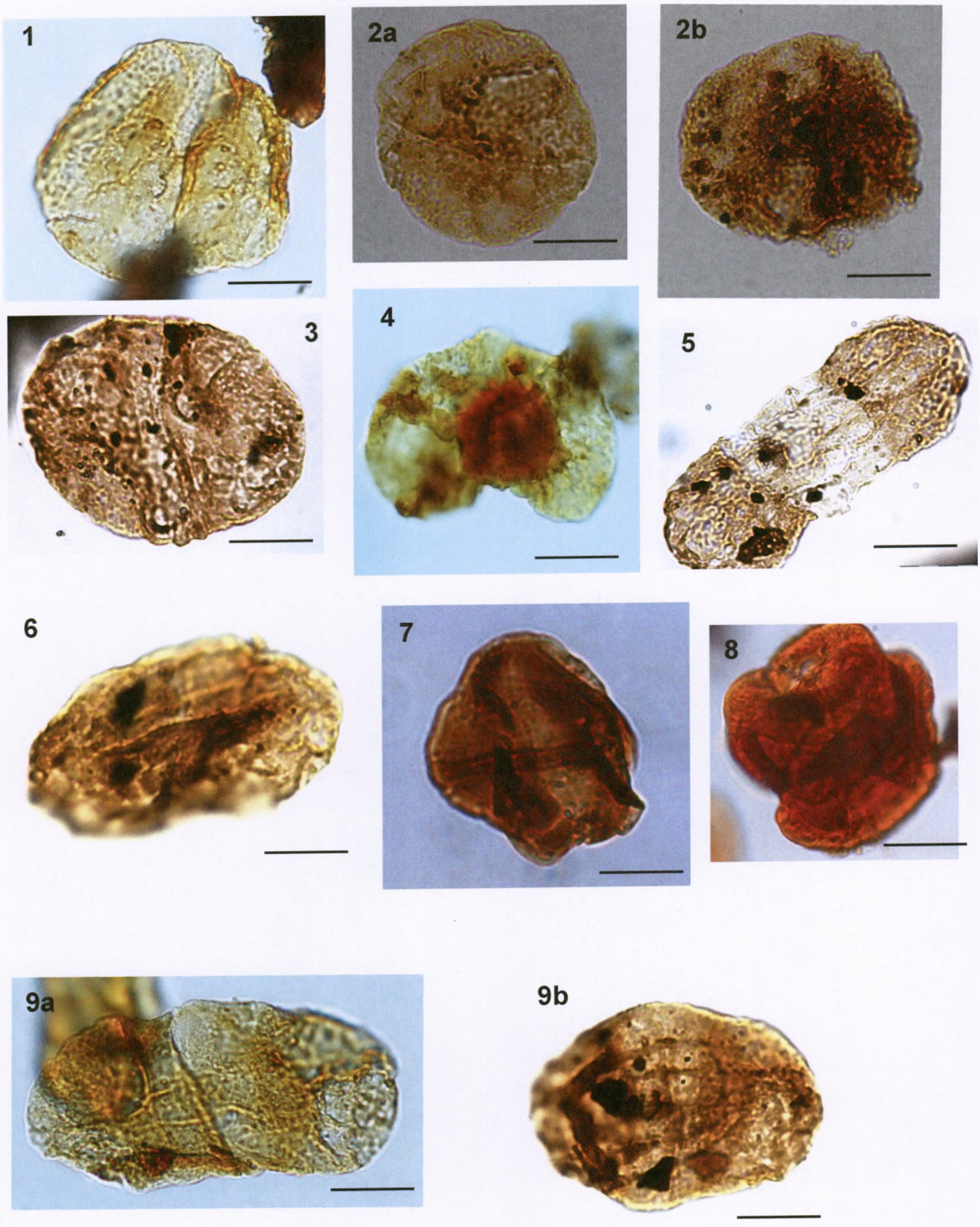

Plate 3

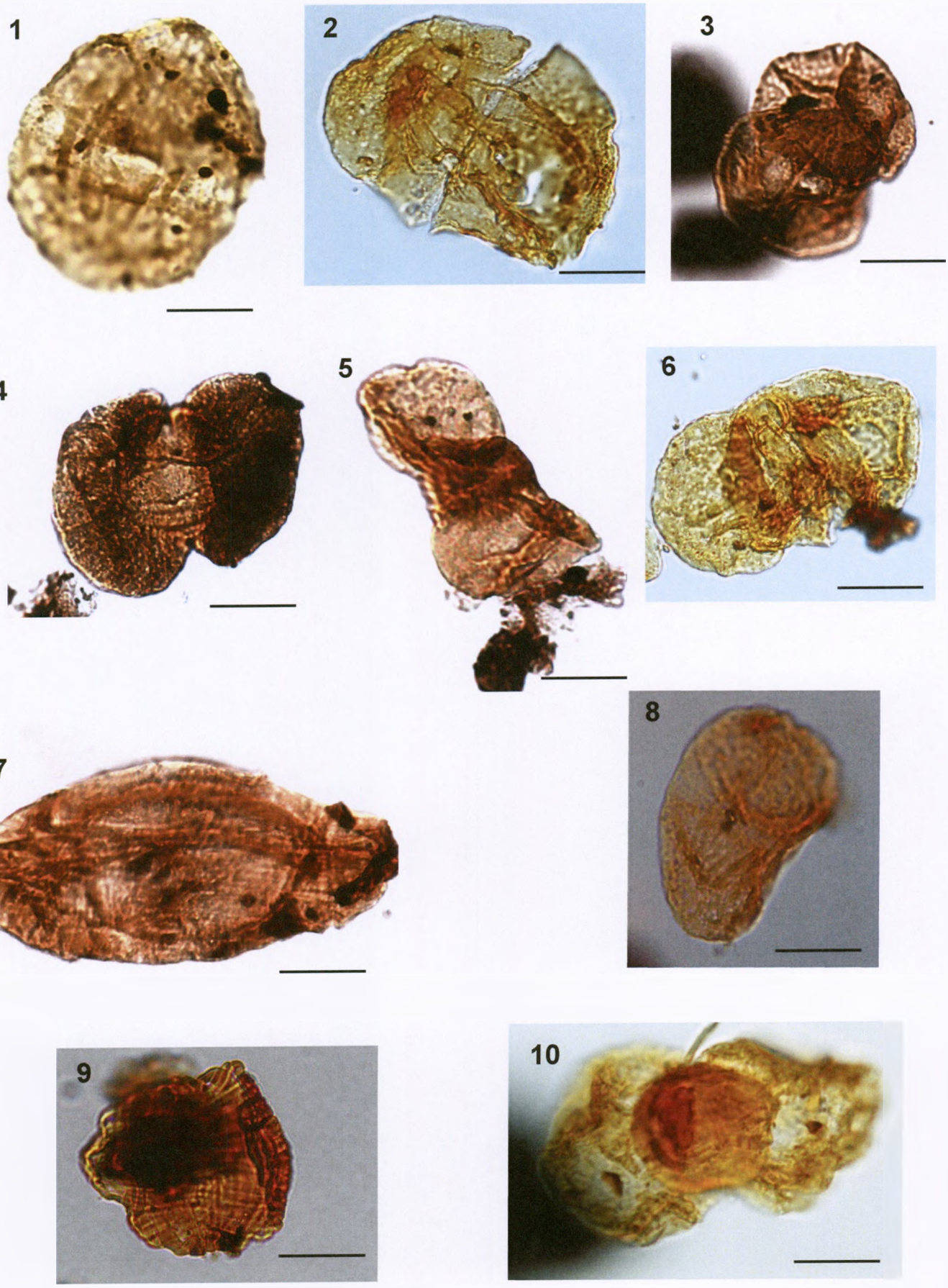

Plate 4

1

2

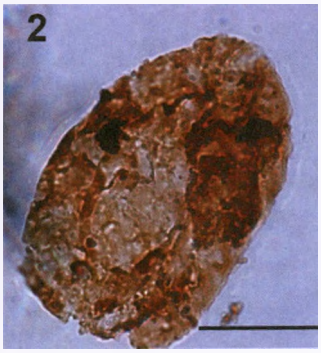

4

3

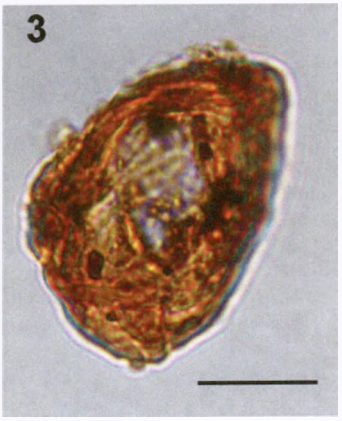

5

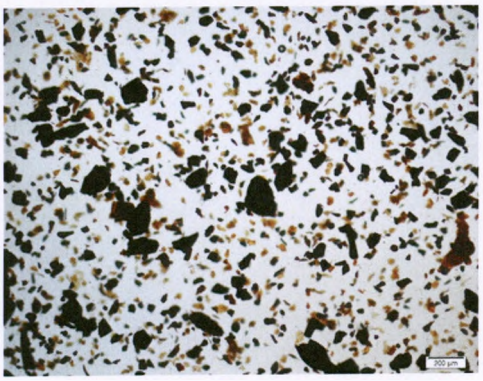

6

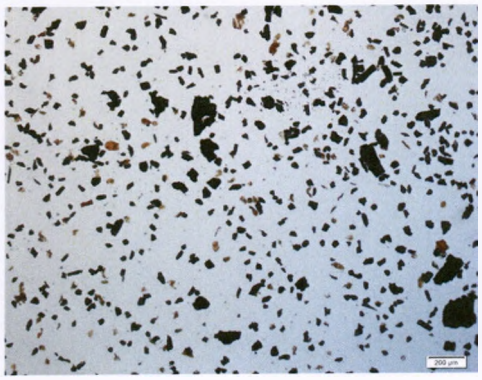

7

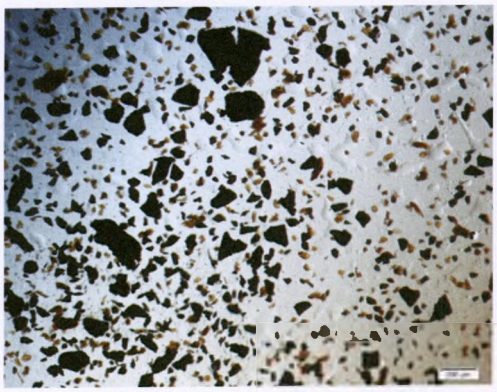

8

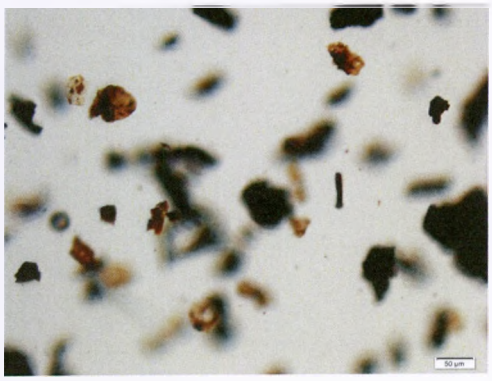

Plate 5

4.2. Statistical Analyses

Statistical analysis was performed using R and R studio for cluster and PCA analysis using the vegan, cluster and rioja packages. The stratigraphic pollen diagrams were made using the C2 program, and Adobe illustrator and Photoshop were used to produce the final diagrams and plates. For the purposes of separating each borehole and its zones, the boreholes are given a simple alphabetic labelling system namely borehole 12 ESD 231 = A, borehole 871D_l012 = B and borehole 12 ESD 218 = C. Borehole 12 ESD 231 zones are labelled as A1 and A2. Borehole 871L_D012 zones are labelled as B1 and B2. Borehole 12 ESD 218 zone is labelled as C1. For PCA biplots, quadrant one is the upper right section, quadrant two is the lower right section, quadrant three is the lower left section and quadrant four is the upper left section.

4.2.1. Borehole 12 ESD 231

4.2.1.1. Productivity

A total of 7 samples were taken from this borehole, with 3 of them being productive. The table below shows the productivity results for borehole 12 ESD 231 (Table 4.1).

Table 4.1: Productivity of borehole 12 ESD 231.

12 ESD 231	
Number of samples	7
Number productive	3
Number unproductive	4
Number Fragmented	0

4.2.1.2. Silhouette Plots and CONISS dendrogram

A series of silhouette plots were produced for a number of possible numbers of clusters within the CONISS dendrogram, from which 2 groups were found most accurate (Figure 4.1). The average silhouette width was 0.28 which meant the 2 clusters were correct. These clusters were then colour coded on the CONISS dendrogram in order to see the exact split of the cluster in sample numbers (Figure 4.2).

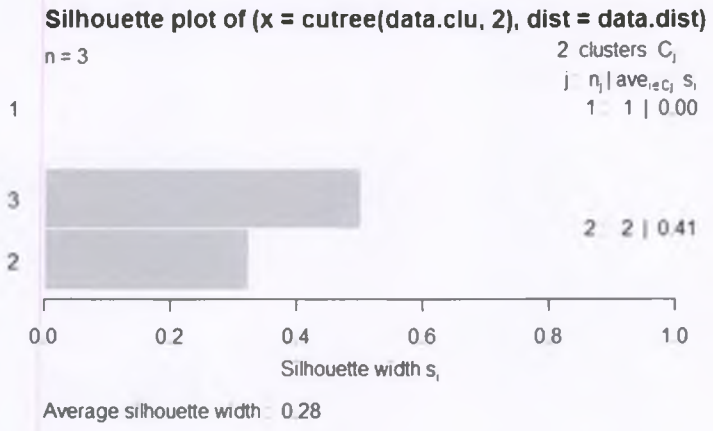

Figure 4.1: Silhouette plot showing a data cluster of 2.

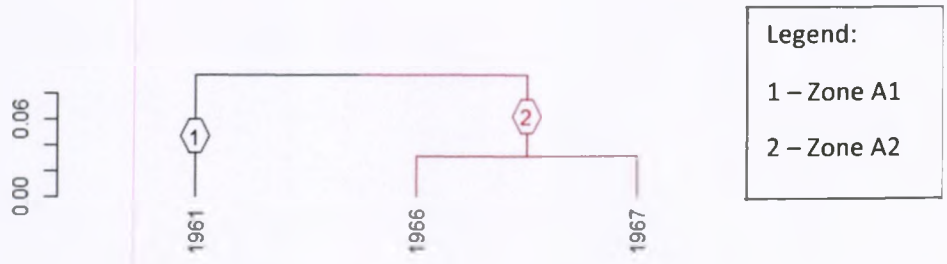

Figure 4.2: CONISS dendrogram showing colour coding of clusters with sample numbers.

4.2.1.3. C2 diagrams with borehole logs

A stratigraphic pollen diagram was plotted using C2 for borehole 12 ESD 231 and the two clusters from the CONISS dendrogram were used to plot two zones on the C2 pollen diagram (Figure 4.3). The zones were plotted at the midpoint depth between the two clusters (approximately 62.30m) in between samples 1961 and 1966. Zone A2 runs from the bottom of the core to 62m. The second zone, zone A1 runs from 63m to the surface.

The C2 diagram shows an almost identical set of species and abundances for both zones in this borehole (Figure 4.3). The most abundant species in borehole 12 ESD 231 are *Scheuringipollenites ovatus* and *Deltoidospora directa* in both zones. Zone A2 has an absence of *Thymospora pseudothiessenii* which is only seen to initiate in zone A1. The latter initiation of this species is most likely the reason for the statistical split of the borehole into two zones.

4.2.1.4. Turmal groups

Borehole 12 ESD 231 shows only four turmal groups being represented (Table 4.2). The most abundant turmal group is the non-taeniate bisaccates (45.66%) followed by triletes (36.52%). Monoletes (10.75%) and aletes (7.07%) are present in lower abundances. A dominance of spore taxa (54.34%) is seen as compared to pollen (45.66%) found in this borehole.

Table 4.2: Table showing percentage abundances of turmal groups found in borehole 12 ESD 231.

Turmal Groups	Percentage Abundance (%)
Triletes	36.52
Monoletes	10.75

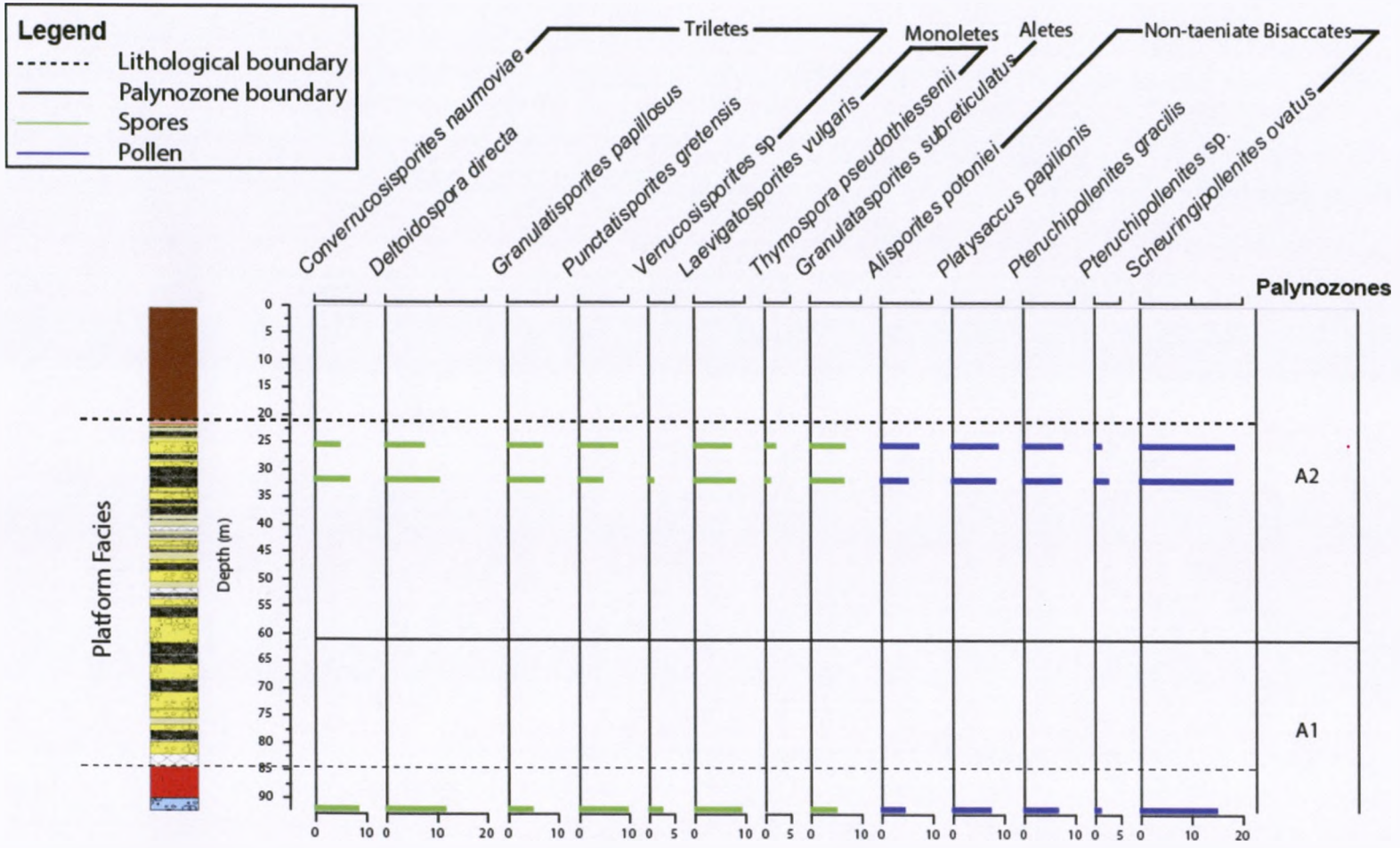

Figure 4.3: Stratigraphic pollen diagram showing palynozones A1 and A2 with geological log for Borehole 12 ESD 231.

Aletes	7.07
Non-taeniate Bisaccates	45.66
Total	100

4.2.1.5. PCA

PC1

PC1 accounts for 84% of the variance based on the sample distribution and sample numbers. PC1 separates the two most positive species scores are *Thymospora pseudothiessenii* (0.7710) and *Alisporites potoniei* (0.2700) from the two most negative species scores *Verrucosisporites* sp. (-0.8014) and *Converrucosisporites naumoviae* (-0.3310). This shows that these species are most statistically different from each other. The sample scores for PC1 were also ranged from highest positive to lowest negative. Since there are only three samples in this borehole, all are included. The two most positive samples are 1967 (0.9639) and 1966 (0.1084). The negative sample score was 1961 (-1.0723) and plotted on the negatively.

PC2

PC2 accounts for another 16% of the variance in samples based on their species distributions. The ranging of most positive to most negative was done for the species scores and sample scores. The two most positive species scores are *Punctatisporites gretensis* (0.3870) and *Alisporites potoniei* (0.0858). The negative of these species scores are *Pteruchipollenites* sp. (-0.2697) and *Verrucosisporites* sp. (-0.2206). The sample scores for PC2 show samples 1961 (0.4939) and 1967 (0.6817) plotting as the most positive with sample 1966 (-1.1756) plotting as most negative.

A PCA biplot was created for sample and species distributions against principal component 1 and 2 (Figure 4.4). The samples are distributed in three of the four

quadrants based on their species abundances. Sample 1967 plots in quadrant one, sample 1966 in quadrant two and sample 1961 in quadrant four. Sample 1967 is driven mostly by the species vector *Alisporites potoniei*. Sample 1966 is driven by the species vectors of *Thymospora pseudothiessenii* and *Pteruchipollenites* sp. Quadrant 3 is driven by the species vector *Verrucosisporites* sp. but no samples plotted here. Sample 1961 is driven by the species vector *Punctatisporites gretensis*. Samples 1966 and 1967 are both from the same CONISS cluster but show a shift of extremes on PC2.

4.2.2. Borehole 871L_D012

4.2.2.1. Productivity

A total of 16 samples were taken from this borehole, with 12 of them being productive. Out of the 12 productive samples, one contained palynomorphs that were too fragmented to identify and count 250 grains. The table below shows the productivity results for borehole 871L_D012 (Table 4.3).

Table 4.3: Productivity of borehole 871L_D012.

871L_D012	
Number of samples	16
Number productive	12
Number unproductive	4
Number Fragmented	1

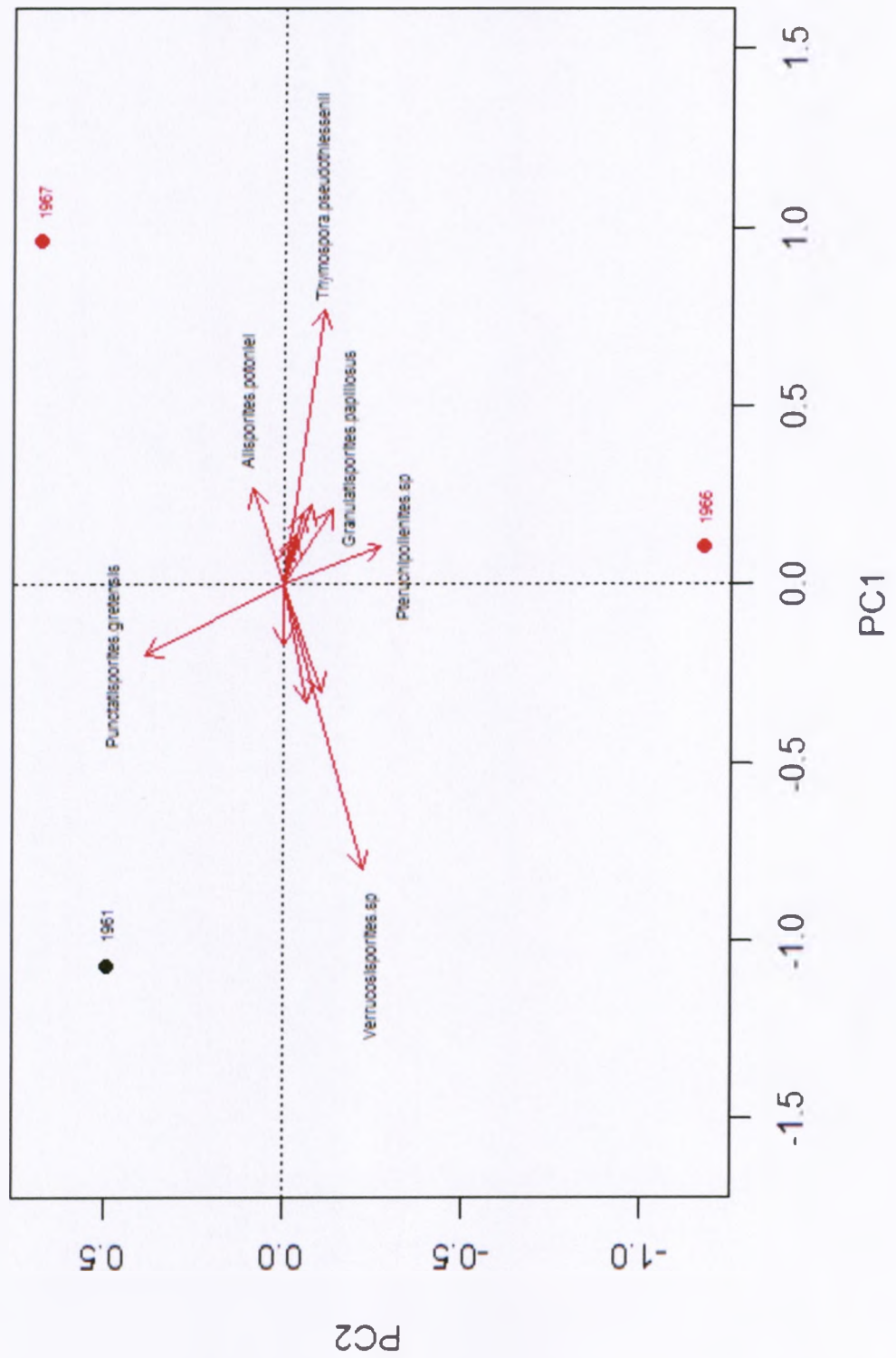

Figure 4.4: PCA biplot showing species and sample number distribution on PC1 and PC2 for borehole 12 ESD 231.

4.2.2.2. Silhouette Plots and CONISS dendrogram

A series of silhouette plots were produced for a number of possible numbers of clusters within the CONISS dendrogram, from which 2 groups were found most accurate (Figure 4.5). The average silhouette width was 0.29 which meant the 2 clusters were correct as most of the samples plotted positively on the silhouette plot (Figure 4.5). These clusters were colour coded on the CONISS dendrogram in order to see the exact split of the cluster in sample numbers (Figure 4.6).

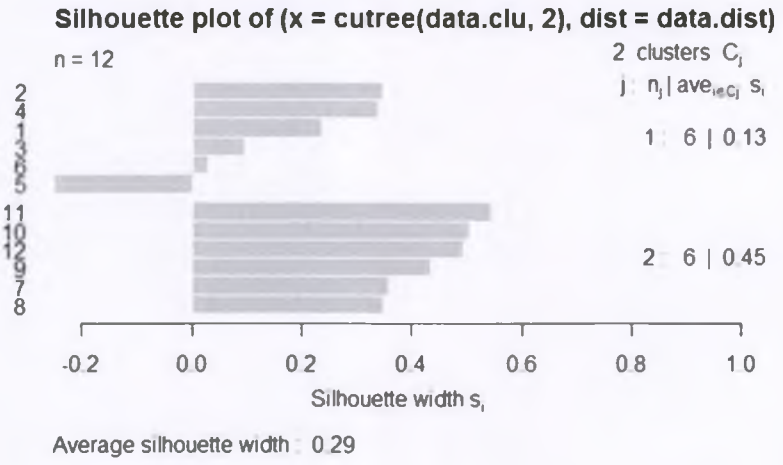

Figure 4.5: Silhouette plot showing a data cluster of 2.

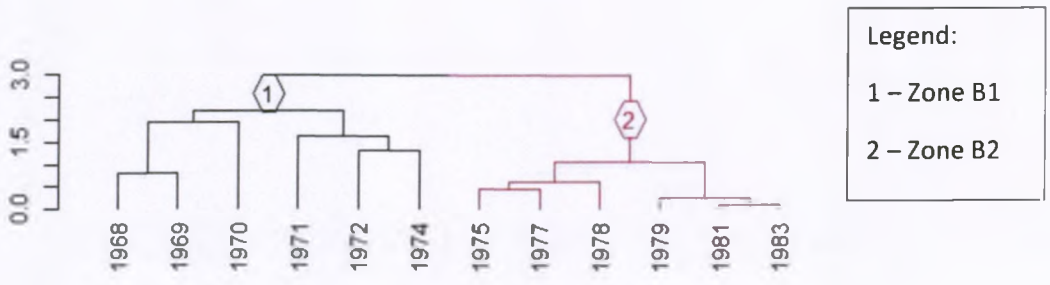

Figure 4.6: CONISS dendrogram showing colour coding of clusters with sample numbers.

4.2.2.3. C2 diagrams with borehole logs

A stratigraphic pollen diagram was plotted using C2 (Figure 4.7). The two clusters from the CONISS dendrogram were used to plot two zones on the C2 pollen diagram. The zones were plotted at the midpoint depth between the two clusters at approximately 116.57m in between sample 1974 and 1975. Zone B2 runs from the bottom of the core to 117m and zone B1 runs from 118m to the surface (Figure 4.7).

Zone B2 is compared with zone A1 and shows the initiation of twenty taxa, two of which are spore taxa and the remaining eighteen being pollen taxa. No termination of taxa is seen in this zone. Zone B1 is then compared to zone B2 and seven taxa initiations are seen with two taxa terminations being visible.

4.2.2.4. Turmal groups

Table 4.4 reflects the percentage abundances for all 9 of the turmal groups found in borehole 871L_012. This borehole shows non-taeniate bisaccates (26.74%) being most abundant followed closely by taeniate bisaccates (25.84%). Triletes have the highest percentage abundance (11.55%) amongst the spores. The borehole is dominated by pollen taxa comprising an overall percentage of 79.28% as compared to spore taxa which comprise a total of 20.72%.

Table 4.4: Table showing percentage abundances of turmal groups found in borehole 871L_D012.

Turmal Groups	Percentage Abundance (%)
Triletes	11.55
Zonotriletes	0.93
Monoletes	5.70
Aletes	2.54

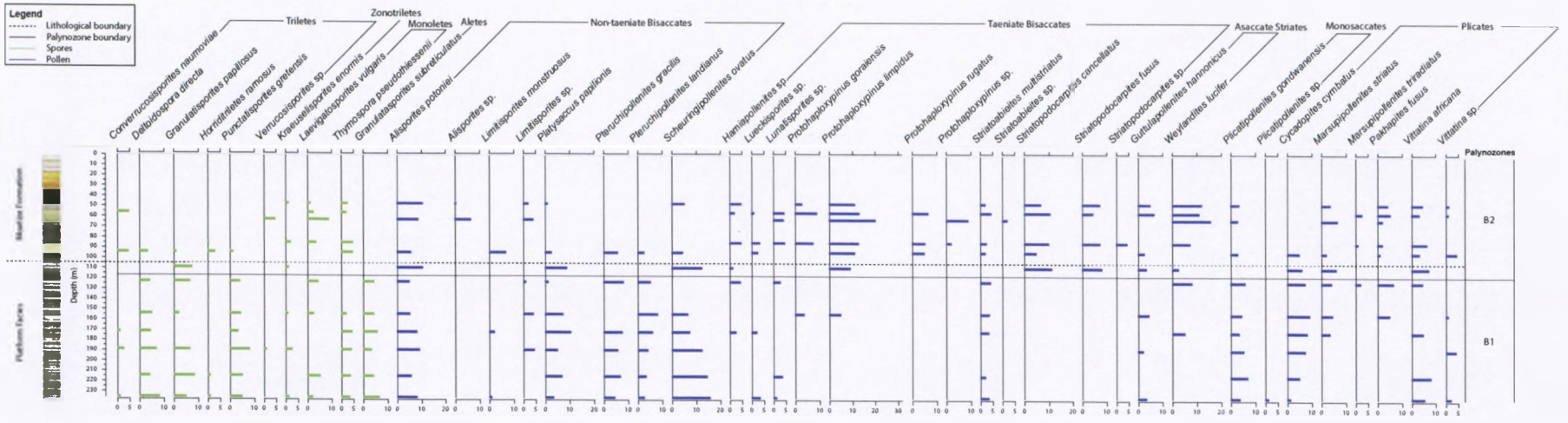

Figure 4.7: Stratigraphic pollen diagram showing palynozones B1 and B2 with geological log for Borehole 871L_D012.

Non-taeniate Bisaccates	26.74
Taeniate Bisaccates	25.84
Asaccate Striates	7.77
Monosaccates	3.42
Plicates	15.51
Total	100

4.2.2.5. PCA

PC1

For borehole 871L_D012, PC1 is explained by 42% of the variance between sample number and species distribution. The species scores and sample scores were sorted to give the extremes on PC1. The two most positive species scores were from *Scheuringipollenites ovatus* (0.8260) and *Deltoidospora directa* (0.7881) are separated on PC1 from the two most negative species score were from *Protohaploxypinus limpidus* (-1.1007) and *Weylandites lucifer* (-0.8631). The sample scores showed samples 1979 (1.7081) and sample 1981 (1.4919) being separated on PC1 positively from sample 1971 (-2.1807) and sample 1969 (-2.1249) which are most negative.

PC2

PC2 is explained by 15% of the variance between samples distribution and sample numbers. This means that PC1 and PC2 explain 57% of the total variance. Sorting of the sample scores showed *Striatopodocarpites cancellatus* (0.6418) and *Vittatina africana* (0.4178) to be the most positive. *Limitisporites* sp. (-0.4671) and *Laevigatosporites* sp. (-0.4331) being most negative. The sample scores for PC2 showed sample 1972 (1.5935) and sample 1969 (1.2871) as most positive and samples 1970 (-3.6206) and sample 1975 (-1.6209) as most negative.

A PCA biplot was then produced showing PC1 and PC2 (Figure 4.6). The first quadrant is influenced mostly by *Scheuringipollenites ovatus.* Sample 1983 seems to cluster mostly with this taxon. Samples 1978, 1981 and 1979 show a cluster forming between quadrant one and two, and is mostly influenced by the vector representing the taxon *Granulatasporites subreticulatus* and *Plicatipollenites gondwanensis.* Samples 1977 and 1975 are most influenced by *Plicatipollenites gondwanensis* and *Limitisporites* sp. Sample 1970 forms an outlier in the third quadrant and the dominating vector in this quadrant is driven by *Weylandites lucifer.* Sample 1968 falls near the negative x-axis as is driven by *Protohaploxypinus limpidus.* The remaining samples in the fourth quadrant (1969, 1971 and 1974) are most likely driven by the dominant vector *Striatopodocarpites cancellatus.*

CONISS cluster 1 is seen to all cluster in quadrants three and four on the negative extreme. Sample 1972 is an outlier from CONISS cluster 1 and plots in quadrant one which shows a slight shift in the species composition and abundances for this sample. CONISS cluster 2 all plot in the extreme of CONISS cluster 1. All the CONISS cluster 2 samples plot in the first and second quadrants.

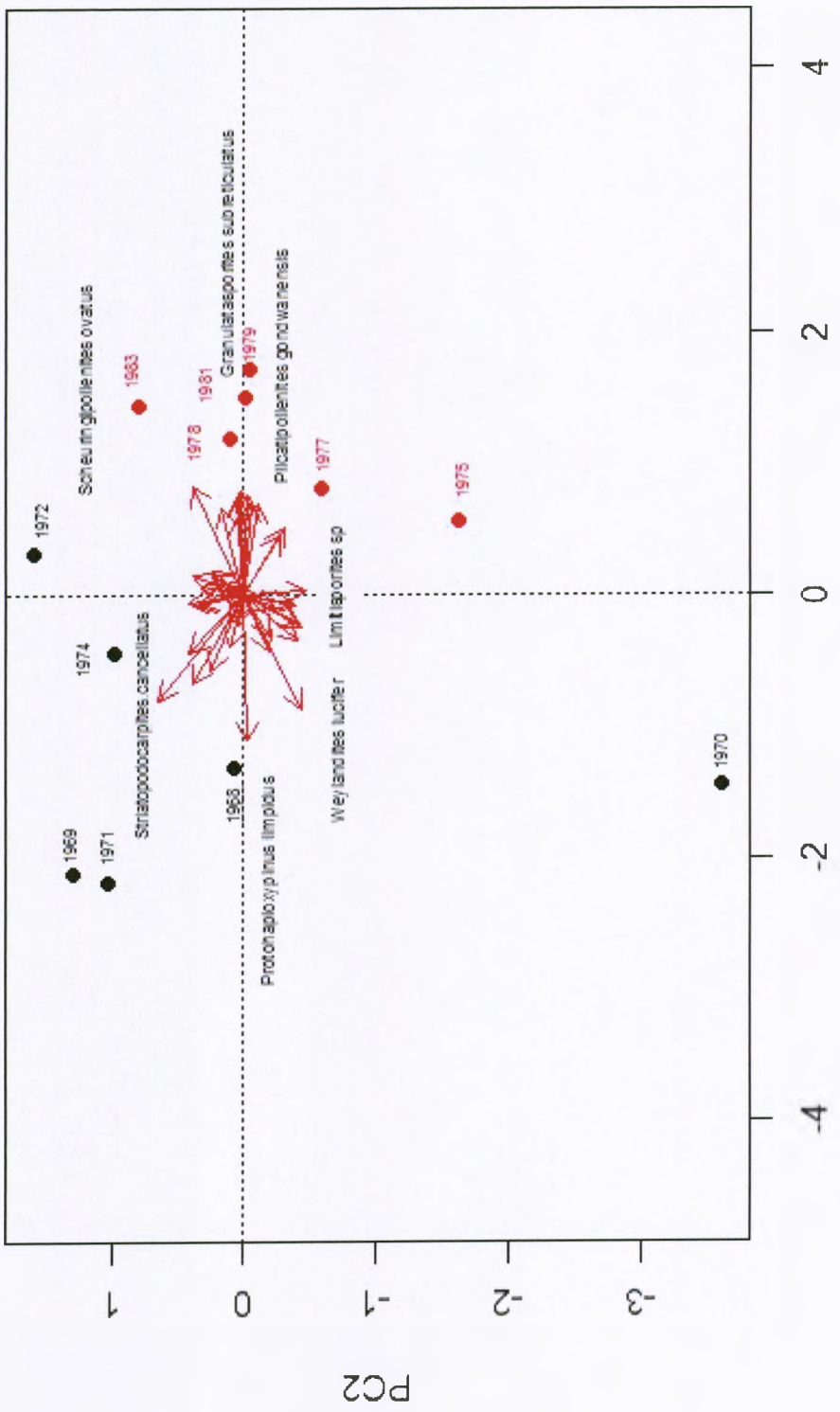

Figure 4.8: PCA biplot showing species and sample number distribution on PC1 and PC2 for borehole 871L_D012.

4.2.3. Borehole 12 ESD 218

4.2.3.1. Productivity

The largest number of samples was taken from this borehole totalling 33 samples. Out of the 33, 19 of them were productive. Out of the 19 productive samples, six of them contained palynomorphs that were too fragmented to identify. The table below shows the productivity results for borehole 12 ESD 218 (Table 4.5).

Table 4.5: Productivity of borehole 12 ESD 218.

12 ESD 218	
Number of samples	33
Number productive	19
Number unproductive	14
Number Fragmented	6

4.2.3.2. Silhouette Plots and CONISS dendrogram

A series of silhouette plots were produced for a number of possible numbers of clusters within the CONISS dendrogram, from which no groups were found most statistically significant for this borehole. Numbers 2 through to 12 were tested as possible data clusters and out of all the results 3 clusters had the best outcome. The average silhouette width was -0.02 which meant the 3 clusters were still not entirely correct (Figure 4.9). However, 3 data clusters gave the least negative silhouette width and the split of the data on the plot was half negative and half positive. This suggests that half the clusters are correct (plotting positively) and half of the clustered samples are incorrect (plotting negatively). Therefore, no statistically significant clusters could be found and the entire dataset for this borehole forms no cluster. The CONISS dendrogram produced shows no clustering of sample numbers (Figure 4.10).

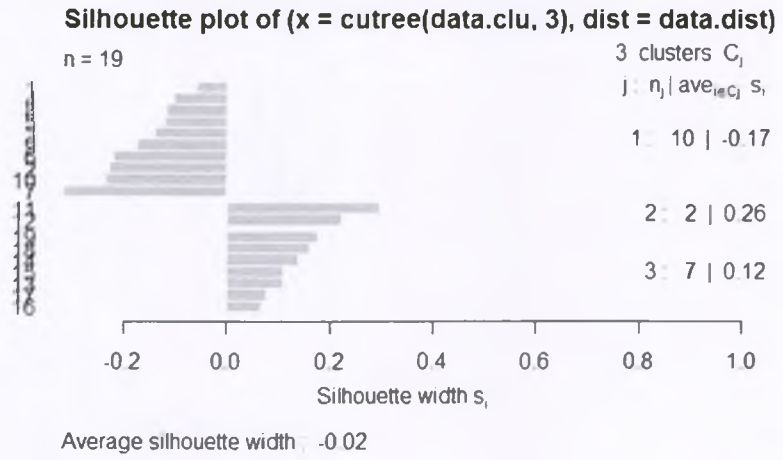

Figure 4.9: Silhouette plot showing a data cluster of 3.

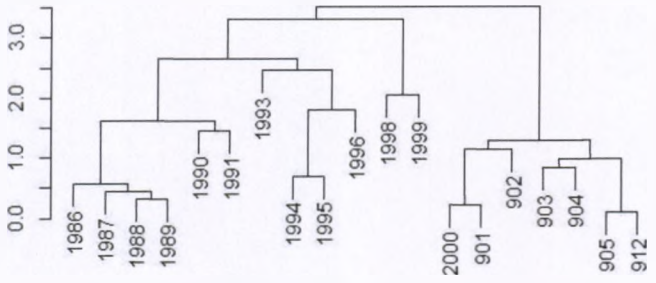

Figure 4.10: CONISS dendrogram showing no clusters with sample numbers.

4.2.3.3. C2 diagrams with borehole logs

A stratigraphic pollen diagram was plotted using C2 (Figure 4.11). The zero clusters from the CONISS dendrogram were used to plot one zone on the C2 pollen diagram. The zone was plotted as the entire stratigraphic range of this borehole. The zone is labelled Zone C1 and runs from the bottom of the core to the surface (Figure 4.11).

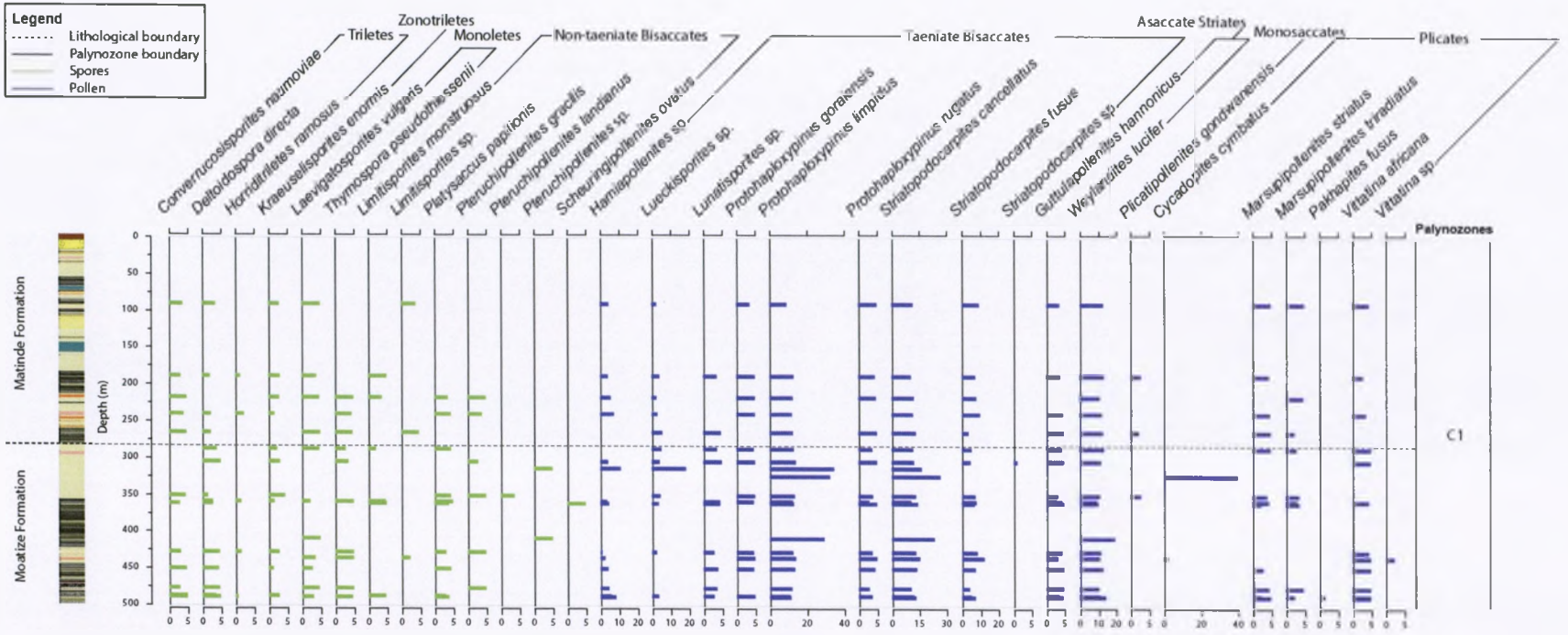

Figure 4.11: Stratigraphic pollen diagram showing palynozone C1 with geological log for Borehole 12 ESD 218.

4.2.3.4. Turmal groups

There are eight turmal groups represented in borehole 12 ESD 218 (Table 4.6). The turmal group that is most dominant in this borehole is the taeniate bisaccates which comprise 52.41%. Asaccate striates (15.10%) and plicates (10.50%) are the next most abundant turmal groups found in borehole 12 ESD 218. Spores comprise an overall percentage of 12.88%, and pollen an overall percentage of 87.12%. This shows that there is a general dominance of pollen species as compared to spores in borehole 12 ESD 218.

Table 4.6: Table showing percentage abundances of turmal groups found in borehole 12 ESD 218.

Turmal Groups	Percentage Abundance (%)
Triletes	5.82
Zonotriletes	1.52
Monoletes	5.54
Non-taeniate Bisaccates	8.69
Taeniate Bisaccates	52.41
Asaccate Striates	15.10
Monosaccates	0.42
Plicates	10.50
Total	100

4.2.3.5. PCA

PC1

For borehole 12 ESD 218, PC1 represents 31% of the variability. *Pteruchipollenites* sp. (0.9007) and *Cycadopites cymbatus* (0.7902) have the two highest species scores and are plotted on the positive extreme. The two most negative scores are *Striatopodocarpites fusus* (-0.8610) and *Weylandites lucifer* (-0.7265). This shows that these species are most statistically different and must have been influenced by the opposite factors to *Pteruchipollenites* sp. and *Cycadopites cymbatus.* The PC1 sample scores show that sample 1998 (2.7988) and sample 1999 (2.5298) are the highest most positive samples. Sample 1995 (-0.7314) and sample 1987 (-0.7121) are the most negative samples scores.

PC2

PC2 accounts for 11% of the total variability between sample distribution and species abundance. This means a total of 42% of total variability is explained by PC1 and PC2. The sample scores show that *Cycadopites cymbatus* (0.8660) and
Thymospora pseudothiessenii (0.4706) are the most positive scores on PC2. On the negative extreme is *Lueckisporites* sp. (-0.7946) and *Pteruchipollenites* sp. (-0.5952). The sample scores for PC2 show samples 1998 (2.5383) and 1990 (2.1388) plotting as most positive. Sample 1999 (-2.3557) and sample 1994 (-1.2896) have the most negative sample scores on PC2.

A biplot was then produced for borehole 12 ESD 218 for PC1 and PC 2 (Figure 4.12). In quadrant one the dominant species vector is *Cycadopites cymbatus* and influences samples 1990 and 1998. There are no clusters seen in quadrant one and therefore both sample 1990 and sample 1998 are seen to be outliers. Quadrant two also has no visible clusters and contains outliers (sample 1993 and 1999). The most dominant vector belongs to *Pteruchipollenites* sp. and is the biggest influencer in this quadrant as seen by the length of the vector. Samples 1996 and 1994 are close to the y-axis and most likely form a cluster based on the

abundance of *Lueckisporites* sp. In quadrant three a cluster is formed with samples 901, 912, 904, 902, 905 and sample 1987. This cluster is driven by a number of species as all the vectors are of relatively similar size and length. Two of the driving vectors in this cluster are *Converrucosisporites naumoviae* and *Marsupipollenites striatus*. Quadrant four shows one cluster of samples 1989, 1988, 1986, 1991 and 1995, 906 and 2000. This cluster is driven by the dominant vectors representing *Thymospora pseudothiessenii, Vittatina africana* and *Striatopodocarpites fusus.*

Samples 1998 and 1999 are plotted on extremes showing that they are major outliers and therefore represent a different set of conditions. Most of the sample points are on the negative axis and near the middle of the biplot showing they all are influenced by similar environmental conditions.

4.3 Palynofloral Composition

The palynofloral composition of the Sanangoé-Mefidezi Basin assemblages comprises trilete, zonotrilete, monolete and alete spores, and non-taeniate bisaccate and taeniate bisaccate, asaccate striate, monosaccate and plicate pollen. Based on the percentage abundances for each turmal group, Table 4.7 shows the level of dominance of each in the individual boreholes respectively. From the table (Table 4.7) triletes and non-taeniate bisaccates are seen in the lowermost borehole (borehole 12 ESD 231). Borehole 871L_D012 shows triletes becoming moderate in abundance with non-taeniate bisaccates remaining dominant, and taeniate bisaccates starting to become dominant as well. The uppermost borehole (borehole 12 ESD 218 shows a shift with triletes and non-taeniate bisaccates becoming rarer, while taeniate bisaccates remain dominant.

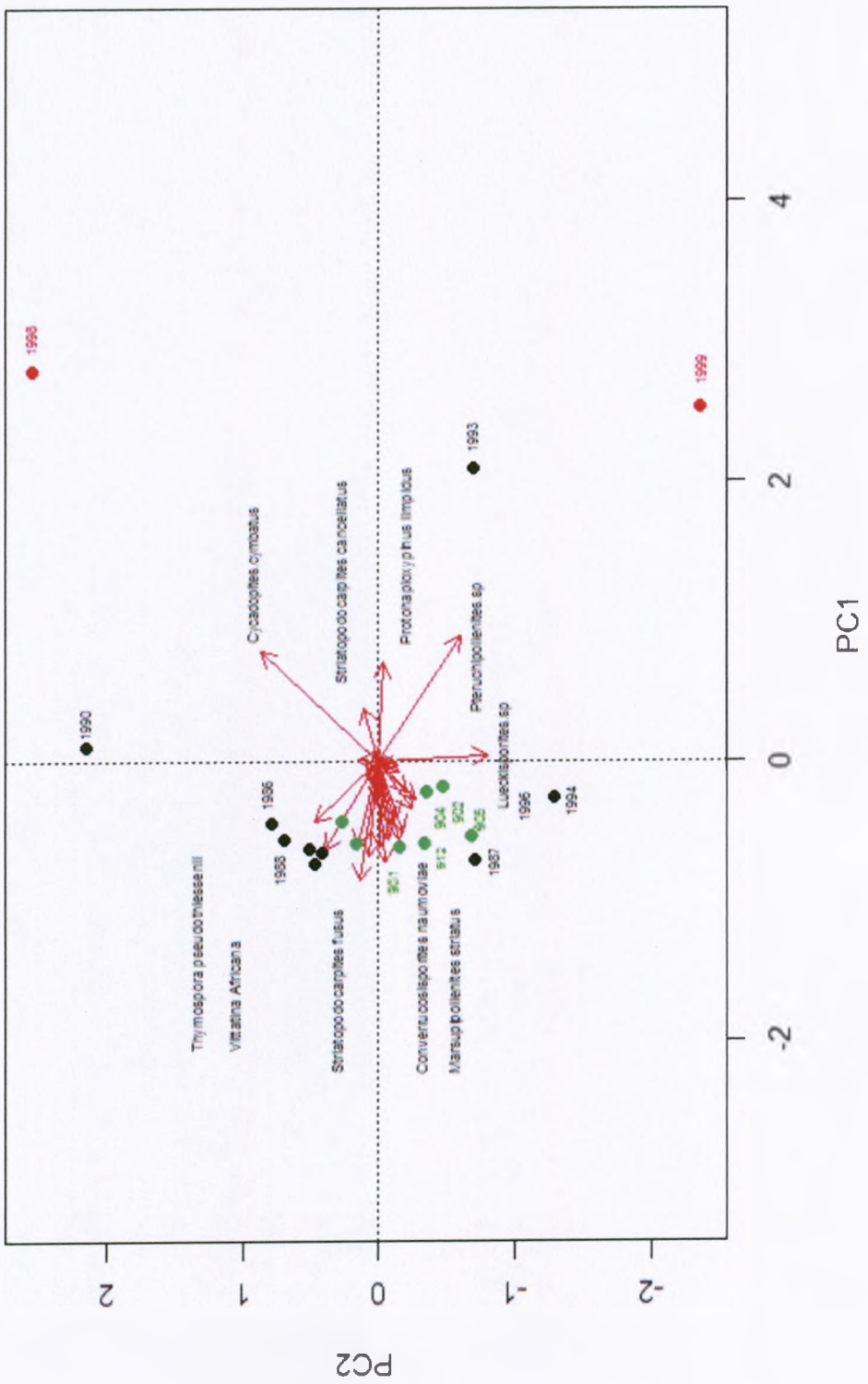

Figure 4.12: PCA biplot showing species and sample number distribution on PC1 and PC2 for borehole 12 ESD 218.

4.3.1 Palynozonation

There are five different kinds of biozones that can be used, namely range zones, interval zones, assemblage zones, abundance zones and linage zones (Murphy & Salvador, 1999). Range zones can be separated into taxon-range zones and concurrent-range zones. Taxon-range zones are the total range occurrence of a specific taxon from all individual section and localities (Murphy & Salvador, 1999). Concurrent-range zones are defined by the overlapping range of two particular taxa (Murphy & Salvador, 1999). Interval zones are defined as the body of fossiliferous strata between two specified biohorizons (Murphy & Salvador, 1999). Assemblage zones are different in that they are defined by three or more taxa that when seen as group separate it from the adjacent strata (Murphy & Salvador, 1999). The fourth type of zone is the abundance zone. Abundance zones are defined by the abundance of specific taxa or group of taxa that are in greater abundance compared to adjacent stata (Murphy & Salvador, 1999). The last type of zone that can be described is the lineage zone. This type is slightly more complex as it requires both identification of taxa and the species following in the successive sections that are part of the same evolutionary linage (Murphy & Salvador, 1999). This may be represented by the entire range of taxa from that lineage or part of the range that occurs beneath the appearance of a descendant taxon (Murphy & Salvador, 1999).

Palynozones can be erected for each of the clusters produced by the CONISS dendrogram (see chapter 3 - results). These zones are named as abundance biozones based on the number of species present. The species present in each zone were totalled and the data ordered from largest to smallest in order to determine the two largest species abundances. The zones are shown in Table 4.7 labelled from the lowermost zone described from the C2 diagrams presented above.

Table 4.7: Turmal group abundance for each borehole with a legend explaining terminology used.

	12 ESD 231	871L_D012	12 ESD 218
Triletes	Dominant	Moderate	Few
Zonotriletes	None	Rare	Few
Monoletes	Moderate	Few	Few
Aletes	Few	Few	None
Non-taeniate Bisaccates	Dominant	Dominant	Few
Taeniate Bisaccates	None	Dominant	Dominant
Asaccate Striates	None	Few	Moderate
Monosaccates	None	Few	Rare
Plicates	None	Moderate	Moderate

Legend
(Based on percentage abundance) None: 0
Rare: 0.1 – 1
Few: 1.01 – 9.99
Moderate: 10 – 19.99
Dominant: > 20

Table 4.8: Table showing the three most abundant species found in each zone described from the C2 diagrams.

Zone	Most Abundant	Second Most Abundant	Third Most Abundant
C1	*Protohaploxypinus limpidus*	*Striatopodocarpites cancellatus*	*Weylandites lucifer*
B2	*Protohaploxypinus limpidus*	*Weylandites lucifer*	*Striatopodocarpites cancellatus*
B1	*Scheuringipollenites ovatus*	*Alisporites potoniei*	*Cycadopites cymbatus*
A2	*Scheuringipollenites ovatus*	*Deltoidospora directa*	*Platysaccus papilionis*
A1	*Scheuringipollenites ovatus*	*Deltoidospora directa*	*Punctatisporites gretensis*

The zones are labelled with the two most abundant species as outlined by the International guidelines for Stratigraphic Nomenclature (Murphy & Salvador, 1999) (Table 4.8). Subzones are given to the zones where two or more zones contain the same two most abundant species. The subzones are named using the name of the third most abundant species (Table 4.8).

The lowermost zone is named the *Scheuringipollenites ovatus-Deltoidospora directa* Zone, with two subzones, the *Punctatisporites gretensis* Subzone (Subzone A1, borehole 12 ESD 231) and the *Platysaccus papilionis* Subzone (Subzone A2, borehole 12 ESD 231).

Borehole 871L_D012 comprises two zones, Zones B1 and B2. Zone B1 is named the *Scheuringipollenites ovatus-Alisporites potoniei* Zone. The overlying zone, Zone B2 is named the *Protohaploxypinus limpidus-Weylandites lucifer* Zone. Both zones B1 and B2 are distinctive.

The third borehole 12 ESD 218 comprises one zone, the *Protohaploxypinus limpidus-Striatopodocarpites cancellatus* Zone, with no subzones. Each zone can be defined by the most abundant and distinctive taxa as well as the initiations and terminations of species that occurs within the zone. The C2 diagrams and cluster analyses as well as the species abundances are used to determine the distinctive taxa for each zone.

***Scheuringipollenites ovatus-Deltoidospora directa* Zone**

***Punctatisporites gretensis* Subzone (A1):**

This subzone extends from approximately 100 m to approximately 50m in borehole 12 ESD 231. This subzone forms part of the "Platform Facies" informal lithostratigraphic unit. The zone is named after two of the most abundant species, with a subzone defined by the third most abundant species, informally called Subzone A1. As this is the lowermost zone defined in the borehole stratigraphic succession, species appearances may not represent true initiation depths. No species terminations are seen within this subzone. The most abundant taxa are listed below:

Scheuringipollenites ovatus

Deltoidospora directa

Punctatisporites gretensis

Laevigatosporites vulgaris

Converrucosisporites naumoviae

Platysaccus papilionis

Pteruchipollenites gracilis

***Platysaccus papilionis* Subzone (A2):**

This subzone is the uppermost zone in borehole 12 ESD 231 and also spans the "Platform Facies" unit. The extent of the subzone is from approximately 51 m to surface. This subzone is informally named Subzone A2. There are only two productive samples in this zone, which is very similar to Subzone A1 but differentiated by the initiation of one new taxon, *Thymospora pseudothiessenii* (designated as an initiation by the symbol I in brackets). No terminations are observed in this subzone.

Thymospora pseudothiessenii (I)

A list of the most abundant species found in this zone are given below:

Scheuringipollenites ovatus

Deltoidospora directa

Platysaccus papilionis

Laevigatosporites vulgaris

Pteruchipollenites gracilis

Granulatisporites papillosus

Granulatasporites subreticulatus

Punctatisporites gretensis

Alisporites potoniei

Converrucosisporites naumoviae

***Scheuringipollenites ovatus-Alisporites potoniei* Zone (B1):**

This zone is the lowermost zone in borehole 871L_D012 and also extends through the "Platform Facies" unit. The extent of this zone is approximately 240 m to approximately 115 m. This zone is distinctive, does not comprise any subzones, and is informally named Zone B1. A very high number of initiations (20) and no terminations are seen in this zone.

Horriditriletes ramosus (I)

Kraeuselisporites enormis (I)

Limitisporites monstruosus (I)

Limitisporites sp. (I)

Hamiapollenites sp. (I)

Lueckisporites sp. (I)

Lunatisporites sp. (I)

Protohaploxypinus goraiensis (I)

Protohaploxypinus limpidus (I)

Striatoabieites multistriatus (I)

Guttulapollenites hannonicus (I)

Weylandites lucifer (I)

Plicatipollenites gondwanensis (I)

Plicatipollenites sp. (I)

Cycadopites cymbatus (I)

Marsupipollenites striatus (I)

Marsupipollenites triradiatus (I)

Pakhapites fusus (I)

Vittatina africana (I)

Vittatina sp. (I)

The most abundant species are listed below:

Scheuringipollenites ovatus

Alisporites potoniei

Platysaccus papilionis

Deltoidospora directa

Pteruchipollenites gracilis

Punctatisporites gretensis

Pteruchipollenites landianus

Granulatasporites subreticulatus

Granulatisporites papillosus

***Protohaploxypinus limpidus* - *Weylandites lucifer* Zone (B2):**

This zone is the uppermost zone in borehole 871L_D012 and spans part of the Moatize Formation, the unit overlying the "Platform Facies" informal unit. The depth of this zone extends from approximately 116 m to surface. This zone is distinct and also contains no subzones, being informally termed Zone B2. Seven species initiations and two terminations (designated by the symbol T in brackets) are noted in this zone.

Alisporites sp. (I)

Protohaploxypinus rugatus (I)

Protohaploxypinus sp. (I)

Striatoabieites sp. (I)

Striatopodocarpites cancellatus (I)

Striatopodocarpites fusus (I)

Striatopodocarpites sp. (I)

Granulatasporites subreticulatus (T)

Plicatipollenites sp. (T)

The most abundant species in this zone are listed below:

Protohaploxypinus limpidus

Weylandites lucifer

Alisporites potoniei

Vittatina africana

Scheuringipollenites ovatus

Protohaploxypinus goraiensis

Marsupipollenites striatus

***Protohaploxypinus limpidus* - *Striatopodocarpites cancellatus* Zone (C1):**

This zone is the only palynozone of borehole 12 ESD 218 and spans the Moatize and Matinde formations. The extent of the zone is from approximately 500 m to surface. The zone is informally named Zone C1. There are no new species initiations in this zone and sixteen species terminations labelled with a (T).

Granulatisporites papillosus (T)

Punctatisporites gretensis (T)

Verrucosisporites sp. (T)

Alisporites potoniei (T)

Alisporites sp. (T)

Pteruchipollenites sp. (T)

Pteruchipollenites landianus (T)

Protohaploxypinus sp. (T)

Striatoabieites multistriatus (T)

Striatoabieites sp. (T)

Striatopodocarpites sp. (T)

Plicatipollenites sp. (T)

Scheuringipollenites ovatus (T)

Cycadopites cymbatus (T)

Pakhapites fusus (T)

Vittatina sp. (T)

A list of the most abundant species are given below for Zone C1.

Protohaploxypinus limpidus

Striatopodocarpites cancellatus

Weylandites lucifer

Striatopodocarpites fusus

Guttulapollenites hannonicus

Vittatina africana

Protohaploxypinus goraiensis

Hamiapollenites sp.

Protohaploxypinus rugatus

Thymospora pseudothiessenii

Deltoidospora directa

Converrucosisporites naumoviae

4.3.2 Palynomorph Ranges

A range diagram was plotted in order to see which species are long ranging species (occur throughout the "Platform Facies", Moatize and Matinde formations) and which species are shorter ranging (Figure 4.13). This helps
identify which are the more useful distinguishing species for biostratigraphic correlation. The longer ranging species (orange lines) are not as useful for correlating or distinguishing palynozones as they occur throughout the three boreholes and are found in every lithological formation in this study (Platform Facies", Moatize and Matinde formations). The shorter ranging species (blue and green lines) are more useful as they only appear for specific periods of time and in certain formations making them more useful for correlation.

A list of the short ranging species that occur in one formation only is given below and displayed as green lines in Figure 4.13:

Granulatasporites subreticulatus ("Platform Facies")

Plicatipollenites sp. ("Platform Facies")

Alisporites sp. (Moatize Formation)

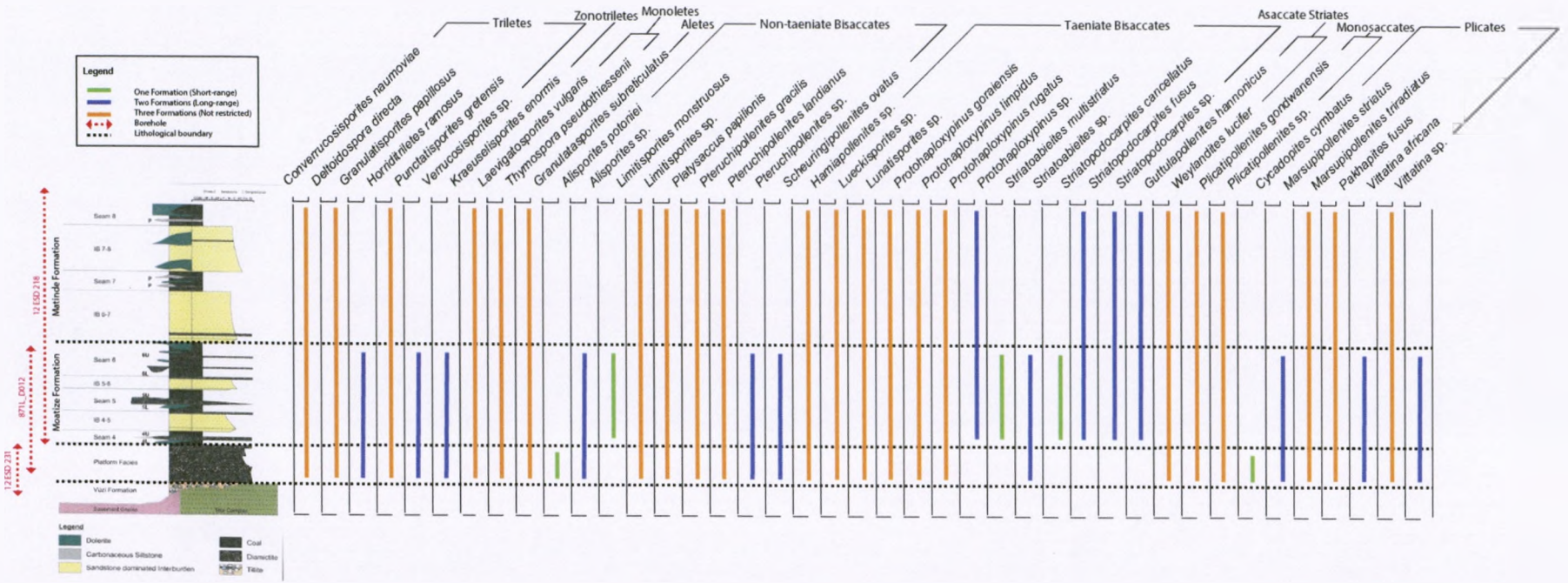

Figure 4.13: Palynomorph range diagram showing species distributions over the "Platform Facies", Moatize and Matinde formations with composite borehole log.

Protohaploxypinus sp. (Moatize Formation)

Striatoabieites sp. (Moatize Formation)

The species that are slightly longer ranging (crossing two formations) are listed below with their lithological units. These are displayed as blue lines in Figure 4.13:

Granulatisporites papillosus ("Platform Facies" and Moatize Formation)

Punctatisporites gretensis ("Platform Facies" and Moatize Formation)

Verrucosisporites sp. ("Platform Facies" and Moatize Formation)

Alisporites potoniei ("Platform Facies" and Moatize Formation)

Pteruchipollenites landianus ("Platform Facies" and Moatize Formation)

Pteruchipollenites sp. ("Platform Facies" and Moatize Formation)

Striatoabieites multistriatus ("Platform Facies" and Moatize Formation)

Cycadopites cymbatus ("Platform Facies" and Moatize Formation)

Pakhapites fusus ("Platform Facies" and Moatize Formation)

Vittatina sp. ("Platform Facies" and Moatize Formation)

Protohaploxypinus rugatus (Moatize Formation and Matinde Formation)

Striatopodocarpites cancellatus (Moatize Formation and Matinde Formation)

Striatopodocarpites fusus (Moatize Formation and Matinde Formation)

Striatopodocarpites sp. (Moatize Formation and Matinde Formation)

The long ranging species which are not as useful in correlating cover all three formations ("Platform Facies", Moatize Formation and Matinde Formation) and are listed below and displayed as orange lines in Figure 4.13:

Converrucosisporites naumoviae

Deltoidospora directa

Horriditriletes ramosus

Kraeuselisporites enormis

Laevigatosporites vulgaris

Thymospora pseudothiessenii

Limitisporites monstruosus

Limitisporites sp.

Platysaccus papilionis

Pteruchipollenites gracilis

Scheuringipollenites ovatus

Hamiapollenites sp.

Lueckisporites sp.

Lunatisporites sp.

Protohaploxypinus goraiensis

Protohaploxypinus limpidus

Guttulapollenites hannonicus

Weylandites lucifer

Plicatipollenites gondwanensis

Marsupipollenites striatus

Marsupipollenites triradiatus

Vittatina africana

4.3.3. Borehole Correlation

The three sampled boreholes were correlated on their palynomorph content using the statistical clustering analyses described in Section 4.2, in order to determine their degree of overlap as well as stratigraphic ordering of the designated palynozones (Figure 4.14).

A dominance of spores is seen in the lower lithological unit ("Platform Facies") with six out of the ten being spore species in borehole 12 ESD 231 (Figure 4.14). to dominate the assemblages. Borehole 871L_D012 contains two spore and eight pollen species (Figure 4.13). The uppermost borehole, 12 ESD 218 displays an overwhelming dominance of pollen species with all ten most abundant species being pollen (Figure 4.14).

Table 4.9: shows that there is a transition from a more spore dominated assemblage in borehole 12 ESD 231 to an assemblage containing similar proportions of spores and pollen in borehole 871L_D012, in turn changing to a pollen dominated assemblage in borehole 12 ESD 218.

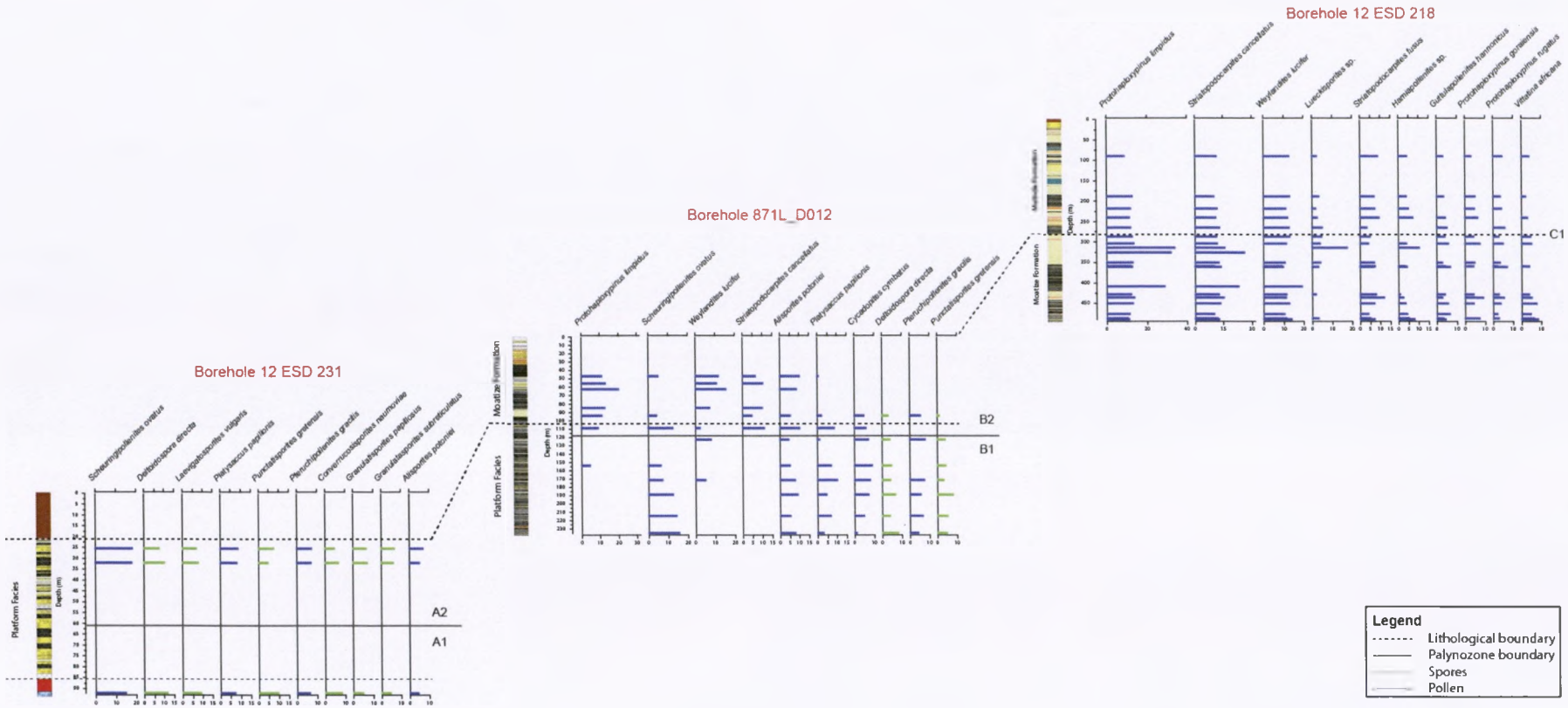

Figure 4.14: Composite diagram of ten most abundant species in all three boreholes showing inferred lithological boundary with palynozones.

Table 4.9: Table showing top ten most abundant species used to plot Figure 4.14. Green represents spore species present in boreholes 12 ESD 231 and 871L_D012. Blue represents the pollen species found in both boreholes 871L_D012 and 12 ESD 218. Species in black are present in one borehole only.

Borehole 12 ESD 231	**Borehole 871L_D012**	**Borehole 12 ESD 218**
Scheuringipollenites ovatus	*Protohaploxypinus limpidus*	*Protohaploxypinus limpidus*
Deltoidospora directa	*Scheuringipollenites ovatus*	*Striatopodocarpites cancellatus*
Laevigatosporites vulgaris	*Weylandites lucifer*	*Weylandites lucifer*
Platysaccus papilionis	*Striatopodocarpites cancellatus*	*Striatopodocarpites fusus*
Punctatisporites gretensis	*Alisporites potoniei*	*Hamiapollenites* sp.
Pteruchipollenites gracilis	*Cycadopites cymbatus*	*Guttulapollenites hannonicus*
Converrucosisporites naumoviae	*Platysaccus papilionis*	*Protohaploxypinus goraiensis*
Granulatisporites papillosus	*Deltoidospora directa*	*Protohaploxypinus rugatus*
Granulatasporites subreticulatus	*Pteruchipollenites gracilis*	*Vittatina africana*
Alisporites potoniei	*Punctatisporites gretensis*	*Lueckisporites* sp.

4.4 Palynofacies

Palynofacies represents the total assemblage of organic components that are acid resistant and are able to survive the chemical process carried out to extract palynomorphs. Palynofacies are a useful palynological tool in order to determine palaeoenvironments and what climatic conditions prevailed during the time of deposition as well as diagenesis (Combaz, 1964). The organic debris is referred to as Amorphous Organic Matter (AOM) which represents altered organic debris that has no definitive cellular structure. In most cases the AOM occur simultaneously with palynomorphs, and can occur in large clusters or can be spread out. By studying the palynofacies we can infer which variables had an impact on the deposition and preservation. A number of factors such as climate, tectonics, and changes in sea level play a role in differentiating depositional environments on a global scale. On a regional scale the sediment amount as well as rate of accumulation, proximity and composition of the water as well as biological activity within it, impact the sediment accumulation and how well the organic matter is preserved (Batten, 1996). Palynofacies has been useful in

representing hydrocarbon potential in a specific lithological unit as palynology can indicate environmental as well as source potential information (Batten, 1996). Amorphous Organic Matter requires anoxic depositional environments in order for successful preservation to occur (Batten, 1982).

The palynofacies from the Sanangoé-Mefidezi Basin show a significant amount of amorphous organic matter (AOM) even after increasing the oxidation time (Plate 5, 5–8). Any longer oxidation would result in the palynomorphs being damaged and over-oxidized. Therefore, the remaining AOM is examined and Figure 4.15 summarizes the results found.

There is a medium to high preservation of opaque phytoclasts that remain in the sample and are usually of irregular shape. An average amount (>50%) of translucent phytoclasts also seen in samples. In most samples however, there is a mixture of both translucent and opaque phytolasts. A high amount of pollen and spores are preserved in all boreholes examined. Overall the Sanangoé-Mefidezi Basin shows a great amount of darkly coloured degraded organic matter. This could be due to transportation and reworking of sediments. No algae is noted in the samples examined in this study.

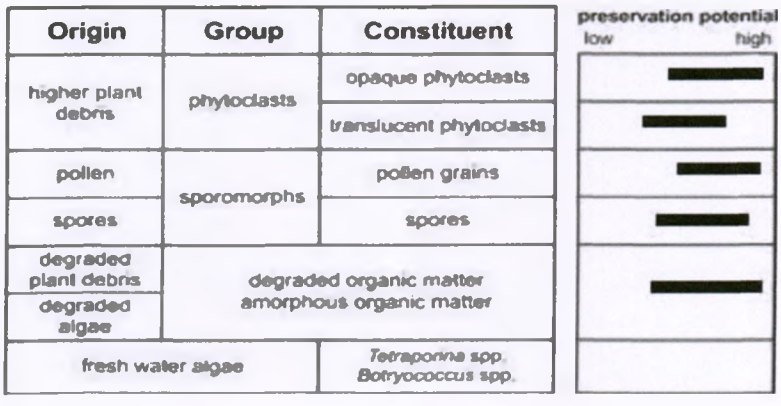

Figure 4.15: Visual composition of the palynofacies of the Sanangoé-Mefidezi Basin rocks, adapted from Batten (1996).

5. Discussion

5.1. Preparation methods

A number of methods exist for preparation of Permian-aged sediments and these should be modified depending on the specific sample lithologies. The method of Phipps and Playford (1984) was found to be best suited for the Mozambique samples in the current study. The samples comprised mostly carbonaceous mudstone with interbedded coal and accordingly acetolysis was not performed as the samples were much older than Quaternary, where sediments can contain cellulose.

5.1.1. Oxidation

Oxidation is a step that needed to be carried out with caution as too little time can create microscope slides with an excess of amorphous organic matter (AOM), which obscures palynomorphs. Too much time spent under oxidation can cause degradation of the palynomorphs making it difficult to identify structures on the palynomorphs (therefore species). An oxidation time of approximately 20 minutes was determined to be the correct period for these samples as they contained a high quantity of amorphous organic matter.

5.1.2. Zinc Chloride

During the Zinc Chloride step caution needed to be taken as the Zinc Chloride needs to be of specific gravity 2.0. During the initial round of preparation an inferior product was delivered by the supplier, the prepared centrifuge tubes were uncharacteristically heavy and the centrifuge could not balance. It was also noted that the zinc chloride step did not separate the samples out sufficiently (three distinct layers of zinc chloride, supernatant and sediment were not visible). This in turn meant that the palynomorphs had not been separated out properly. Although microscope slides were made from these samples, they could not be used as a true representation of the palynomorph concentration. Therefore, all samples had to be

reprocessed from the start, making sure the zinc chloride was of the correct specific gravity in order to get an accurate representation of the palynomorph concentration.

5.2. Modern contamination

Throughout the entire process caution was taken in order to not cause contamination of the samples. Clean labelled equipment was used for each sample and preparation was carried out in a closed laboratory. However, some contamination can occur with modern pollen. In these samples (Figure 5.1), a few modern grains and a diatom were seen under the microscope, but as the samples were of Permian age, these modern contaminants were easily distinguished from the fossil palynomorphs due to the large size, colour and cells being present indicating that reproduction can still occur (Moore *et al.*, 1991). Therefore, these did not affect the counts of Permian palynomorphs.

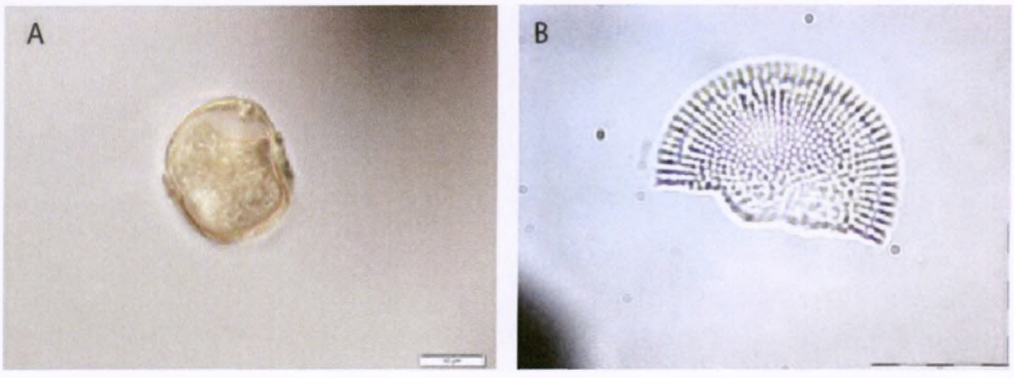

Figure 5.1: Images of modern contamination. A = modern pollen, B = modern diatom.

5.3. Thermal Maturity

An assessment of the thermal maturity of coal-bearing strata is useful in that it can give an indication of the hydrocarbon potential of the rocks, and can also predict the quality of coal that can be mined. A number of methods exist on how to determine the thermal maturity of the sediments but are mostly expensive and require advanced testing methods. The colour method used by palynology is easier as well as more cost effective and can give a good indication of thermal maturity. Palynological testing makes use of the fact that when rocks

are subjected to certain degrees of metamorphism, their contained palynomorphs change colour which is an indicator of the thermal maturity (Barbolini, 2010). However, as with all methods some disadvantages do exist, such as palynomorphs of the same thermal maturity can appear different in colour due to the wall
thickness and composition of each individual grain (Barbolini, 2010; Pross *et al.*, 2007). Yule *et al.* (1998) also noted that small changes in temperature can cause rapid colour changes within individual samples.

Palynomorph colouration is most often judged by eye so a number of classification charts exist and can be subjective due to different interpretations of colour. A number of improvements are being worked on but are not being used frequently yet. Due to this the method chosen for the determination of thermal maturity in the Sanangoé-Mefidezi Basin was determination of colour by eye using the Thermal Alteration Scale of Batten (1980) as a comparative chart (Table 5.1).

Table 5.1: Thermal Alteration Scale of Batten (1980).

Observed colour of palynomorphs	**Significance for hydrocarbons**
1. colourless, pale yellow, yellowish green	Chemical change negligible; organic matter immature, having no source potential for hydrocarbon
2. yellow	Some chemical change, but organic matter still immature
3. light brownish yellow, yellowish orange	Some chemical change, marginally mature but not likely to have potential as a commercial source
4. light medium brown	Mature, active volatilization, oil generation
5. dark brown	Mature, production of wet gas and condensate, transition to dry gas phase
6. very dark brown-black	Over-mature, source potential for dry gas
7. black (opaque)	Traces of dry gas only

Based on observations of colour of the Sanangoé-Mefidezi palynomorphs before oxidation treatment, the sedimentary rocks range from 4 to 5 on the Thermal Alteration Scale of Batten (1980) (Table 5.1). Borehole 12 ESD 231 has a TAI
(thermal alteration index) of 4, with the colour of palynomorphs being mostly light medium brown in colour. Boreholes 871L_D012 and 12 ESD 218 both had a TAI of 4 to 5 with the palynomorph colours ranging from light medium brown to dark brown. In general the colours of the palynomorphs ranged from a light medium brown through to dark brown. This means that the samples range from active volatilization and oil generation to samples that have the potential for oil generation as well as wet gas production and transition into dry gas. This is a good indication for mining as it shows the potential for oil. Although the Sanangoé-Mefidezi Basin is currently exploited for coal, further preliminary exploration for unconventional hydrocarbons should be carried out in the area.

5.4. Sample productivity

The samples from the Sanangoé-Mefidezi Basin yielded a high palynomorph productivity with 34 out of the 56 samples (61%) being classified as productive (250 or more palynomorphs). However, 7 of the productive samples were too fragmentary to identify and count individual grains. This meant that 27 samples were used for actual identification and counting up to 250 palynomorphs. The 7 fragmented samples were still included in statistical analyses for a complete overview of the assemblages present in the Sanangoé-Mefidezi Basin.

5.5. Botanical Affinities

The palynofloras of the Sanangoé-Mefidezi Basin show distinct changes from the "Platform Facies" to the Moatize and Matinde formations. The "Platform Facies" palynoassemblage shows a strong dominance of trilete spores represented by eusporangiate and leptosporangiate ferns, lycopods and sphenophytes (Table 5.2). The palynoflora of the Moatize Formation also indicates the presence of eusporangiate and leptosporangiate ferns, lycopods, sphenophytes, conifers, peltasperms, and glossopterids (Table 5.2). In the Matinde Formation a further shift is seen, with glossopterids being dominant and lesser numbers of peltasperms, conifers, sphenophytes, lycopods and ferns present (Table 5.2).

Botanical affinities of palynomorphs found in the "Platform Facies" and Moatize Formation indicate that the likely environment during this time was a swampy alluvial plain. The overlying Matinde Formation shows greater dominance of the glossopterid flora, suggesting a waterlogged or woodland environment with ferns, conifers, lycopods and sphenophytes also present. The presence of *Protohaploxypinus* and *Striatopodocarpites* in the Moatize and Matinde formations further emphasises the dominance of the glossopterid flora across Gondwana in the Permian (Anderson et al., 1999). The palaeoenvironment can be supported by the presence of coal seams in these deposits as coal only forms under specific conditions (a surplus of dead vegetation such as ferns, conifers, lycopods and the overall dominance of glossopterid flora collecting on swamp floors with cycles of waterlogging occurring, with this process repeating in cycles). All the sediment examined in this study was carbonaceous mudstone interbedded with coal further supporting the paleoenvironment being a wet swamp. Table 5.2. describes the species found in the Sanangoé-Mefidezi Basin sediments and their associated parent plant group.

Table 5.2: Pollen and spores identified from the Sanangoé-Mefidezi Basin and their botanical affinities with references.

Species	Plant Group	Reference
Converrucosisporites naumoviae	Early fern-like order Zygopteridales Eusporangiate ferns (Marattiales) ?Leptosporangiate ferns (Botryopteridales)	Balme, 1995; Taylor et al., 2009; Meyen, 2012
Deltoidospora directa	Eusporangiate ferns (Marattiales) Leptosporangiate ferns (Gleicheniaceae, Dipteridaceae, Dicksoniaceae, Schizaeaceae, Polypodiaceae)	Balme, 1995; Taylor et al., 2009
Granulatisporites papillosus	Rhyniopsida (Rhyniales) Lycopsida (Drepanophycales) Filicopsida	Ibrahim, 1933

	(Botryoptoridales), Equisetopsida (Equiseltales) □ Cyadopsida (Lagenostomales)	
Horriditriletes ramosus	□ Filicopsida (Order uncertain)	Bharadwaj & Salujha, 1964
	□ Ginkgoopsida (Calamopityales)	
Punctatisporites gretensis	□ Early fern-like order Zygopteridales □ Lycopodiophyta □ Sphenophyta (Equisetales) □ Eusporangiate ferns (Marattiales) □ ?Leptosporangiate ferns (Botryopteridales) □ Progymnosperms (Noeggerathians)	Balme, 1995
Verrucosisporites sp.	□ Early fern-like order Zygopteridales □ Lycopodiophyta □ Eusporangiate ferns (Marattiales) □ ?Leptosporangiate ferns (Botryopteridales) □ Progymnosperms (Noeggerathians)	Balme, 1995
Laevigatosporites vulgaris	□ Eusporangiate ferns (Marattiales, Polypodiaceae) □ Progymnosperms (Noeggerathians)	Balme, 1995; Taylor et al., 2009
Thymospora pseudothiessenii	□ ?Sphenophyta (Equisetales) □ Filicopsida (Marattiales)	Balme, 1995; Wilson & Venkatachala, 1963
Granulatasporites subreticulatus	□ ?Sphenophyta (Equisetales)	Balme, 1995
Alisporites potoniei	□ Peltasperms □ Podocarp and voltzian conifer cones	Balme, 1995; Lindström and McLoughlin, 2007
Limitisporites monstruosus *Platysaccus papilionis* *Lueckisporites* sp.	□ Coniferophytes	Balme, 1995; Taylor et al., 2009

Lunatisporites sp.	□ Podocarpaceae	Balme, 1995; Taylor et al., 2009
Protohaploxypinus goraiensis *Protohaploxypinus rugatus*	□ Glossopteridales □ Peltaspermales	Balme, 1995; Taylor et al., 2009

Striatopodocarpites fusus *Marsupipollenites striatus* *Marsupipollenites triradiatus* *Vittatina africana*		
Protohaploxypinus limpidus *Striatopodocarpites cancellatus*	□ Glossopterid sporangium *Arberiella*	Lindström et al., 1997; Lindström and McLoughlin, 2007
Weylandites lucifer	□ *Rugatheca* = ?Glossopterid	Pant and Basu, 1977; Balme, 1995
Cycadopites cymbatus	□ ?Bennettitaleans (first known from the Triassic)	Balme, 1995

5.6. Correlation

5.6.1. Correlations with Africa

5.6.1.1 South Africa

MacRae (1988)

Correlations with MacRae (1988) are made on the basis of abundance and turmal patterns. Examination of these allowed for correlation between Zones A1 to C1 of this study and the biozones of MacRae (1988).

The zones and subzones in this study are considered to be at finer stratigraphic resolution than those of MacRae (1988) for the Waterberg. Therefore, Zones A1, A2 and a portion of Zone B1 all correlate with Biozone D (*Laevigatosporites vulgaris-Alisporites* sp.1 Concurrent Range Zone) of MacRae (1988) based on the dominance of the following species:

Scheuringipollenites ovatus

Deltoidospora directa

Laevigatosporites vulgaris

The following species also occur in both Biozone D of MacRae (1988) and Zones A1, A2 and B1 of this study:

Granulatisporites papillosus

Horriditriletes ramosus

Punctatisporites gretensis

Thymospora pseudothiessenii

Granulatasporites subreticulatus

Alisporites potoniei

Limitisporites monstruosus

Platysaccus papilionis

Pteruchipollenites gracilis

Zones B2 and C1 are more similar to Biozone E (*Kraeuselisporites enormis-Striatopodocarpites cancellatus* Concurrent Range Zone) of MacRae (1988) based on abundances and turmal patterns observed. The distinguishing species of this zone that occur both in Biozone E of MacRae (1988) and Zones B2 and C1 of this study are listed below:

Kraeuselisporites enormis

Alisporites potoniei

Protohaploxypinus limpidus

Striatopodocarpites cancellatus

The other species that occur in both Biozone E of MacRae (1988) and Zones B2 and C1 of this study are listed below:

Converrucosisporites naumoviae

Verrucosisporites sp.

Protohaploxypinus goraiensis

Striatopodocarpites fusus

Weylandites lucifer

Plicatipollenites gondwanensis

The upper part of Zone C1 of this study can be correlated with the lower part of Biozone F (*Striatopodocarpites fusus-Weylandites lucifer* Concurrent Range Zone) of MacRae (1988). The most distinctive species from both Biozone F of MacRae (1988) and Zone C1 of this study are listed below:

Striatopodocarpites fusus

Weylandites lucifer

Other common abundant species that occur in both Biozone F of MacRae (1988) and Zone C1 of this study are given below:

Protohaploxypinus goraiensis

Protohaploxypinus limpidus

Striatopodocarpites cancellatus

Pteruchipollenites gracilis

Pteruchipollenites sp.

Aitken (1988)

Correlations can be made between the palynofloral zones of the Sanangoé-Mefidezi Basin and the biozones of Aitken (1998) for the northern Karoo Basin, South Africa. These correlations are also made on the basis of abundances and turmal patterns observed.

Zones A1, A2 and B1 of this study can be correlated with Biozone II (*Mehlisphaeridium colliensis-Alisporites splendens* Zone) of Aitken (1998) based on the species listed below:

Deltoidospora directa

Laevigatosporites vulgaris

The following other species occur in both Biozone II of Aitken (1998) and Zones A1, A2 and B1 of this study:

Granulatisporites papillosus

Horriditriletes ramosus

Punctatisporites gretensis

Alisporites potoniei

Limitisporites monstruosus

Converrucosisporites naumoviae

Thymospora pseudothiessenii

Zones B2 and C1 of the Sanangoé-Mefidezi Basin can be correlated with Biozone III (*Striatopodocarpites cancellatus-Marsupipollenites triradiatus* Zone) of Aitken (1998) based on abundances of the following distinctive taxa:

Striatopodocarpites cancellatus

Marsupipollenites triradiatus

Alisporites potoniei

Kraeuselisporites enormis

Other taxa that can be found in both Biozone III of Aitken (1998) and Zones B2 and C1 of this study are listed below:

Plicatipollenites gondwanensis

Striatoabieites multistriatus

Platysaccus papilionis

Pteruchipollenites gracilis

Scheuringipollenites ovatus

The upper part of Zone C1 in the Sanangoé-Mefidezi Basin can be correlated with Biozone IVB (*Striatopodocarpites fusus-Weylandites lucifer* Zone) of Aitken (1998). This correlation is based on the abundance of the following distinctive taxa:

Striatopodocarpites fusus

Weylandites lucifer

Striatopodocarpites cancellatus

Protohaploxypinus goraiensis

Protohaploxypinus limpidus

A list of other taxa found within both Biozone IVB and upper Zone C1 are given below:

Marsupipollenites striatus

Pteruchipollenites sp.

Pteruchipollenites gracilis

Plicatipollenites gondwanensis

Striatoabieites multistriatus

5.6.1.2 Botswana

A tentative correlation is made between Zone C1 of this study and the *Platysaccus papilionis-Striatopodocarpites fusus* Assemblage Zone (Biozone KK3) of Modie and Le Hérissé (2009). This is based on the dominance of the taxa *Platysaccus papilionis* and *Striatopodocarpites fusus*, and the presence of the other species:

Alisporites splendens

Striatopodocarpites fusus

Protohaploxypinus limpidus

Alisporites ovatus

Laevigatosporites vulgaris

5.6.1.3 Zimbabwe

Correlation of Zone B2 of this study with Assemblage II of Falcon (1975) is possible based on the occurrence of *Marsupipollenites* sp., *Striatoabieites* sp., *Striatopodocarpites* sp., *Laevigatosporites* sp., *Alisporites splendens* and *A. potoniei*.

5.6.1.4 Zambia

Zone B2 of this study and the palynoassemblage from the Gwembe Formation (Nyambe & Utting, 1997; Barbolini et al., 2016b) can be correlated and share the following species:

Alisporites potoniei

Guttulapollenites hannonicus

Striatopodocarpites cancellatus

Limitisporites sp.

Protohaploxypinus sp.

A tentative correlation can be made between Zone C1 of this study and the palynoflora of the Madumabisa Formation (Nyambe & Utting, 1997; Barbolini et al., 2016b), based on the presence of the following species:

Cycadopites cymbatus

Marsupipollenites triradiatus

Platysaccus papilionis

Weylandites lucifer

5.6.1.5 Mozambique

Other Mozambique palynoassemblages are very similar to the palynofloras of this study and can be correlated as follows:

Zones A1 and A2 of this study can be correlated with Seam 4 of the Mucanha-Vúzi Basin (Falcon *et al.* (1984) and share *Cycadopites cymbatus*, *Marsupipollenites triradiatus*, *M. striatus*, *Striatopodocarpites cancellatus* and *Alisporites* sp. These species are characteristic of the *Protohaploxypinus-Vittatina-Striatopodocarpites* Sub-Assemblage, and *Protohaploxypinus-Vittatina-Guttulapollenites-Lueckisporites* Sub-Assemblage.

Pereira *et al.* (2016) identified two palynoassemblages for the Matinde Formation, of late Permian and early Triassic age. Both of these assemblages are younger than those of the current study, indicating that Zone C1 represents a lower part of the Matinde Formation than those described by Pereira *et al.* (2016).

A recently published study of palynomorphs from the Moatize Basin, eastern Tete province, Mozambique was assigned a Guadalupian–Lopingian age (Götz *et al.*, 2017) can be compared with palynofloras of the Sanangoé-Mefidezi Basin. The lower part of the assemblage is dominated by triletes and can be correlated with zones A1 and A2 of

this study, the middle part is dominated by non-taeniate bisaccate pollen and can be correlated with Zone B2 of this study, and the upper part is characterised by *Protohaploxypinus* and *Lueckisporites*, which can be correlated with Zone C1 of this study.

5.6.2 Correlations with Antarctica

A tentative correlation can be made between Zone C1 of this study and the Buckley Formation of Antarctica based on the following shared species:

Deltoidospora directa

Laevigatosporites sp.

Marsupipollenites striatus

Marsupipollenites triradiatus

Protohaploxypinus limpidus

Striatopodocarpites cancellatus

Striatopodocarpites fusus

5.6.3 Correlations with Australia

Australia has a finely resolved Permian palynozonation that serves as the standard biostratigraphic scheme for the southern hemisphere, but contains some endemic species that can complicate correlation (Barbolini et al., 2016c). Correlation of zones B1 and the lower part of B2 of this study can be made with the *Striatopodocarpites fusus* Zone of Backhouse (1991). This is based on the first appearance of both *Striatopodocarpites fusus* and *Striatopodocarpites cancellatus* seen in Zone B1. *Scheuringipollenites* and *Cycadopites cymbatus* are also common in both zones. A possible correlation with Zone B1 and lower B2

is extended to the upper part of Stage 3a of Price (1983) and Unit IV of the Canning Basin (Kemp *et al.*, 1977).

Zone C1 and upper B2 shows a possible correlation with the *Microbaculispora trisina* Zone of Backhouse (1991). Shared species are listed below:

Granulatisporites papillosus / Granulatisporites trisinus

Marsupipollenites striatus

Striatopodocarpites fusus

Protohaploxypinus limpidus

5.6.4 Age Determination

The age of the Sanangoé-Mefidezi Basin rocks is determined based on the correlation of palynomorph zones with other palynological assemblages from Gondwana. Zones A1, A2 and the lower part of Zone B1 (which represents the "Platform Facies") correlates to Biozone D of MacRae (1988) and Biozone II of Aitken (1998) and is therefore assigned an Artinskian (Cisuralian) age. The upper part of zones B1 (which represents the upper "Platform Facies") can be assigned a Kungurian (Cisuralian) age on the basis of correlation with Biozone III of Aitken (1998). Zone B2 (which represents the lower part of the Moatize Formation) is correlated with Biozone E of MacRae (1988), the Gwembe Formation, Zambia palynoassemblage (Nyambe & Utting, 1997; Barbolini et al., 2016b), the middle part of the Moatize Basin assemblage (Götz *et al.*, 2017), and the *Striatopodocarpites fusus* and *Microbaculispora trisina* zones of Backhouse (1991). Therefore, Zone B2 is assigned a Roadian–Wordian (Guadalupian) age. Zone C1 (which represents the Moatize and Matinde formations) is assigned a late Guadalupian (Capitanian) age based on correlation with Biozone F of MacRae (1988), Biozone IVB of Aitken (1998), Biozone KK3 of Modie and Le Hérissé (2009), the palynoflora of the Madumabisa Formation, Zambia (Nyambe & Utting, 1997; Barbolini et al., 2016b), the upper part of the Moatize Basin assemblage (Götz *et al.*, 2017), and the Buckley Formation of Antarctica.

5.6.5 Statistical Analyses

Statistical analyses were performed on palynomorph abundance data in order to ensure an unbiased method of clustering samples from a borehole core together. Statistics can group samples with similar palynofloral compositions based on numerical data (e.g. Falcon, 1976), but visual methods of clustering can give similar results and are generally easier, quicker and more straightforward to apply (Falcon, 1976). In order to avoid possible bias in this study, statistical analyses were applied as the primary method of subdivision, but it was noted that the same clusters were produced from visual analysis, similar to the findings of Falcon (1976).

5.6.6. Lithology

The palynomorph assemblages of the "Platform Facies" and the Moatize Formation were found to be distinct in this study, supporting the current stratigraphic assignment of the "Platform Facies" to the underlying Vúzi Formation. Palynofloral composition supports lithology in that the reworked diamictites of the "Platform Facies" represent a significantly different palaeoenvironment to the lacustrine deposits of the Moatize Formation. A palynofloral "event" (Samples 1998 and 1999) occurs within Zone C1 at the base of the Matinde Formation, which may be a useful marker for this unit in future exploration work. Many species temporarily disappear during this event, but reappear in higher stratigraphic horizons suggesting that the floral community quickly returned to a similar composition to that found within the underlying Moatize Formation. Therefore, the lithologies of these two units are different, but this did not significantly affect regional vegetation composition on the landscape.

5.6.7 Conclusions and Future Work

This study has identified and described Artinskian–Capitanian palynofloras from coal deposits located in Tete province, Mozambique. Although other studies have assigned to a Lopingian age to palynoassemblages from the Matinde Formation, palynology of the current

study indicates that the lower part of this formation is Guadalupian. The Sanangoé-Mefidezi Basin is abundant in palynomorphs which are useful in biostratigraphic correlation with other parts of Gondwana. The majority of samples were derived from high-energy debris flows which contributed to the fragmentary and damaged nature of the palynomorph grains. The "Platform Facies" is dominated by spores which is consistent with the current stratigraphic assignment of this unit to the glacial Vúzi Formation. Statistical analyses subdivided palynomorph ranges into four zones and two subzones, and demonstrated that visual clustering of palynology samples produces similar results to statistical clustering of samples. The PCA biplots showed no great differences in environment and climate of the coal seams (since all species vectors clustered in the centre). Biostratigraphic correlation was possible between the zones of the Sanangoé-Mefidezi Basin and palynofloras of southern Africa, Antarctica and Australia and this suggested an Artinskian age for zones A1 and A2, a Kungurian age for Zone B1, a Roadian–Wordian age for Zone B2, and a Capitanian age for Zone C1. Due to the fragmentary nature of the grains, higher resolution sampling of the Permian Sanangoé-Mefidezi Basin would be useful in establishing more precise correlations with other Gondwanan assemblages. In particular, a detailed examination of the Matinde Formation would be useful in determining its full age extent, as this study has showed that part of this formation is older than previously thought. Radio-isotopic ages would assist in calibrating the palynomorphs of Mozambique in order to clarify palaeogeographical patterns of plant migration in the Permian.

6. Reference List

Aitken, G.A., 1993. Palynology of the Number Five Seam in the Witbank / Highveld coalfields. Unpublished M.Sc. Thesis, University of the Witwatersrand.

Aitken, G., 1994. Permian palynomorphs from the Number 5 Seam, Ecca Group, Witbank Highveld Coalfields, South Africa. Palaeontologia africana 31: 97-109.

Aitken, G.A., 1998. A palynological and palaeoenvironmental analysis of Permian and early Triassic sediments of the Ecca and the Beaufort groups, Northern Karoo Basin, South Africa. Unpublished Ph.D. Thesis, University of the Witwatersrand.

Anderson, J.M., 1977. The Biostratigraphy of the Permian and Triassic, Part 3. Memoirs of the Botanical Survey of South Africa No. 41.

Anderson, J.M., Anderson, H.M., Cruickshank, A.R.I. 1998. Late Triassic ecosystems of the Molteno/Lower Elliot biome of southern Africa. Palaeontology, 41: 387-421.

Backhouse, J., 1991. Permian palynostratigraphy of the Collie Basin, Western Australia. Review of Palaeobotany and Palynology 67: 237-314.

Balme, B. E., Hennelly, J. P. F., 1956. Monolete, Monocolpate, and Alete sporomorphs from Australian Permian sediments. Australian Journal of Botany 4(1): 54-67.

Balme, B.E. 1995. Fossil in situ spores and pollen grains: an annotated catalogue. Review of Palaeobotany and Palynology 87: 81-323.

Barbolini, N. 2010. Palynology of a coal seam in Karoo deposits of Botswana and correlation with Southern African coal-bearing strata, Unpublished M.Sc. Thesis, University of the Witwatersrand.

Barbolini, N. 2014. Palynostratigraphy of the South African Karoo Supergroup and correlations with coeval Gondwana successions, Unpublished Ph.D. Thesis, University of the Witwatersrand.

Barbolini, N., Bamford, M.K., 2014. Palynology of an Early Permian coal seam from the Karoo Supergroup of Botswana. Journal of African Earth Sciences 100: 136-144.

Barbolini N., Bamford M.K., Tolan S.C., 2016a. Permo-Triassic palynology and palaeobotany of Zambia: a review. Palaeontologia africana 50: 18–30.

Barbolini N., Smith R.M.H., Tabor N., Sidor C.A., Angielcyzk K., 2016b. Resolving the age of Madumabisa vertebrates: Palynological evidence from the mid-Zambezi Basin of Zambia. Palaeoecology, Palaeoclimatology, Palaeogeography 457: 117–128.

Barbolini N., Rubidge B.S., Bamford M.K., 2016c. Radiometric dating demonstrates that Permian spore-pollen zones of Australia and South Africa are diachronous. Gondwana Research 37: 241–251.

Batten, D. J. 1996. Palynofacies. Palynology: Principles and Applications. American Association of Stratigraphic Palynologists Foundation, Dallas, Texas, 1011-1064.

Batten, D. J. 1982. Palynofacies, palaeoenvironments and petroleum. Journal of Micropalaeontology, 1(1), 107-114.Beri, Á., Gutiérrez, P., Balarino, L., 2011. Palynostratigraphy of the late Palaeozoic of Uruguay, Paraná Basin. Review of Palaeobotany and Palynology 167: 16-29.

Bharadwaj, D.C., Salujha, S.K., 1964. Sporological study of seam VIII in Raniganj Coalfield, Bihar (India). The Palaeobotanist 12: 181-215.

Cadle, A.B., Cairncross, B., Christie, A.D.M. and Roberts, D.L., 1993. The Karoo Basin of South Africa: type basin for coal-bearing deposits of southern Africa. International Journal of Coal Geology, 23, 117-157.

Catuneanu, O., Wopfner, H., Eriksson, P. G., Cairncross, B., Rubidge, B. S., Smith, R. M. H., Hancox, P. J., 2005. The Karoo basins of south-central Africa. Journal of African Earth Sciences 43: 211-253.

Cairncross, B. 2001. An overview of the Permian (Karoo) coal deposits of southern Africa, Journal of African Earth Sciences 33: 529-562.

Cairncross, B., 2004. Field guide to rocks and minerals of southern Africa, Struik New Holland Publishing, Cape Town, South Africa.

Césari, S. N., Gutiérrez, P. R., 2000. Palynostratigraphy of Upper Palaeozoic sequences in central-western Argentina. Palynology 24: 113-146.

Césari, S.N., Limarino, C.O., Gulbranson, E.L., 2011. An Upper Paleozoic biochronostratigraphic scheme for the western margin of Gondwana. EarthScience Reviews 106(1-2): 149-160.

Cilek, V., 1989. Industrial minerals of Mozambique: mines and mineral resources – Mozambique. Prague: Geological Survey.

Combaz, A. 1964. The palynofacies. Micropaleontology Review, 7 (3), 205-218.

Daemon, R.F., Quadros, L.P., 1970. Bioestratigrafia do Neopaleozóico da Bacia do Paraná. In: Congresso Brasileiro de Geologia, XXIV, Brasília, 1970. Anais 1 Sociedade Brasileira de Geologia, Brasília: 359-412.

de Jekhowsky, B., Goubin N., 1964. Subsurface palynology in Madagascar; a stratigraphic sketch of the Permian, Triassic and Jurassic of the Morondava Basin. Special Publication - Society of Economic Paleontologists and Mineralogists 11: 116-130.

Goubin, N., 1965. Description et repartition des principaux pollenites Permiens, Triassiques et Jurassiques des sondages du Basin de Morondava (Madagascar). Revue de l'Institut Francais du Petrole 20: 1415-1461.

Falcon, R.M.S., 1975. Application of Palynology in Sub-dividing the Coal-bearing Formations of the Karoo Sequence in Southern Africa. South Journal of Science 71: 336-344.

Falcon, R.M.S., Pinheiro, H.J. & Sheperd, P., 1984. The palynostratigraphy of the major coal seams in the Witbank Basin with lithostratigraphic, chronostratigraphic and palaeoclimatic implications. Comunicações dos Serviços Geológicos de Portugal 70: 215-243.

Falcon, R.M.S., 1988. Collaborative investigation of the Witbank No. 2 Seam – Petrographic and Palynological aspects. National Geoscience Programme. Final Report for sub-programme COAL. CSIR Internal Report, 40 pp.

Falcon, R.M.S., 1989. Macro- and micro-factors affecting coal-seam quality and distribution in southern Africa with particular reference to the No. 2 seam, Witbank coalfield, South Africa. International Journal of Coal Geology 12: 681731.

Farabee, M.J., Taylor, E.L., Taylor, T.N., 1990. Correlation of Permian and Triassic palynomorph assemblages from the central Transantarctic Mountains, Antarctica. Review of Palaeobotany and Palynology 65: 257-265.

Fernandes P., Cogne N., Chew D.M., Rodrigues B., Santos Jorge R.C.G., Marques M., Jamal D. & Vasconcelos L. 2015. The thermal history of the Karoo Moatize-Minjova Basin, Tete Province, Mozambique: An integrated vitrinite reflectance and apatite fission track thermochronology study. Journal of African Earth Science: 101: 55–72.

Finkelstein, S.A., Peros, M.C. and Davis, A.M. 2005. Late Holocene palaeoenvironmental change in a Great Lakes coastal wetland: integrating pollen and diatom datasets. Journal of Palaeolimnology, 33: 1-12.

Fitchett, J.M. 2015. Towards a muti-proxy Holocene palaeoenvironmental and palaeoclimatic reconstruction for Eastern Lesotho. Unpublished Ph.D. Thesis, University of the Witwatersrand.

Foster, C.B., 1982. Spore-pollen assemblages of the Bowen Basin, Queensland (Australia): their relationship to the Permian/Triassic boundary. Review of Palaeobotany and Palynology 36: 165-183.

Götz, A.E., Hancox, P.J., Lloyd, A. 2017. Permian climate change recorded in palynomorph assemblages of Mozambique (Moatize Basin, eastern Tete Province) Acta Palaeobotanica: DOI: 10.1515/acpa-2017-0001

GTK Consortium Geological Surveys in Mozambique 2002-2007, 2008. In: Yrjö, Pekkala, Tapio, Lehto, Hannu, Mäkitie (Eds.). Geological Survey of Finland, Special Paper, 48, 7-22.

Hancox, P.J. 2016. The coalfields of South-Central Africa: A current perspective. Episodes, 407-428.

Hancox, P.J. and Götz, A.E., 2014. South Africa's coalfields — A 2014 perspective. International Journal of Coal Geology, 132, 170-254.

Hankel, O., 1987. Lithostratigraphic subdivision of the Karoo rocks of the Luwegu Basin (Tanzania) and their biostratigraphic classification based on microfloras, macrofloras, fossil wood and vertebrates. Geologische Rundschau 76: 539-565.

Hankel, O., 1992. Late Permian to Early Triassic microfloral assemblages from the Maji ya Chumvi Formation, Kenya. Review of Palaeobotany and Palynology 72: 129-147.

Hart, G.F., 1965. The systematics and distribution of Permian miospores. Witwatersrand University Press, Johannesburg, 252 pp.

Ibrahim, M.I.A., 1933. Aptian-Turonian palynology of the Ghazalat-I Well (GTX-I), Qattara Depression, Egypt. Review of Palaeobotany and Palynology 94: 137-168.

Johnson, M.R., 1996. Stratigraphy of the Karoo Supergroup in southern Africa: an overview. Journal of African Earth Sciences 23: 3-15.

Juggins, S. 2007. C2, Software for ecological and palaeoecological data analysis and visualisation, User guide Version 1.5. Retrieved on 11 July 2014 from www.staff.ncl.ac.uk/stephen.juggins/software/code/C2.pdf

Kar, R.K., Bose, M.N., 1967. Palaeozoic sporae dispersae from Congo III. - Assise des schistes noirs de la Lukuga. Annales Musée Royal de l'Afrique Centrale, Tervuren, Belgique, Serie in-8°, Sciences Géologiques 54: 1-83.

Kaufman, L. and Rousseeuw, P.J. 2009. Finding groups in data: An introduction to cluster analysis. John Wiley & Sons: New Jersey, pp. 87-98, 242-243.

Key, R.M., Tidi, J., McGeorge, I., Aitken, G., Cadman, A., Anscombe, J., 1998. The Lower Karoo Supergroup geology of the southeastern part of the Gemsbok Sub-basin of the Kalahari Basin, Botswana. South African Journal of Geology 101(3): 225-236.

Lächelt, S., 2004.The Geology and Mineral Resource of Mozambique. Council of Geosciences.

Legendre, P. and Birks, H.J.B. 2012. Clustering and Partitioning. In Birks, H.J.B., Lotter, A.F., Juggins, S. and Smol, J.P. (eds.). Tracking environmental change using lake sediments, volume 5: Data handling and numerical techniques. Springer: Dordrecht, pp. 167-200.

Lindström, S., 1995. Early Permian palynostratigraphy of the northern Heimefrontfjella mountain-range, Dronning Maud Land, Antarctica. Review of Palaeobotany and Palynology 89: 359-415.

Lindström, S., McLoughlin, S., Drinnan, A.N., 1997. Intraspecific variation of taeniate bisaccate pollen within Permian glossopterid sporangia, from the Prince Charles Mountains, Antarctica. International Journal of Plant Sciences 158: 673–684.

Lindström, S., McLoughlin, S., 2007. Synchronous palynofloristic extinction and recovery after the end-Permian event in the Prince Charles Mountains. Antarctica: implications for

palynofloristic turnover across Gondwana. Review of Palaeobotany and Palynology 145: 89–122.

Lloyd, A., 2015. Tete Coal Basin - What do we know? What do we still have to learn? Presentation delivered at the Fossil Fuel Foundation Solid fossil fuels in southern Africa and Madagascar, March 2015.

Mackay, A.W., Bezrukova, E.V., Leng, M.J., Meaney, M., Nunes, A., Piotrowska, N., Self, A., Shchetnikov, A., Shilland, E., Tarasov, P., Wang, L. and White, D. 2012. Aquatic ecosystem responses to Holocene climate change and biome development in boreal, central Asia. Quaternary Science Reviews, 41: 119-131.

Mackay, A.W., Bezrukova, E.V., Boyle, J.F., Holmes, J.A., Panizzo, V.N., Piotrowska, N., Shchetnikov, A., Shilland, E.M., Tarasov, P. and White, D. 2013. Multiproxy evidence for abrupt climate change impacts on terrestrial and freshwater ecosystems in the Ol'khon region of Lake Baikal, central Asia. Quaternary International, 290-291: 46-56.

MacRae, C.S., 1978. Palaeozoic Palynology of Botswana. M.Sc. thesis, University of the Witwatersrand.

MacRae, C.S., 1988. Palynostratigraphic correlation between the Lower Karoo sequence of the Waterberg and Pafuri coal-bearing basins and the Hammanskraal plant macrofossil locality, Republic of South Africa. Memoirs of the Geological Survey of South Africa 75: 1–217.

Mahabeer, K.C. 2015. Palynology of the Permian Ecca Mucanha-Vuzi Basin, Tete province, Mozambique. Unpublished Honours Thesis, University of the Witwatersrand.

McLoughlin, S. 2012. "Two new Senotheca (Glossopteridales) species from the Sydney Basin, Australia, and a review of the genus". Review of Palaeobotany and Palynology. 171: 140–151. doi:10.1016/j.revpalbo.2011.12.004.

Meyers, P.A. and Teranes, J.L. 2001. Sediment organic matter. In Last, W.M. and Smol, J.P. (eds.). Tracking environmental change using lake sediments, volume 2: Physical and Geochemical Methods. Springer Science and Media: Dordrecht, pp. 239-262

Modie, B.N., 2007. The Palaeozoic palynostratigraphy of the Karoo Supergroup and Palynofacies insight into palaeoenvironmental interpretations, Kalahari Karoo Basin, Botswana. Ph.D. thesis, Université de Bretagne Occidentale, Brest. 301 pp.

Modie, B.N., Le Hérissé, A., 2009. Late Palaeozoic palynomorph assemblages from the Karoo Supergroup and their potential for biostratigraphic correlation, Kalahari Karoo Basin, Botswana. Bulletin of Geosciences 84(2): 337–358. Czech Geological Survey, Prague.

Moore, P.D. and Webb, J.A., 1978. An Illustrated Guide to Pollen Analysis. Hodder and Stoughton, London, 133 pp. Moore, P. D., Webb, J. A., Collinson, M. E., 1991. Pollen Analysis (Second Edition). Blackwell Scientific Publications, Osney Mead, Oxford.

Mory, A.J., Backhouse, J., 1997. Permian stratigraphy and palynology of the Carnarvon Basin, Western Australia. Geological Survey of Western Australia Report 46: 1–101.

Mukhopadhyay, G., Mukhopadhyay, S. K., Roychowdhury, M., Parui, P. K., 2010. Stratigraphic Correlation between Different Gondwana Basins of India. Journal of the Geological Society of India 76: 251-266.

Murphy, M., Salvador, A., 1999. International Stratigraphic Guide, an abridged edition. Episodes 22: 255-271.

Nyambe, I. A., Utting, J., 1997. Stratigraphy and palynostratigraphy, Karoo Supergroup (Permian and Triassic), mid-Zambezi Valley, southern Zambia. Journal of African Earth Sciences 24(4): 563 -583.

Potonié, R., 1956. Synopsis der Gattungen der Sporae dispersae, I. Teil: Sporites. Beih. Geol. Jahrb., 23: 1-103

Pereira, Z., Fernandes, P., Lopes, G., Marques, J., Vasconcelos, L., 2016. The Permian-Triassic transition in the Moatize-Minjova Basin, Karoo Supergroup, Mozambique: A palynological perspective. Review of Palaeobotany and Palynology 226: 1-19.

Phipps, D., Playford, G., 1984. Laboratory techniques for extraction of palynomorphs from sediments. Papers of the Department of Geology, University of Queensland 11: 1-23.

Playford, G., Dino, R., 2000. Palynostratigraphy of upper Palaeozoic strata (Trapajós Group), Amazonas Basin, Brazil: Parts One and Two. Palaeontographica Abteilung B 255: 1–46, 87-145.

Pross, J., Pletsch, T., Shillington, D.J., Ligouis, B., Schellenberg, F., Kus, J., 2007. Thermal alteration of terrestrial palynomorphs in mid-Cretaceous organic-rich mudstones intruded by an igneous sill (Newfoundland Margin, ODP Hole 1276A). International Journal of Coal Geology 70: 277–291.

Smith, R.M.H., 1990. A review of the stratigraphy and sedimentary environments of the Karoo basin of South Africa. Journal of African Earth Sciences 10: 117137.

Stephenson, M.H., McLean, D., 1999. International correlation of Early Permian palynofloras from the Karoo sediments of Morupule, Botswana. South African Journal of Geology 102(1): 3-14.

Stevenson, R.J. and Pan, Y. 2004. Assessing environmental conditions in rivers and streams with diatoms. In Stoermer, E.F. and Smol, J.P. (eds.). The Diatoms: Applications for the environmental and earth science. Cambridge University Press: Cambridge, pp. 11-40.

Souza, P.A., 2006. Late Carboniferous palynostratigraphy of the Itararé Subgroup, northeastern Paraná Basin, Brazil. Review of Palaeobotany and Palynology 138: 9-29.

Souza, P. A., Marques-Toigo, M., 2003. An overview on the Palynostratigraphy of the Upper Paleozoic strata of the Brazilian Paraná Basin. Revista del Museo Argentino de Ciencias Naturales 5(2): 205-214.

Souza, P. A., Marques-Toigo, M., 2005. Progress on the palynostratigraphy of the Permian strata in Rio Grande do Sul State

Taylor, T.N., Taylor, E.L., Krings, M., 2009. Paleobotany: the Biology and Evolution of Fossil Plants (2nd Edition). Elsevier.

Tripathi, A., Vijaya, Murthy, S., Chakarborty, B., Das, D K., 2012. Stratigraphic status of coal horizon in Tatapani–Ramkola Coalfield, Chhattisgarh, India. Journal of Earth System Science 121(2): 537-557.

Traverse, A., 2007. Paleopalynology, Second Edition (Topics in Geobiology 28). Springer, Dordrecht, Netherlands.

Truswell, E. M., 1981. Pre-Cenozoic palynology and continental movements. Paleoreconstruction of the Continents, Geodynamics Series 2: 13-25.

Utting, J., 1976. Pollen and spore assemblages in the Luwumbu Coal Formation (Lower Karroo) of the North Luangwa Valley, Zambia, and their biostratigraphic significance. Review of Palaeobotany and Palynology 21: 295-315.

Utting, J., 1978. Lower Karroo Pollen and Spore Assemblages from the Coal Measures and Underlying Sediments of the Siankondobo Coalfield, Mid-Zambezi Valley, Zambia. Palynology 2: 53-68.

Vasconcelos, L.S., 2000. Overview of the Moatize Coal Basin geology, Tete province, Republique of Mozambique. Chronicles of Mineral Research and Exploration 538, 25-36.

Vasconcelos, L.S. 2009. Coal in Mozambique. Proceedings of the 3rd Symposium on Gondwana Coals, Porto Alegre, Brazil 2009.

Vasconcelos, L.S. 2012. Overview of the Mozambique Coal Deposits. Proceedings of the 34th International Geological Congress 2012, Australian Geosciences Council, Brisbane, Australia.

Vasconcelos, L.S., 2013. Coal Deposits in Mozambique – An Overview. Presentation at the FFF Mozambique Coal Conference, October 2013, Johannesburg, South Africa.

Vijaya, Tripathi, A., Roy, A., Mitra, S., 2012. Palynostratigraphy and age correlation of subsurface strata within the sub-basins in Singrauli Gondwana Basin, India. Journal of Earth System Science 121(4): 1071-1092.

Wright, R. P., Askin, R. A., 1987. The Permian-Triassic boundary in the southern Morondava Basin of Madagascar as defined by plant microfossils. American Geophysical Union: 157-166.

Yule, B., Roberts, S., Marshall, J.E.A., Milton, J. A., 1998. Quantitative spore colour measurement using colour image analysis. Organic Geochemistry 28(3/4): 139-149.

7. Appendix A

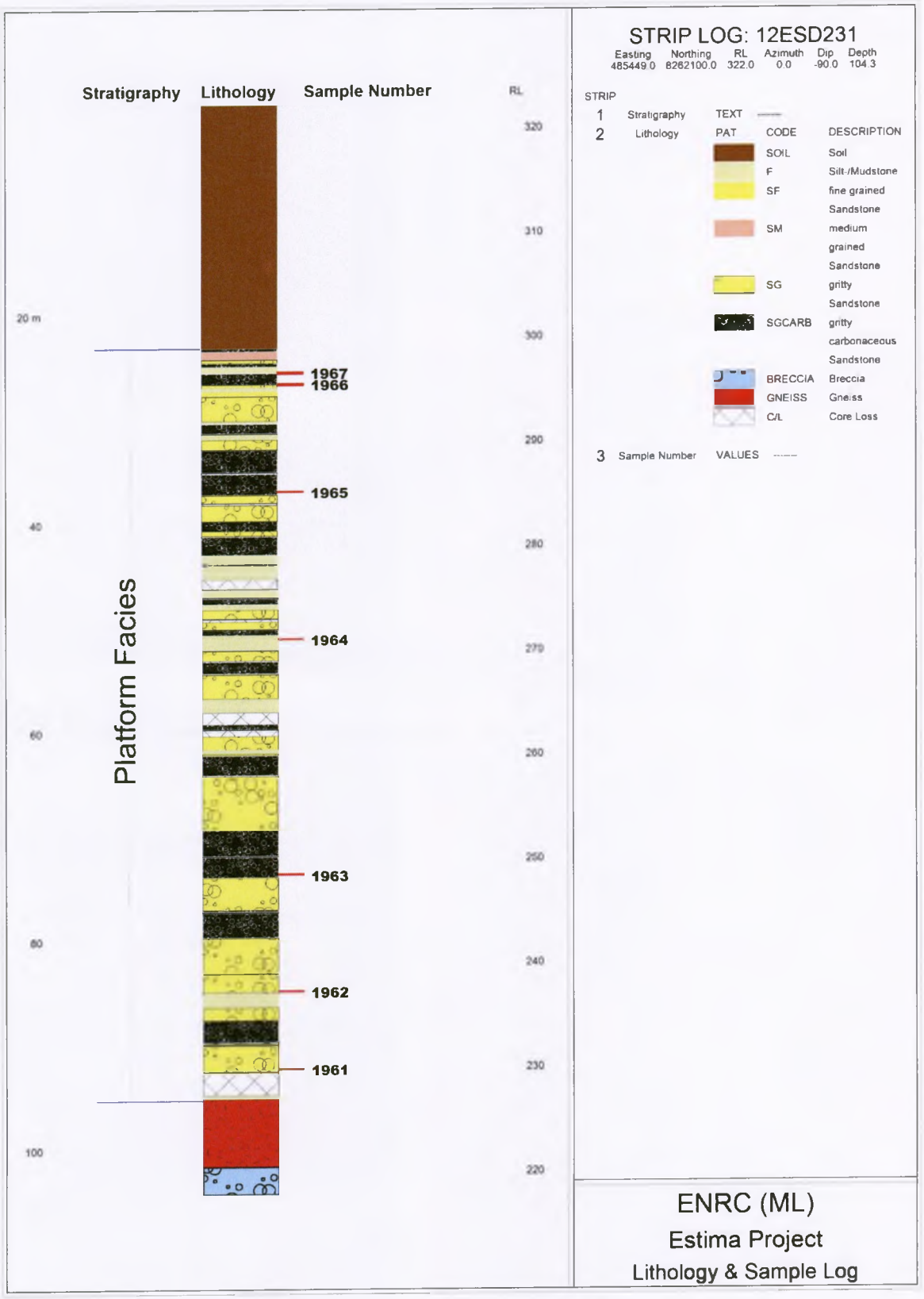
Stratigraphy
Lithology
Sample Number
RL
Platform Facies
20 m
40
60
80
100
320
310
300
290
280
270
260
250
240
230
220
1967
1966
1965
1964
1963
1962
1961
STRIP LOG: 12ESD231
Easting Northing RL Azimuth Dip Depth
485449.0 8262100.0 322.0 0.0 -90.0 104.3
STRIP
1 Stratigraphy TEXT
2 Lithology PAT CODE DESCRIPTION
SOIL Soil
F Silt-/Mudstone
SF fine grained Sandstone
SM medium grained Sandstone
SG gritty Sandstone
SGCARB gritty carbonaceous Sandstone
BRECCIA Breccia
GNEISS Gneiss
C/L Core Loss
3 Sample Number VALUES
ENRC (ML)
Estima Project
Lithology & Sample Log

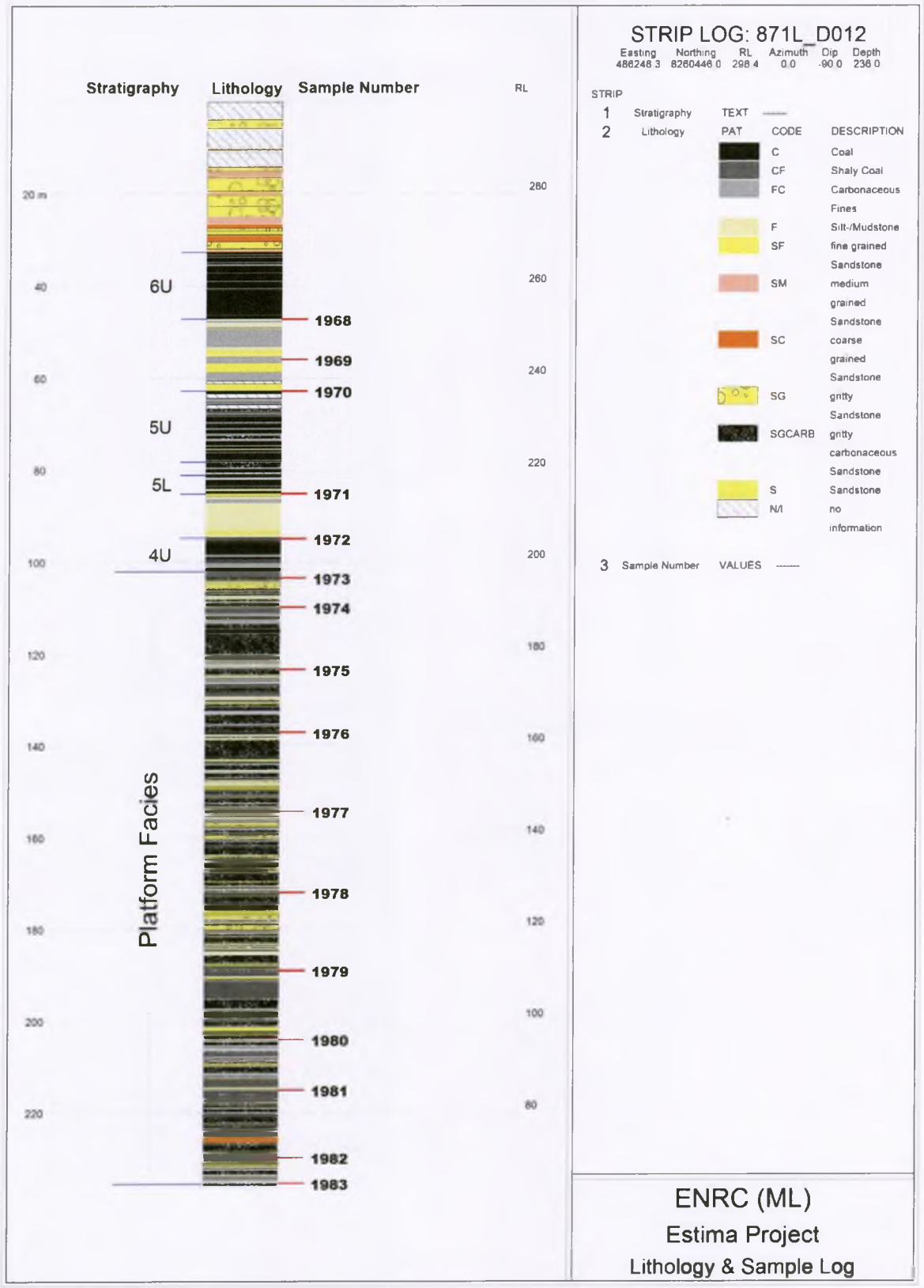
Stratigraphy
Lithology
Sample Number
RL
20 m
40
60
80
100
120
140
160
180
200
220
280
260
240
220
200
180
160
140
120
100
80
6U
5U
5L
4U
Platform Facies
1968
1969
1970
1971
1972
1973
1974
1975
1976
1977
1978
1979
1980
1981
1982
1983
STRIP LOG: 871L_D012
Easting Northing RL Azimuth Dip Depth
486248.3 8260446.0 298.4 0.0 -90.0 236.0
STRIP
1 Stratigraphy TEXT
2 Lithology PAT CODE DESCRIPTION
C Coal
CF Shaly Coal
FC Carbonaceous Fines
F Silt-/Mudstone
SF fine grained Sandstone
SM medium grained Sandstone
SC coarse grained Sandstone
SG gritty Sandstone
SGCARB gritty carbonaceous Sandstone
S Sandstone
N/I no information
3 Sample Number VALUES
ENRC (ML)
Estima Project
Lithology & Sample Log

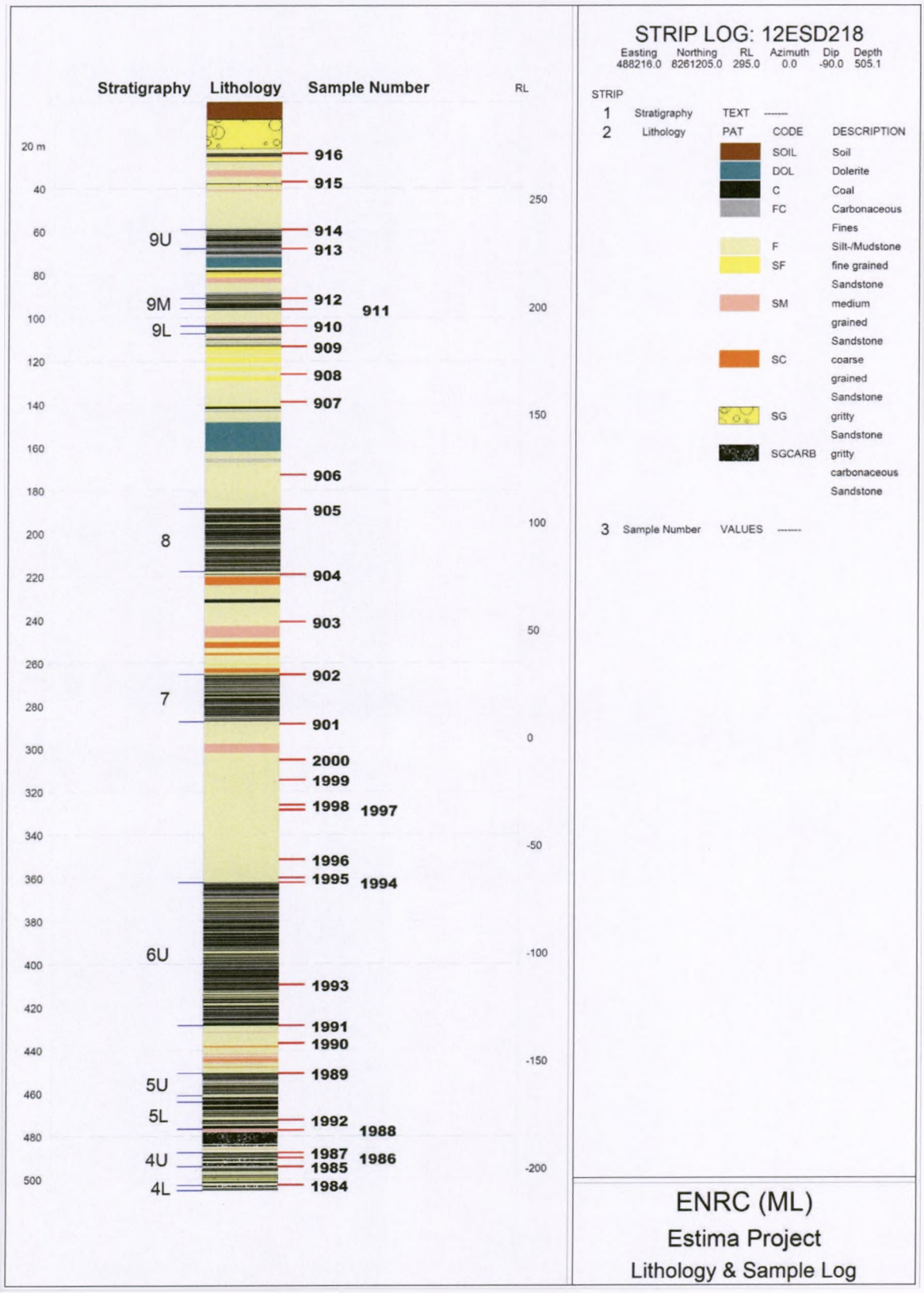
Stratigraphy
Lithology
Sample Number
RL
20 m
40
60
80
100
120
140
160
180
200
220
240
260
280
300
320
340
360
380
400
420
440
460
480
500
250
200
150
100
50
0
-50
-100
-150
-200
9U
9M
9L
8
7
6U
5U
5L
4U
4L
916
915
914
913
912
911
910
909
908
907
906
905
904
903
902
901
2000
1999
1998
1997
1996
1995
1994
1993
1991
1990
1989
1992
1988
1987
1986
1985
1984
STRIP LOG: 12ESD218
Easting Northing RL Azimuth Dip Depth
488216.0 8261205.0 295.0 0.0 -90.0 505.1
STRIP
1 Stratigraphy TEXT ------
2 Lithology PAT CODE DESCRIPTION
SOIL Soil
DOL Dolerite
C Coal
FC Carbonaceous Fines
F Silt-/Mudstone
SF fine grained Sandstone
SM medium grained Sandstone
SC coarse grained Sandstone
SG gritty Sandstone
SGCARB gritty carbonaceous Sandstone
3 Sample Number VALUES ------
ENRC (ML)
Estima Project
Lithology & Sample Log